TÍTULO

STUDY OF ORBITAL GEOMETRY FOR MISSION ANALYSIS

CÓDIGO O.T.

AC-E-400

PREPARADO POR

ASS. Válder matos de medi	Válder Matos de Medeiros	8 / 7 / 86 DATA
ASS. KRamaRao	Kondapalli Rama Rao	8 / 7 / 86 DATA
ASS. Valdemir	Valdemir Carrara	8 / 7 / 86 DATA
ASS. Gadelha	Luis Carlos Gadelha	8 / 7 / 86 DATA
ASS.		/ / DATA

APROVAÇÕES

ASS. Décio C. Ceballos	Décio C. Ceballos	30 / 07 / 86 DATA
ASS.		/ / DATA
ASS.		/ / DATA
ASS.		/ / DATA
ASS.		/ / DATA

PÁGINA	VERSÃO	DATA	REFERÊNCIA DA MODIFICAÇÃO	OBSERVAÇÃO
01	01	30/07/86		
02	01	30/07/86		
03	01	30/07/86		
04	01	30/07/86		
05	01	30/07/86		
06	01	30/07/86		
07	01	30/07/86		
08	01	30/07/86		
09	01	30/07/86		
10	01	30/07/86		
11	01	30/07/86		
12	01	30/07/86		
13	01	30/07/86		
14	01	30/07/86		
15	01	30/07/86		
16	01	30/07/86		
17	01	30/07/86		
18	01	30/07/86		
19	01	30/07/86		
20	01	30/07/86		
21	01	30/07/86		
22	01	30/07/86		
23	01	30/07/86		
24	01	30/07/86		
25	01	30/07/86		
26	01	30/07/86		
27	01	30/07/86		
28	01	30/07/86		
29	01	30/07/86		
30	01	30/07/86		
31	01	30/07/86		
32	01	30/07/86		
33	01	30/07/86		
34	01	30/07/86		
35	01	30/07/86		
36	01	30/07/86		
37	01	30/07/86		
38	01	30/07/86		
39	01	30/07/86		

PÁGINA	VERSÃO	DATA	REFERÊNCIA DA MODIFICAÇÃO	OBSERVAÇÃO
40	01	30/07/86		
41	01	30/07/86		
42	01	30/07/86		
43	01	30/07/86		
44	01	30/07/86		
45	01	30/07/86		
46	01	30/07/86		
47	01	30/07/86		
48	01	30/07/86		
49	01	30/07/86		
50	01	30/07/86		
51	01	30/07/86		
52	01	30/07/86		
53	01	30/07/86		
54	01	30/07/86		
55	01	30/07/86		
56	01	30/07/86		
57	01	30/07/86		
58	01	30/07/86		
59	01	30/07/86		
60	01	30/07/86		
61	01	30/07/86		
62	01	30/07/86		
63	01	30/07/86		
64	01	30/07/86		
65	01	30/07/86		
66	01	30/07/86		
67	01	30/07/86		
68	01	30/07/86		
A1	01	30/07/86		
A1	01	30/07/86		

CONTENTS

STUDY OF ORBITAL GEOMETRY FOR MISSION ANALYSIS

1 - INTRODUCTION

The purpose of this study is to define the orbital geometry in order to know the behaviour of the mission evolution in terms of the orbital coverage and observation of the satellite. The results published here are not complete but are sufficient at the present state of the mission.

First of all, in the second section are given the true geometry and dispersions of the orbit. These values are used throughout the other sections as nominal but, of course, deviations from these values may occur in further studies.

In the third section, the lifetime study is presented for the initial orbits derived in the preceding section. Several possibilities of solar activity are simulated for effective comparison of the results. In all these studies, a six-month operational lifetime is assumed, and all the possible geometries are shown suitable for the proposed mission.

In the fourth section, a launch window is presented. The studies have been done supposing that the solar flux cannot illuminate the "back side" of the satellite, which is defined as the panel with no solar cells. As the satellite is a spin-stabilized one, a residual magnetic momentum, responsible for precession of the satellite, is also considered in this study. It is observed from the results that one can get a launch window throughout the year but the preference is for a negative residual magnetic momentum.

In the fifth section, a view of the satellite from observing station is presented. This geometrical study was necessary because of the blind angle of the satellite at which the communications are blocked. The occurence of this blind angle is due to the fact that the position of the satellite is fixed in the space and the satellite moves around the Earth. The results obtained here are also used for first three orbits in the case of some ground track stations in the sixth section.

In the sixth section, charts and diagrams about the observation and coverage of the satellite are presented. A main emphasis is given for the first day orbits but the results are general. The first day orbits are considered important for several analyses. In several diagrams the geometry of observation of the main tracking stations relative to the orbit is shown for the purposes of preliminary orbit determination which needs to be done in the initial orbits. The results obtained are very decisive and lead to the conclusion that a good use of the observing geometry of Kourou and Mas Palomas is possible. A third station also is under study because of the proximity of these two stations at the burn-out point. In this respect, a choice is leading to a diametrically opposite station.

2 - ORBITAL GEOMETRY

The choice of the orbital geometry depends on the launcher constraints. The launcher available can deliver a satellite of about 150 kg at 700 km altitude. Combining these data with the mission requirements, it is concluded that a 700 km circular orbit with an inclination of 25° is needed. As the orbit is generated by a spin-stabilized last stage, the dispersions may endanger the circularity of the orbit due to pitch angle error at the injection point (Figure 2.1).

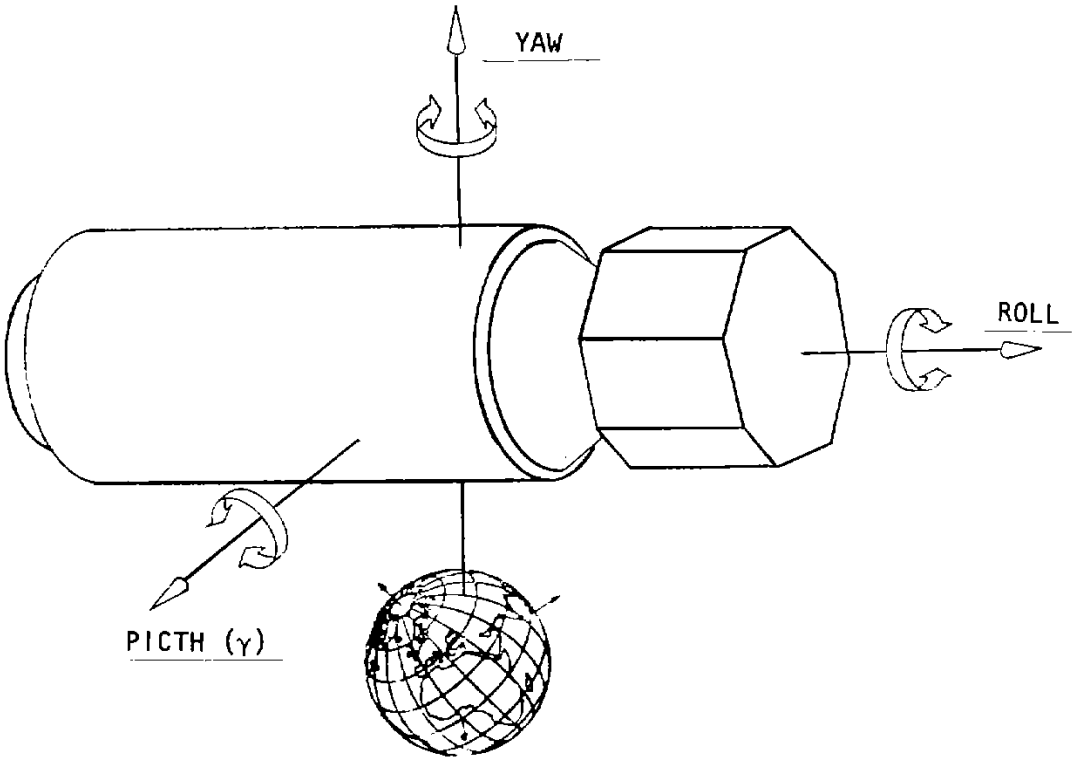

Fig. 2.1 - Angles at the injection point.

The launcher guarantees to produce an orbit with eccentricity not more than 0.042 which puts the perigee at 400 km and apogee at 1000 km. Using these data and using a study of the dispersions and injection geometry (Kondapalli and Medeiros, 1986), the nominal orbits have been determined for mission analysis and simulations. This is done for three distinct cases of injection angle erros:

$\gamma_1 = + 2.429^{o}$,

$\gamma_2 = \quad 0.000^{o}$,

$\gamma_3 = - 2.429^{o}$.

The orbital elements are calculated in such a way that the sidereal time is zero in which case the ascending node angle is a fictitius number. However, the latter can easily be determined by adding the sidereal time at launch epoch.

The argument of perigee is calculated from the burn-out point geometry supposing that no errors in altitude occur except the errors in the pitch angle (Fig. 2.2)

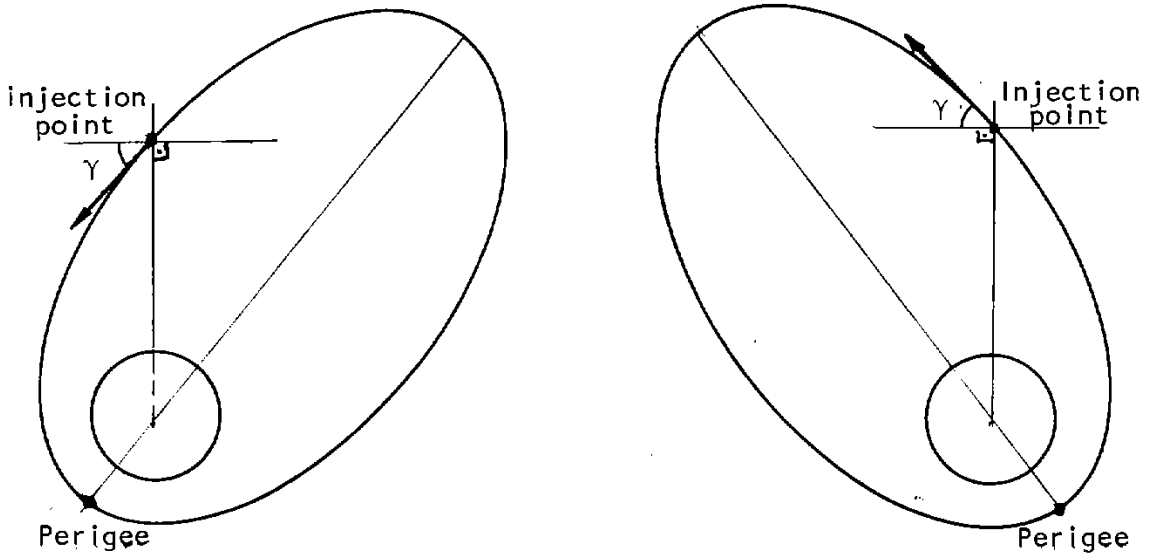

Fig. 2.2 - Perigee geometry for pitch angle erros.

Starting from these considerations, the Keplerian elements, namely, semi-major axis (a), eccentricity (e), inclination (i), longitude of ascending node (Ω), argument of perigee (ω) and mean anomaly (M) are

obtained and listed in the Table 2.1. In this table, true anomaly (f) and eccentric anomaly (E) are also included.

TABLE 2.1

NOMINAL ORBITAL ELEMENTS

	CASE 1	CASE 2	CASE 3	UNITS
γ	+ 2.429	0.000	- 2.429	Degrees
a	7078	7078	7078	Km
e	0.0424	0.0000	0.0424	-
i	25.2500	25.2500	25.2500	Degrees
Ω	- 39.6880	- 39.6880	- 39.6880	Degrees
ω	279.8400	12.2700	104.7000	Degrees
M	87.5729	0.0000	272.4270	Degrees
E	90.0011	0.0000	269.9990	Degrees
f	92.4300	0.0000	267.5700	Degrees

3 - ORBITAL LIFETIME

Keeping in view the importance of having a pre-launch estimate of orbital lifetime of the satellite, an analysis has been made choosing four different initial orbits, namely:

1) A circular orbit with an altitude of 700 km;
2) A circular orbit with an altitude of 750 km;
3) An elliptic orbit with a perigee height of 400 km and an apogee height of 1000 km;
4) An elliptic orbit with a perigee height of 400 km and an apogee height of 1100 km.

The inclination angle used for each one of these orbits is 25°. The orbital lifetimes have been calculated for all the four orbits in three different cases of solar activity, namely:

1) A most realistic case, choosing a fictitious launch date (01/12/1989) and using the solar activity predictions of Marshall Space Flight Center (MSFC) - NASA for that period;

2) A general case, valid for any launch date, supposing a moderate solar activity during the whole lifetime of the satellite;

3) A most eccentric case, included just out of curiosity, supposing a maximum solar activity during the whole lifetime of the satellite.

In all the three cases, the atmospheric model used is that of "COSPAR International Reference Atmosphere (CIRA) - 1972". The results obtained by using a lifetime estimator PRETEV (Kondapalli, 1984) are given in the Table 3.1 and shown in the figures 3.1, 3.2, 3.3 and 3.4.

TABLE 3.1

DECAY OF THE FIRST BRAZILIAN SATELLITE FOR DIFFERENT INITIAL ORBITS IN VARIED CASES OF SOLAR ACTIVITY

INITIAL ORBIT (km)	CASE 1			CASE 2			CASE 3		
	Orbit After 2 years (km)	Orbit After 6 years (km)	Lifetime (Days)	Orbit After 2 years (km)	Orbit After 6 years (km)	lifetime (Days)	Orbit After 2 years (km)	Orbit After 6 years (km)	Lifetime (Days)
700 x 700	678 x 678	617 x 617	-	688 x 688	658 x 658	-	644 x 644	-	1686
750 x 750	730 x 730	710 x 710	-	743 x 743	729 x 729	-	718 x 718	600 x 600	-
400 x 1000	340 x 572	-	828	374 x 729	-	1127	-	-	535
400 x 1100	367 x 749	-	977	383 x 859	-	1385	-	-	654

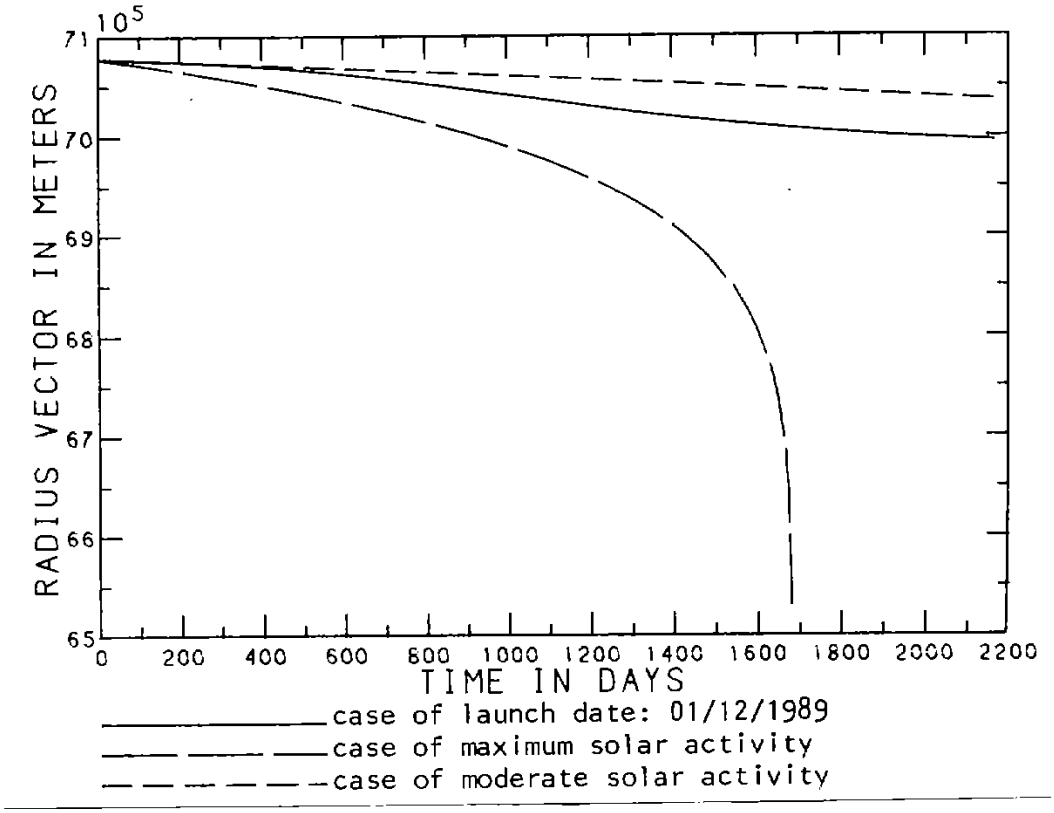

Fig. 3.1 - Decay of the circular orbit with initial altitude of 700 km.

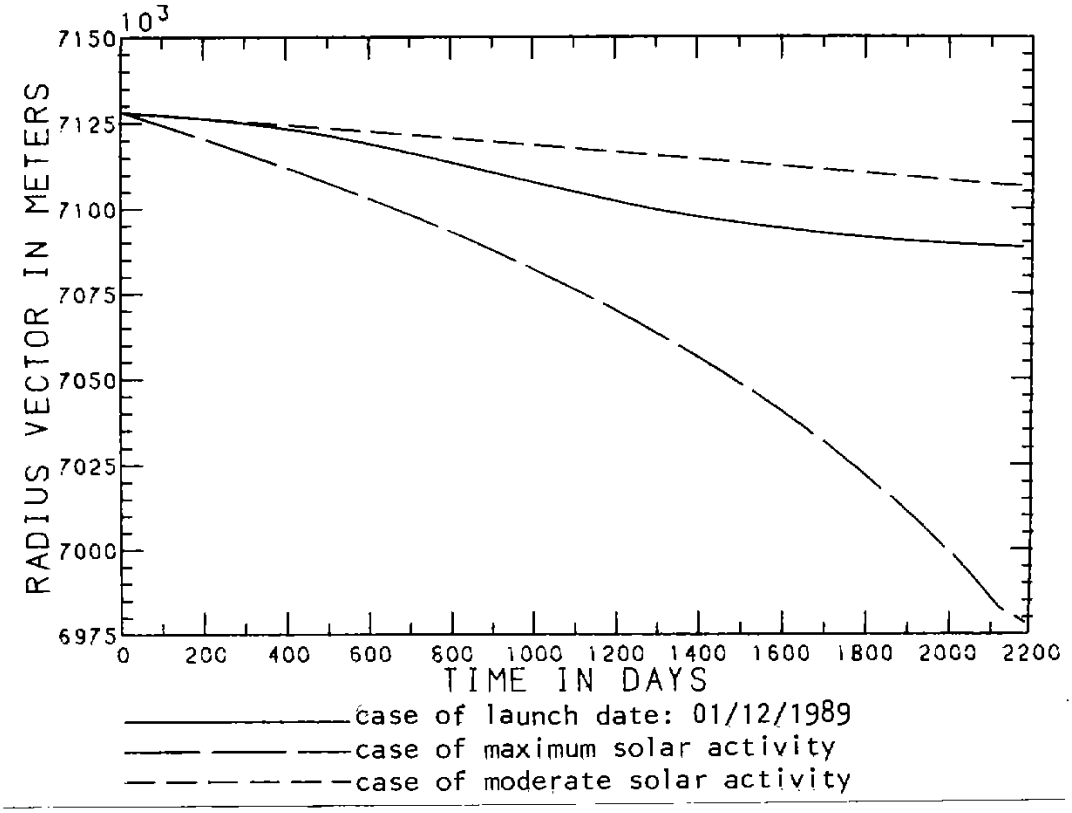

Fig. 3.2 - Decay of the circular orbit with initial altitude of 750 km.

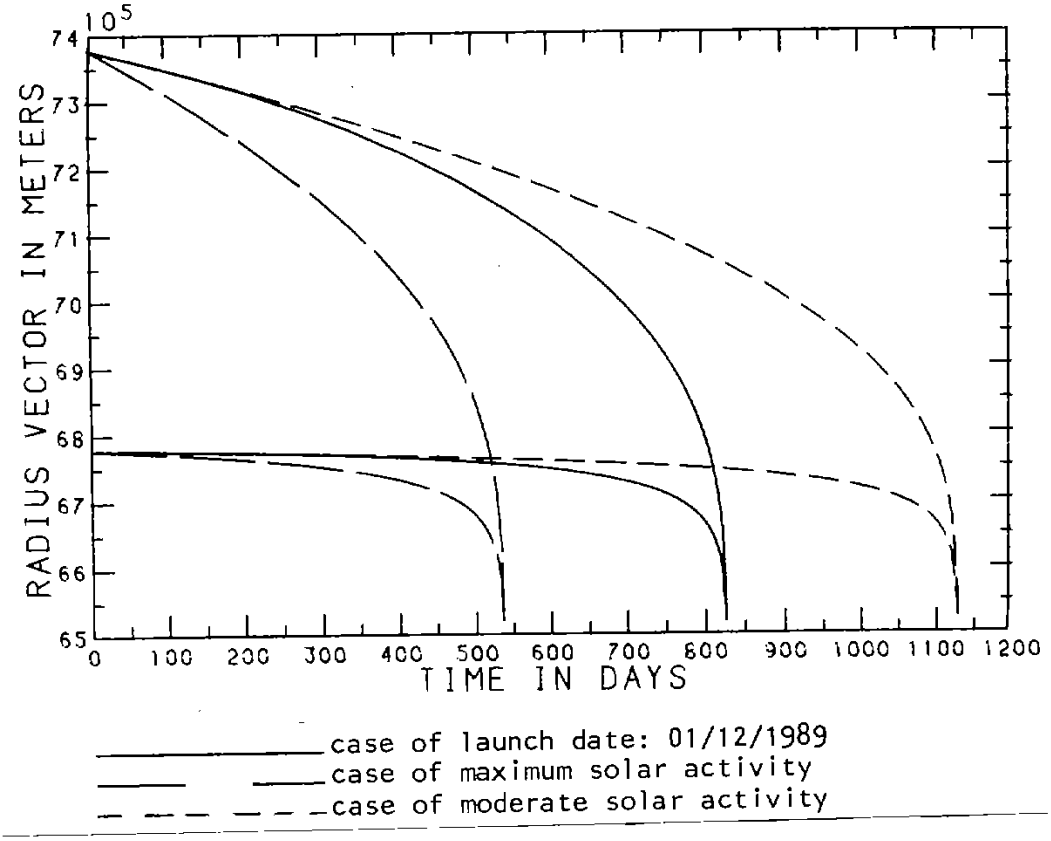

Fig. 3.3 - Decay of the elliptic orbit with an initial perigee of 400 km and an initial apogee of 1000 km.

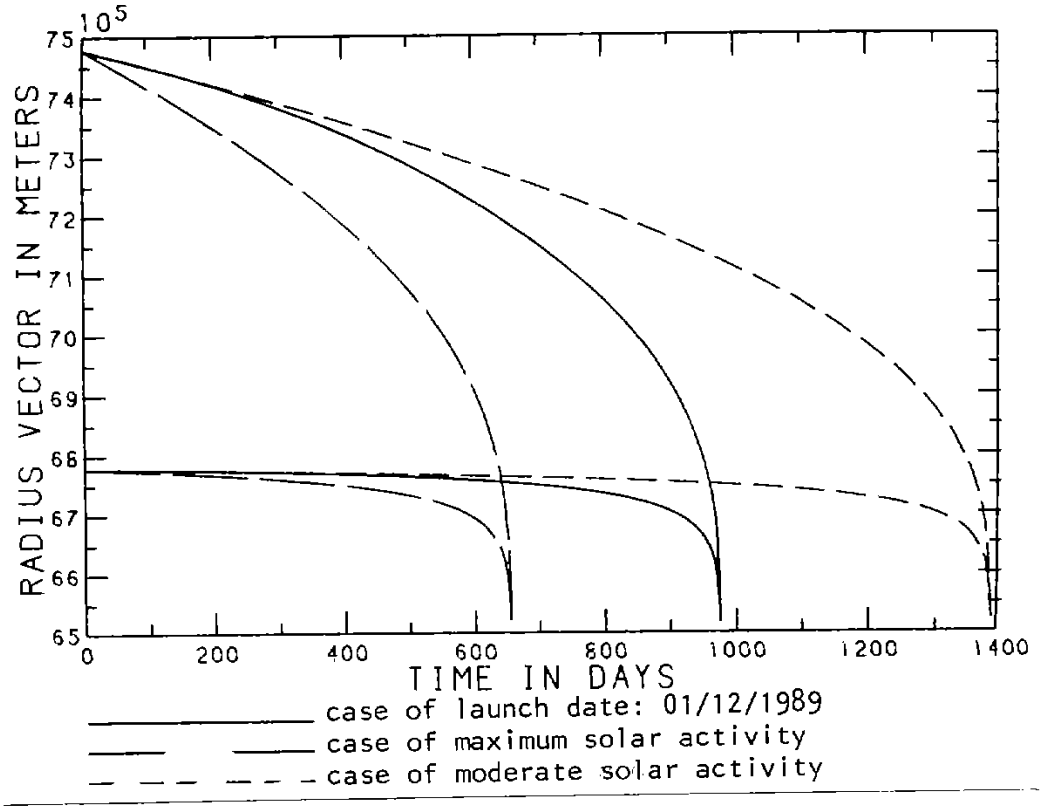

Fig. 3.4 - Decay of the elliptic orbit with an initial perigee of 400 km and an initial apogee of 1100 km.

4 - LAUNCH WINDOW

The main forces that disturb a spin-stabilized satellite are the eddy currents that decrease the rotation velocity, and the magnetic torque that precesses the rotation axis. This torque is due to the electric currents in the payload equipments that create a magnetic dipole on the satellite. This dipole interacts with the Earth's magnetic field causing a torque.

The spin decay velocity due to the eddy currents is exponential as can be seen in the computer simulation shown in the Figure 4.1. The Figure 4.2 shows the right ascention and the declination components of the spin axis, in the inertial frame for a residual magnetic moment of - 0.63 Am^2. The total period of simulation is 6 months or 180 days. In obtaining the results it is supposed that there was a nutation damper on-board.

The Figure 4.2 also shows that the spin axis motion is more predominant in the right ascention (about 95^o) than in the declination (pulsating with a 14^o of maximum amplitude), in 180 days. This suggests that the motion of the spin axis can be described simply as a pure right ascention variation, with a mean declination of 27^o approximately. Then the spin drift is given by:

$$\dot{\alpha} = \frac{T_m}{I\omega} \quad , \tag{4.1}$$

where T_m is the mean magnetic torque, I is the moment of inertia about the spin axis and ω is the angular velocity of the satellite. The spin decay can be adjusted by an analytical expression in the form:

$$\omega = a\, e^{-bt} \quad , \tag{4.2}$$

where a and b are obtained by fitting the expression to the curve in the Figure 4.2:

a = 18.8 radians/sec.,
b = 0.19035/month.

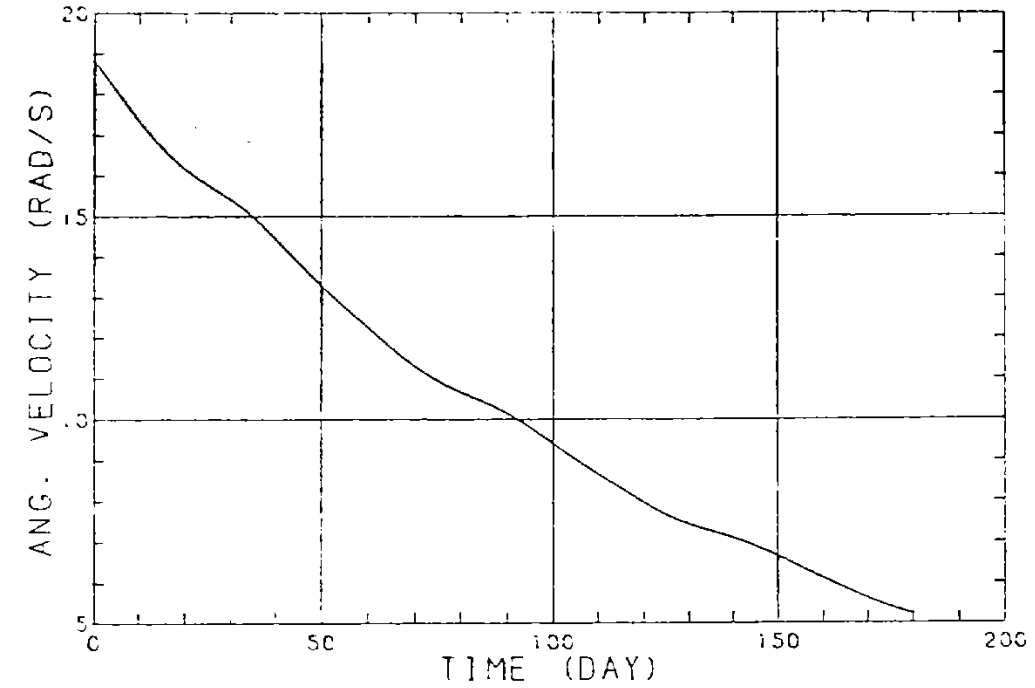

Fig. 4.1 - Spin decay of the satellite

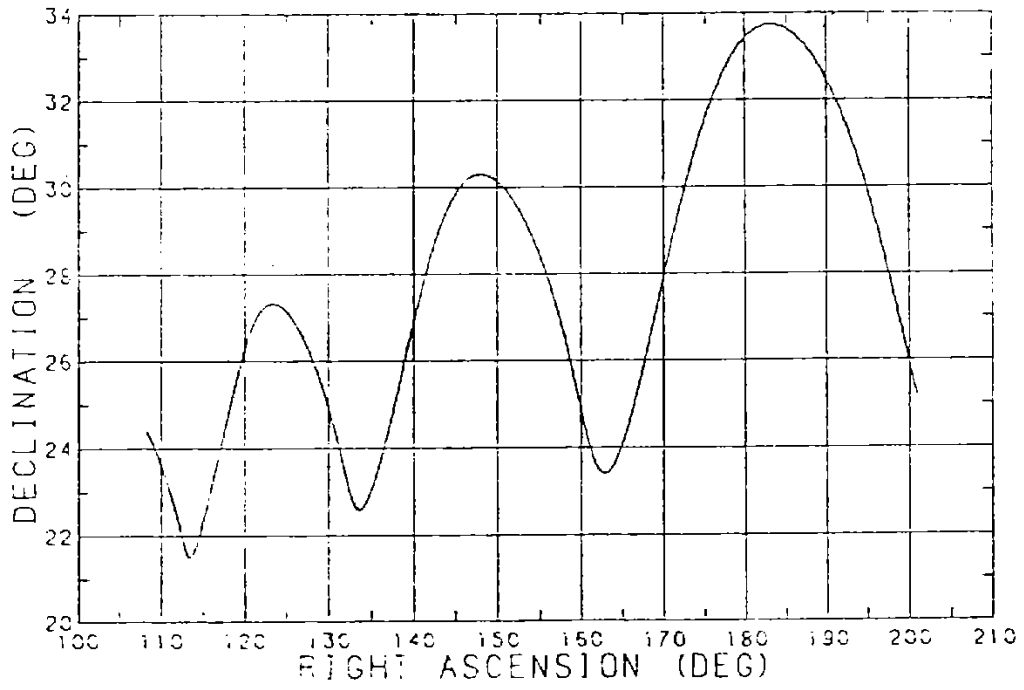

Fig. 4.2 - Variation of right ascention and declination of the spin axis.

The equation 4.1 can now be integrated from zero to t, resulting for the right ascention motion:

$$\alpha = \alpha_0 + \frac{T_m}{Iab} (e^{bt} - 1) , \qquad (4.3)$$

where α_0 is the right ascention of the spin axis at the orbit injection point.

Remembering that the magnetic torque is proportional to the residual magnetic moment intensity M, the equation 4.3 can be modified into the form:

$$\alpha = \alpha_0 + KM (e^{bt} - 1) , \qquad (4.4)$$

where the constant K is obtained in the same way as that of the constants a and b, resulting:

$$K = 55.4^{o}/Am^2 .$$

Note that the angle α_0 is the variable that will give the hour of launching as a function of the magnetic residual moment and the epoch year.

The spin axis direction, in the inertial system can be given by:

$$\hat{r} = \cos \alpha \cos \delta \hat{i} + \sin \alpha \cos \delta \hat{j} + \sin \delta \hat{k}, \qquad (4.5)$$

where δ is the spin axis mean declination which is equal to 27^{o}.

The major force that influences the lifetime of the satellite is the temperatures of the equipments on-board. In fact, if the lower panel (a thermal radiator) becomes illuminated by the sun, the temperatures of some equipments will fall out of range. Consequently, the condition that the angle between the sun and the spin-axis η

should be smaller than 90° must be satisfied during the estimated useful lifetime i.e. 6 months. This imposition keeps the sun's direction over the upper hemisphere of the satellite, as can be seen in the Figure 4.3.

The sun's direction is given by:

$$\hat{s} = \cos \alpha_{\odot} \cos \delta_{\odot} \hat{i} + \sin \alpha_{\odot} \cos \delta_{\odot} \hat{j} + \sin \delta_{\odot} \hat{k}, \tag{4.6}$$

where $\alpha_{\odot}$ and $\delta_{\odot}$ are the sun's right ascention and declination, respectively.

During the useful lifetime of the satellite, the sun's movement in the celestial sphere can be obtained by series expansion of the right ascention, where the 2nd order terms in the eccentricity of the Earth orbit are neglected:

$$\alpha_{\odot} = \omega_{\odot} + M_{\odot} + 2e_{\odot} \sin M_{\odot} - \tan^2 \frac{\varepsilon}{2} \sin 2(\omega_{\odot} + M_{\odot}) , \tag{4.7}$$

and

$$\sin \delta_{\odot} = \sin \varepsilon \sin \alpha_{\odot} . \tag{4.8}$$

The angle $\omega_{\odot}$ is the perihelion argument ($\omega_{\odot} \cong 282.6^{\circ}$), $e_{\odot}$ is the eccentricity of the Earth orbit ($e_{\odot} = 0.0167$) and ε is the inclination of the ecliptic plane ($\varepsilon \cong 23.4^{\circ}$). The Earth's mean anomaly, $M_{\odot}$ is given by:

$$M_{\odot} = n_{\odot} (t + t_1 - t_0) , \tag{4.9}$$

where $n_{\odot}$ is the mean motion of the Earth ($n_{\odot} \cong 0.9856^{\circ}$/day), t_1 is the date of launch in days of the year and t_0 is the date of the Earth's passage through the perihelion ($t_0 \cong 4.5$ days).

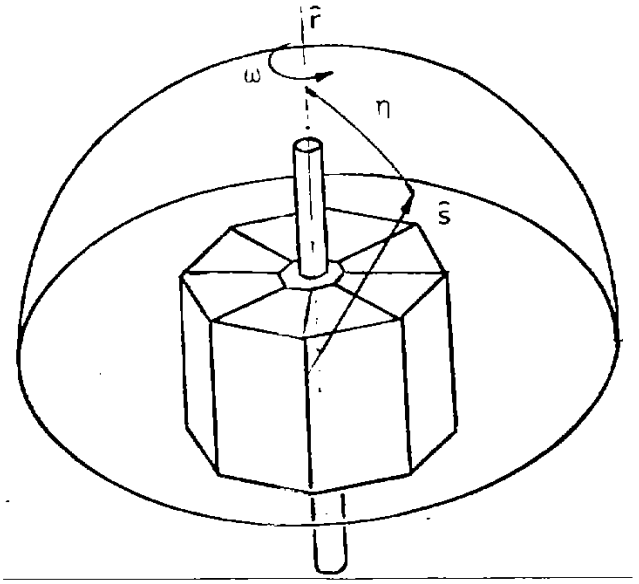

Fig. 4.3 - Angle η between the sun's direction and the spin axis.

The angle η between the sun's direction and the spin axis can now be written as:

$$\cos \eta = \hat{r}.\hat{s} = \cos \delta \cos \delta_{\odot} \cos(\alpha - \alpha_{\odot}) + \sin \delta \sin \delta_{\odot} . \qquad (4.10)$$

By imposing the launch window criterion that this angle must be smaller than 90°, one gets:

$$\cos (\alpha - \alpha_{\odot}) \geq - \tan \delta \tan \delta_{\odot} \qquad (4.11)$$

which results, on substituting the Equation (4.4):

$$\alpha_{o\,min} \leq \alpha_{o} \leq \alpha_{o\,max} \qquad (4.12)$$

where $\alpha_{o\,min}$ and $\alpha_{o\,max}$ are:

$$\alpha_{o\,min} = \alpha_{\odot} - KM\,(e^{bt} - 1) - \arccos\,(- \tan \delta \tan \delta_{\odot}) \qquad (4.13)$$

and

$$\alpha_{o\,max} = \alpha_{\odot} - KM\,(e^{bt} - 1) + \arccos\,(- \tan \delta \tan \delta_{\odot}). \qquad (4.14)$$

Note that both $\alpha_{o\,min}$ and $\alpha_{o\,max}$ are time-dependent variables. Then the condition (4.12) will be satisfied only if the maximum value of $\alpha_{o\,min}$ and the minimum value of $\alpha_{o\,max}$ are taken along the lifetime duration, or 180 days. However, the equations for $\alpha_{o\,min}$ and $\alpha_{o\,max}$ are nonlinear and so a numerical solution is developed varying the time t in one day intervals and taking the $\alpha_{o\,min}$ and $\alpha_{o\,max}$ for all possible days of launching during the year, t_1.

The longitude of the ascending node, Ω, is correlated with the angle α_o through the relation obtained from the orbital geometry:

$$\tan \Omega = \frac{-\sin \alpha_o \sin \omega - \cos \alpha_o \cos i \cos \omega}{-\cos \alpha_o \sin \omega + \sin \alpha_o \cos i \cos \omega} \qquad (4.15)$$

where the minimum and maximum values for Ω are corresponding to the minimum and maximum values for α_o. The i and ω represents the orbital inclination and argument of the injection point respectively ($i = 25^o$ and $\omega = 9.2^o$). In the relation (4.15) it is supposed that the rotation axis , at the injection point, is lying in the orbital plane and perpendicular to the local vertical.

On the other hand, the limits of the launch hour can be obtained as functions of the minimum and maximum values of the longitude of ascending node as:

$$t = \frac{\Omega + \text{arc} \tan(\cos i \tan \omega) - \lambda_i - \theta_{g0}}{\dot{\theta}} . \qquad (4.16)$$

This relation is obtained by geometry, as can be seen in the Figure 4.4, where λ_i is the longitude of the injection point ($\lambda_i \cong 326^o$) and $\dot{\theta}$ is the rotation velocity of the Earth ($\dot{\theta} \cong 15.04^o$/hour) relative to inertial system. θ_{g0} is the Greenwich sideraal time at 0:00 hours of the launching day, and is given by:

$$\theta_{g0} = 99.6909833^o + 36000.7689^o . T + 0.00038708 . T^2 .$$

Here T is a function of the number of days between January, 1st and the launching day, d, which for the year of 1989 is:

$$T = (32507 + d)/36525 \ . \qquad (4.17)$$

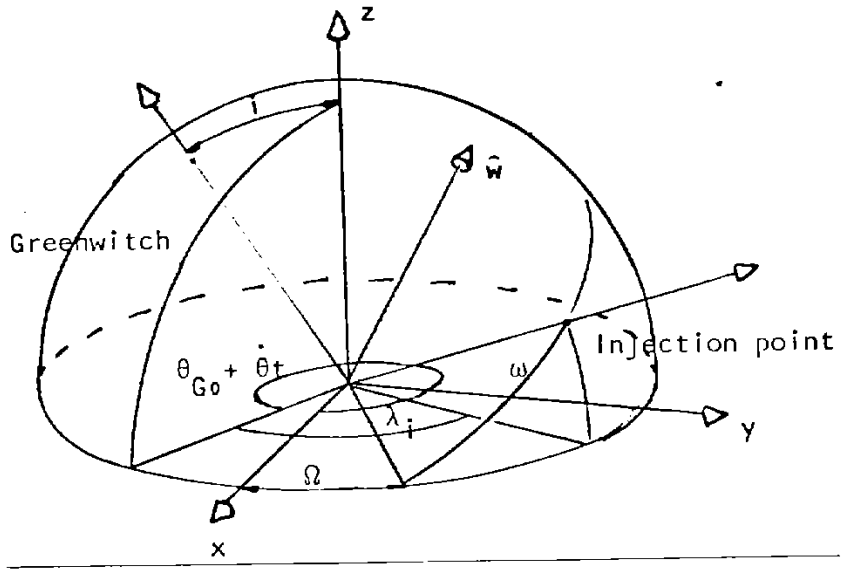

Fig. 4.4 - Definition of various orbital angles

The two values of the launching hour, obtained using the Ω_{min} and Ω_{max} values in the relation (4.16) are plotted in the Figure 4.5, where the residual magnetic moment used is equal to - 0.5 Am^2. The launch window indicates the possible launching hours in a day for a given epoch year. Note that there are even a four-hour windows (around 9:00 hours, Brazilian local time) for all days in the year.

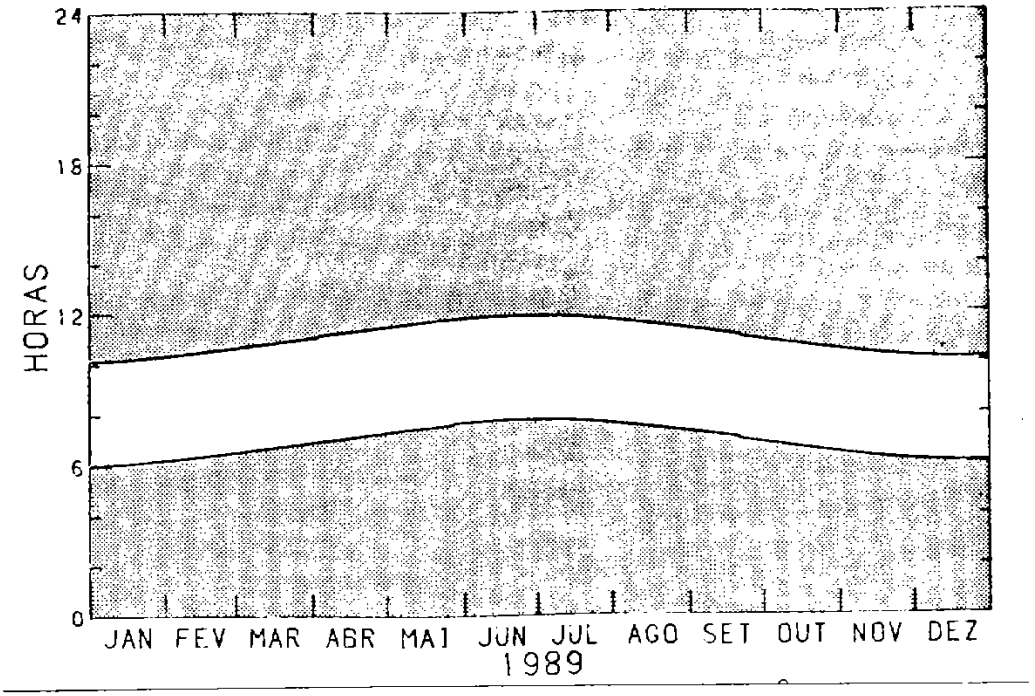

Fig. 4.5 - Launch window for a residual magnetic moment of $-0.5\ Am^2$.

The figures 4.6 and 4.7 show the same window for residual magnetic moments of $-1.52\ Am^2$ and $-2.5\ Am^2$, respectively. The window shown in the Figure 4.6 is bigger than the others, because the mean motion in right ascention of the spin axis is near to the mean motion of the sun's right ascention (0.98^o per day). In other words, the spin axis follows the sun's movement and thus it is possible to launch the satellite over a period of almost 12 hours in a day.

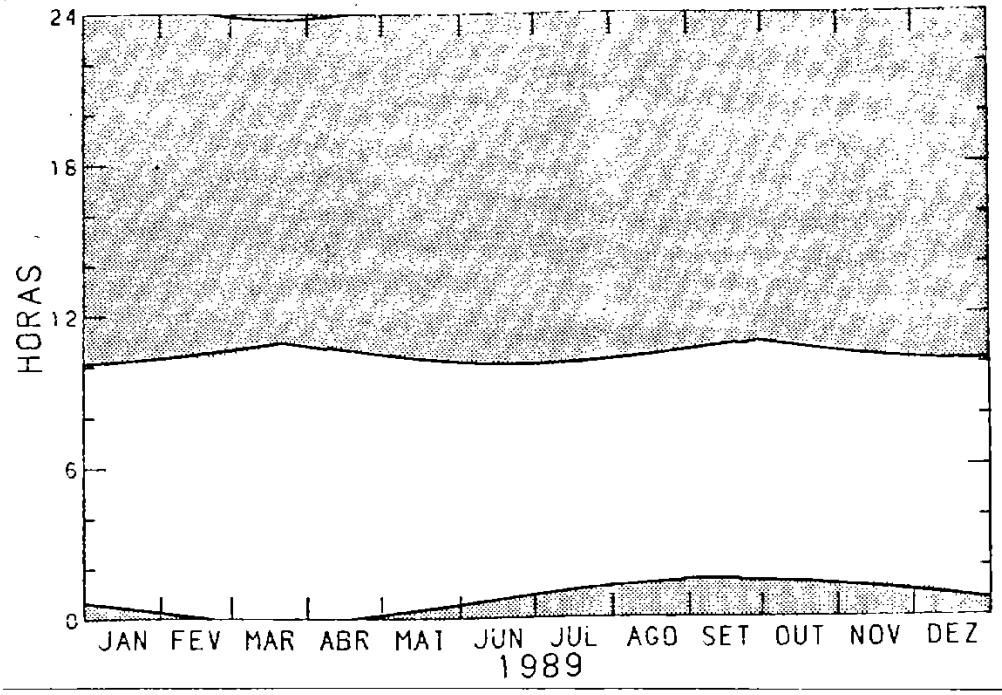

Fig. 4.6 - Launch window for a residual magnetic moment of $-1.52\ Am^2$.

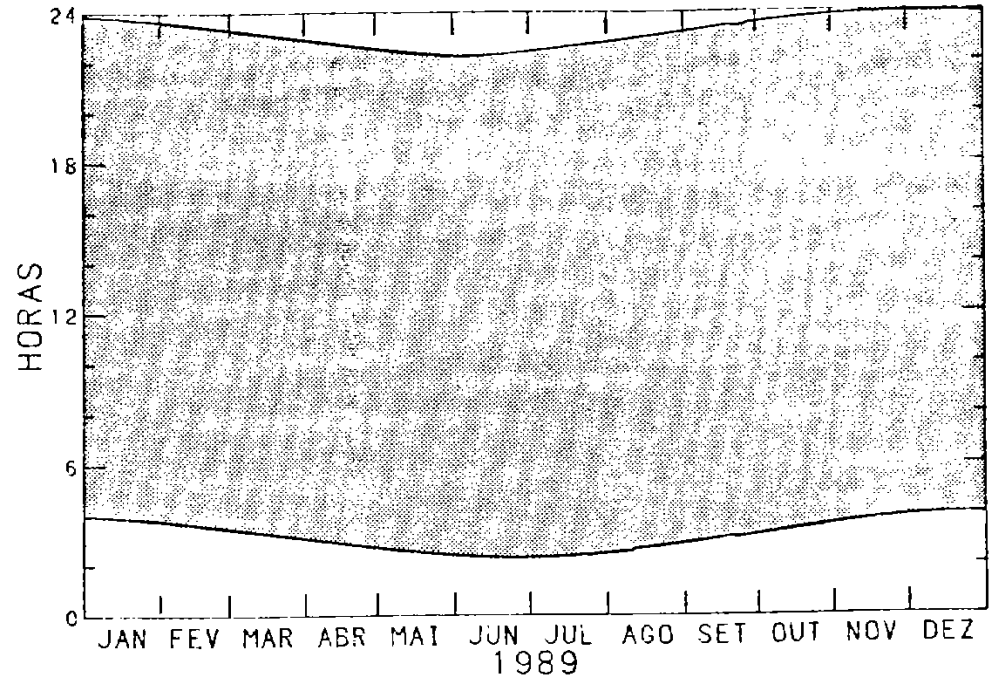

Fig. 4.7 - Launch window for a residual magnetic moment of $-2.5\ Am^2$.

5 - OBSERVING STATIONS' VIEW OF THE SATELLITE

For telemetry, telecommand and tracking purposes, one needs to know how the satellite is being seen by the observing stations. Diagrams depicting the view of various observing stations are helpful in application problems too. To draw these diagrams the observing station chosen, at first, is Cuiabá-Brazil whose coordinates are given by:

. Longitude, λ = - 56.1 E

. Latitude, ϕ = - 15.53°

. Altitude, h = 277 m.

The Keplerian set chosen for initial orbit is:

. Semi-major axis, a = 7078151 m

. Eccentricity, e = 0

. Inclinação, i = 25°

. Longitude of ascending node, Ω = 0°

. Argument of perigee, ω = 0°

. Mean anomaly, M = 0°

Based on the preliminary launch data provided extra-officially by IAE, the launch conditions used here are:

. Latitude of the injection point = 5.202°

. Longitude of the injection point = -28.558° E

. Altitude of the injection point = 700 km

. Launch azimuth = 65.231°

. Total velocity at the injection point = 7504.306 m/sec.

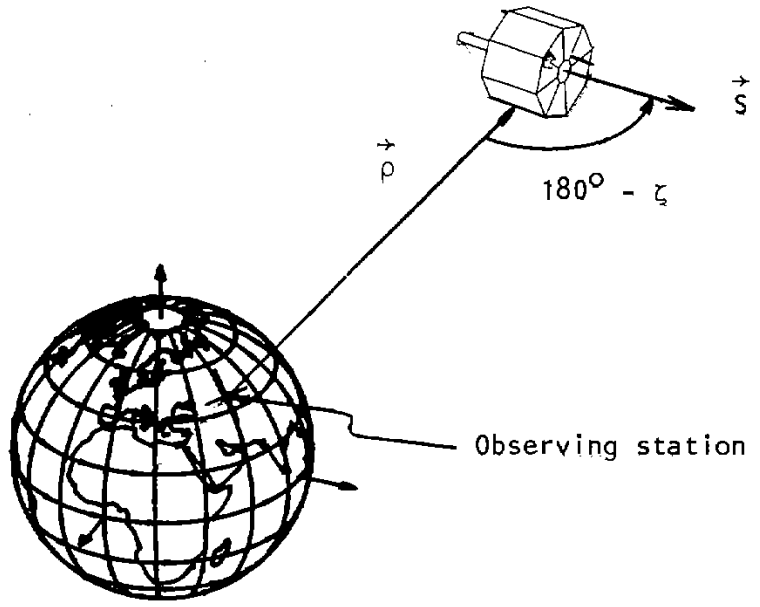

Fig. 5.1 - Definition of the angle ζ.

Since the launch data provided are not final, the results obtained here also should be considered as preliminary. More accurate results can be obtained once the final launch data are available.

Now, since the satellite is a spin-stabilized one, in observation point of view, the main thing to be considered is the angle ζ defined in Figure 5.1. This is an angle between the station-satellite vector $\vec{\rho}$ and the spin-axis vector $\vec{S}$ of the satellite. The direction of the spin-axis is fixed in the space, and due to this fact the angle ζ, defined when satellite is in the visibility circle, varies continuously. Taking Cuiabá as a tracking station, the variation of ζ has been studied in various orbits during a period of one day.

The angle ζ is also affected by precession of the orbit in which case the spin-axis leaves the orbital plane as shown in figure 5.2.

To simulate the effect of the orbital precesion on the angle ζ, its variation has been calculated for various values of Ω, starting from 0^{o}, with increments of 45^{o} each time.

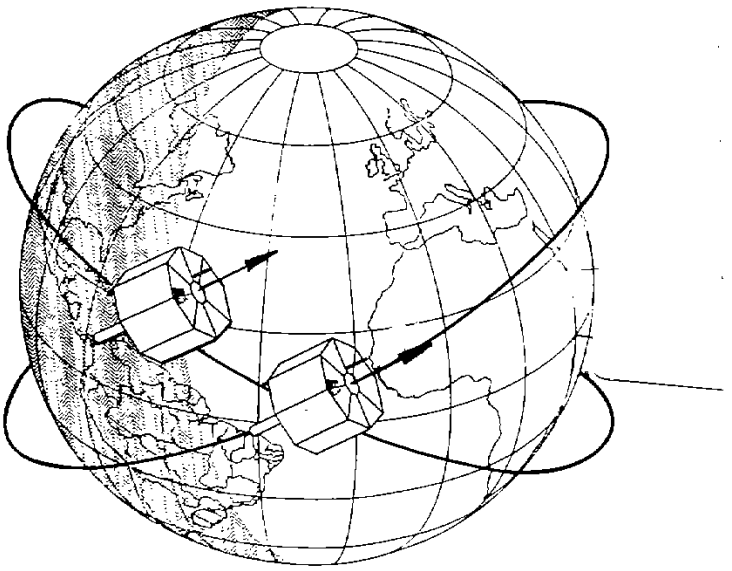

Fig. 5.2 - Effect of orbital precession on the spin-axis.

The combined results obtained by using the computer programs of Medeiros (1983) are given in figures 5.3 through 5.11. The 8 curves given in the top part of figure 5.3 represent the variation of ζ in the first orbits of different days obtained with 8 different values of Ω. In the same way, the variation of ζ in second through ninth orbit of different days obtained with 8 different values of Ω are given in figures 5.4 through 5.11 respectively. The continuous line in the top part of all the figures represent the angle of 90 degrees which corresponds to the blind angle of the satellite at which the satellite loses contact with the tracking station. The various dotted lines in the figures represent various values of Ω as follows:

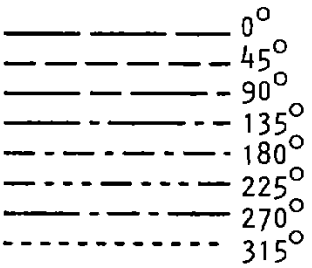

The bottom part of each figure gives variation of elevation angle of the satellite at the station during the time of contact. This makes one possible to see the better observing positions of the satellite.

Besides the contact between the satellite and the observing station, for application purposes it is also necessary to have an idea of simultaneous contact of station-satellite and satellite-data collection platform. In this connection, two stations-Chuí of extreme south and Oiapoque of extreme north - have been chosen for the study. Same as in the case of Cuiabá, the top parts of the figures 5.12 through 5.17 give the variation of ζ at Chuí in the orbits in which the simultaneous contact of Cuiabá-satellite-Chuí is possible. The same for Oiapoque is given in the top parts of the figures 5.18 through 5.25.

The bottom parts of the figures 5.12 through 5.17 give the variation of elevation angles of the satellite at Cuiabá as well as at Chuí during the intersection of time of contact. The curves are defined as follows:

_____ Cuiabá

__ __ Chuí

The same for Oiapoque is given in the bottom parts of the figures 5.18 through 5.25, with the curves defined as follows:

_____ Cuiabá

__ __ Oiapoque

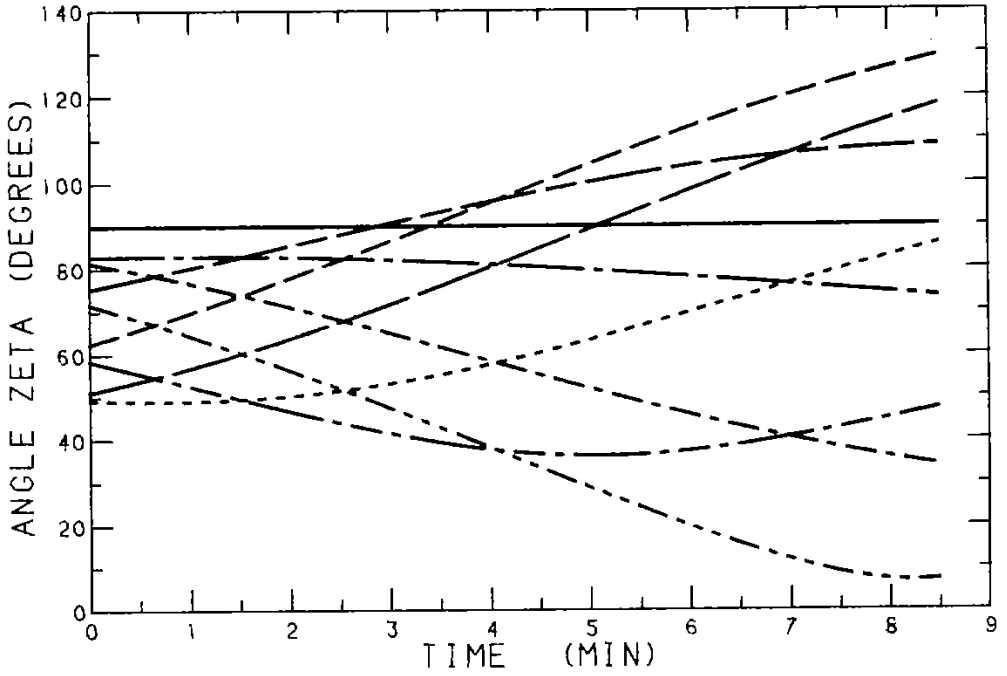

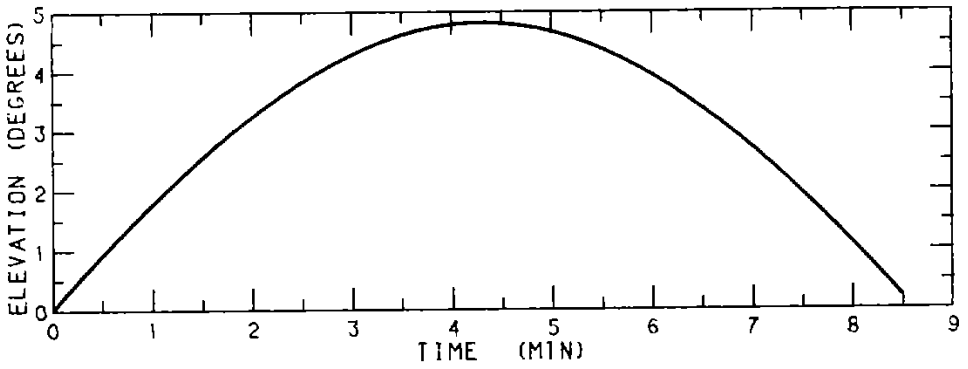

Fig. 5.3 - View of the satellite in the first orbit

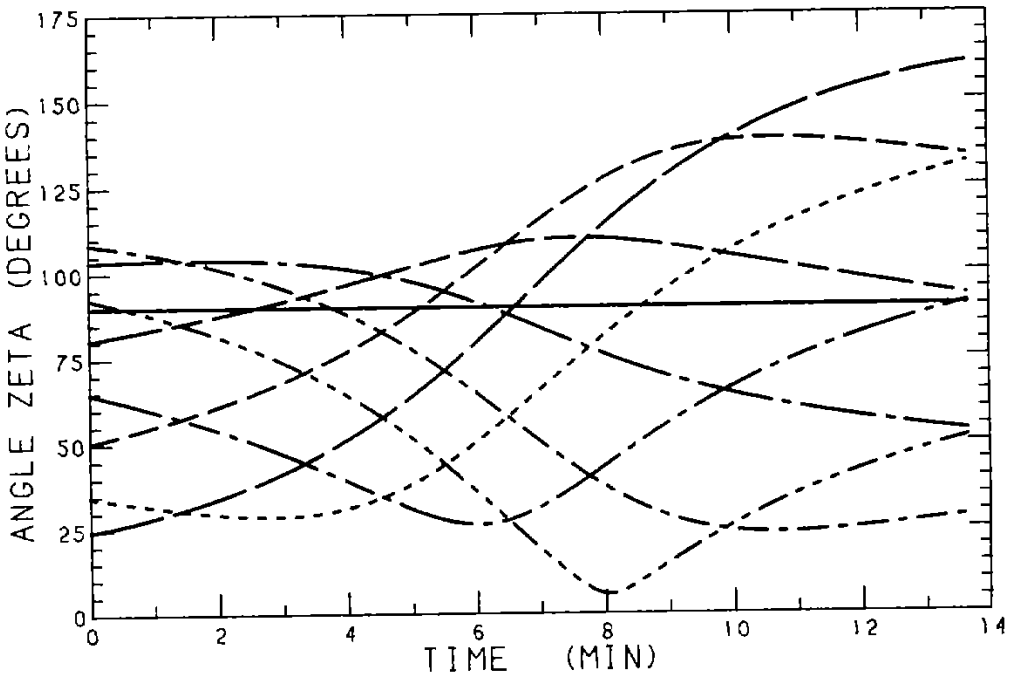

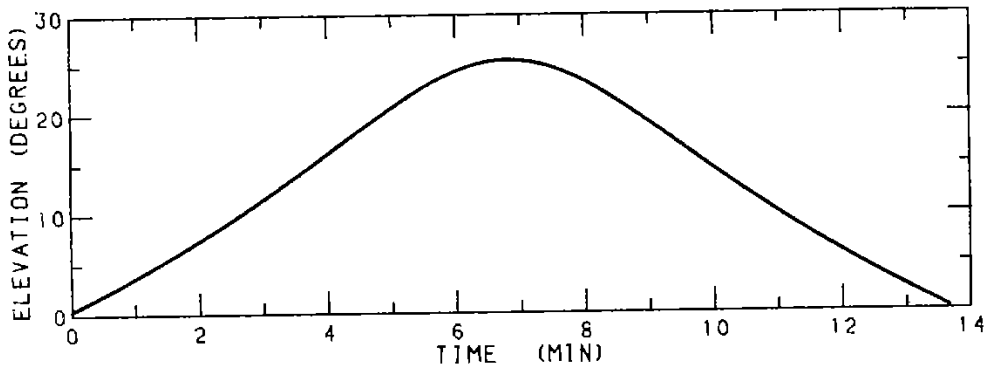

Fig. 5.4 - View of the satellite in the second orbit.

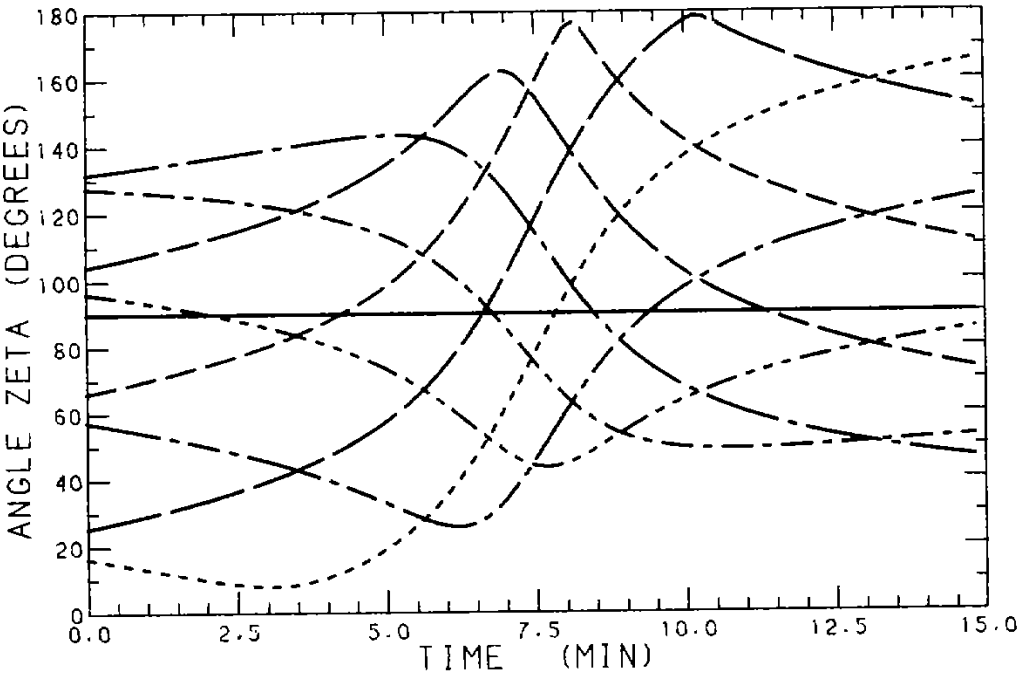

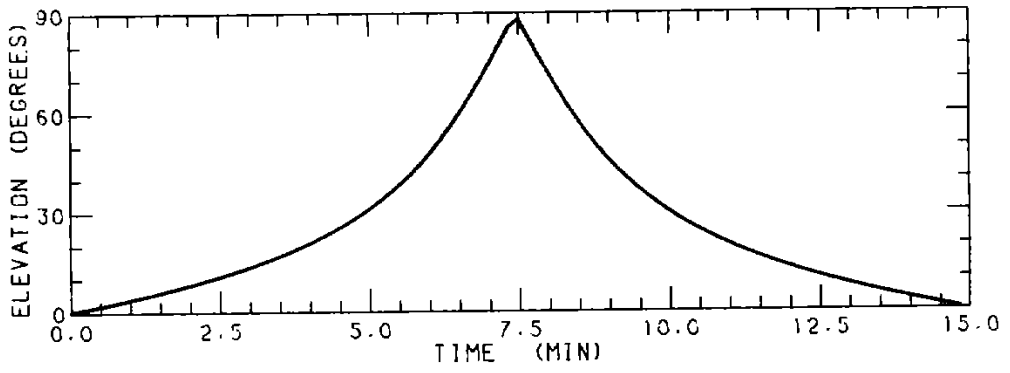

Fig, 5.5 - View of the satellite in the third orbit.

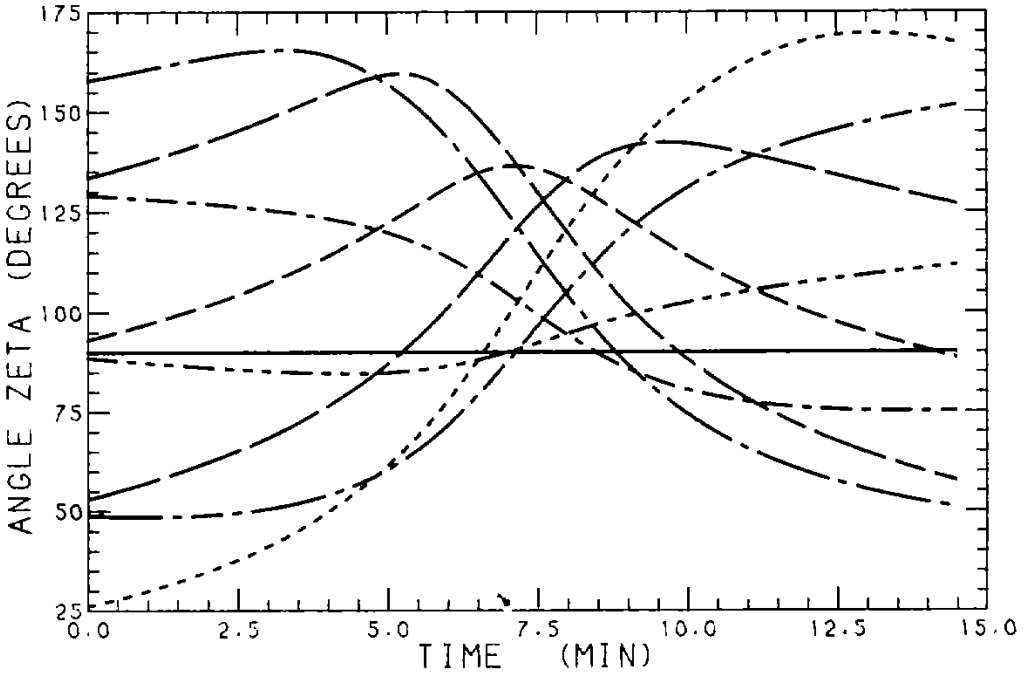

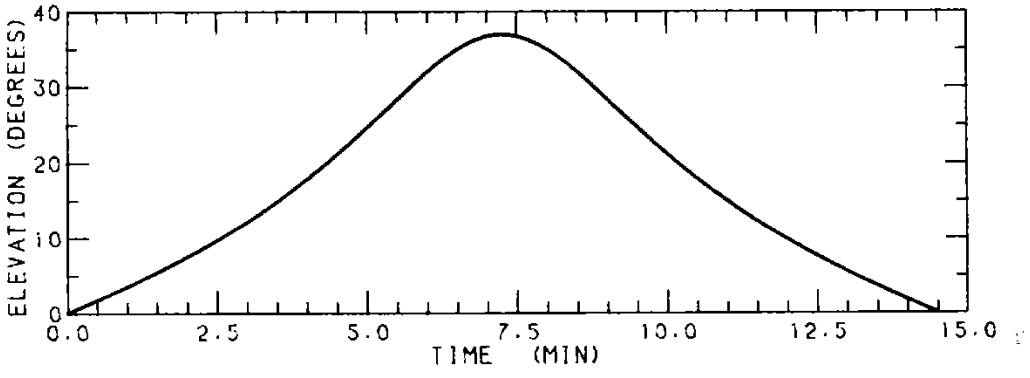

Fig. 5.6 - View of the satellite in the fourth orbit.

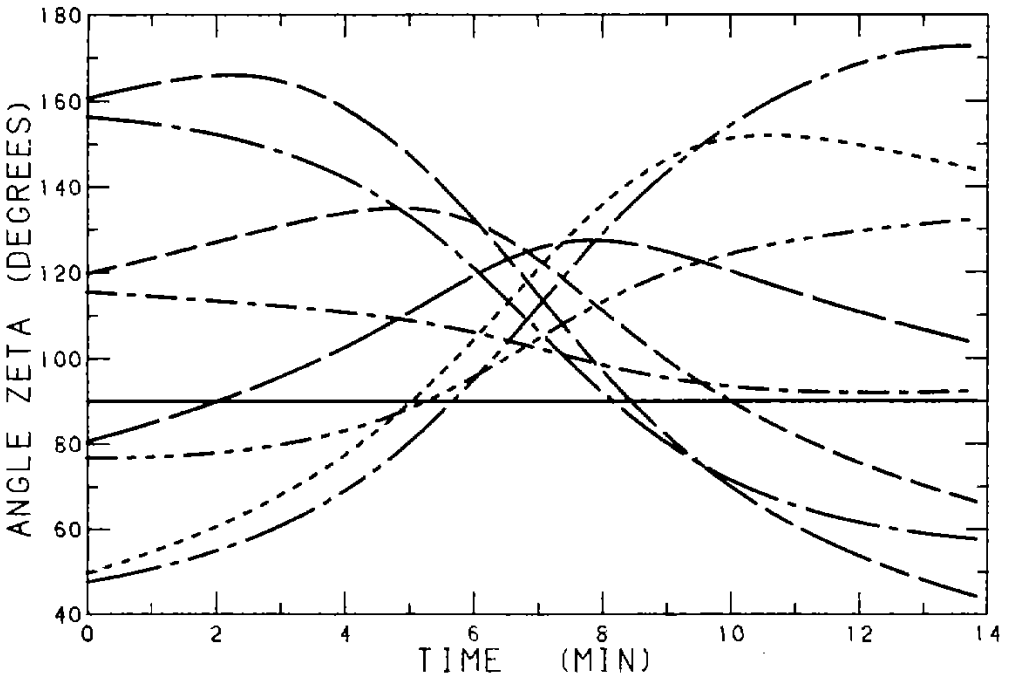

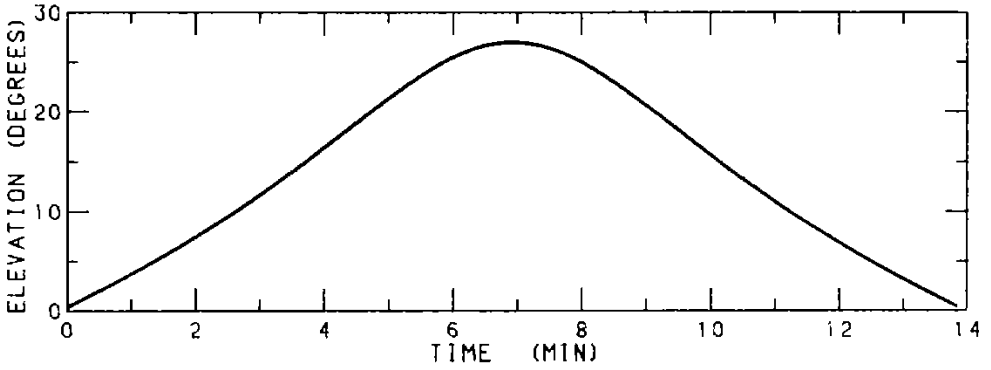

Fig. 5.7 - View of the satellite in the fifth orbit.

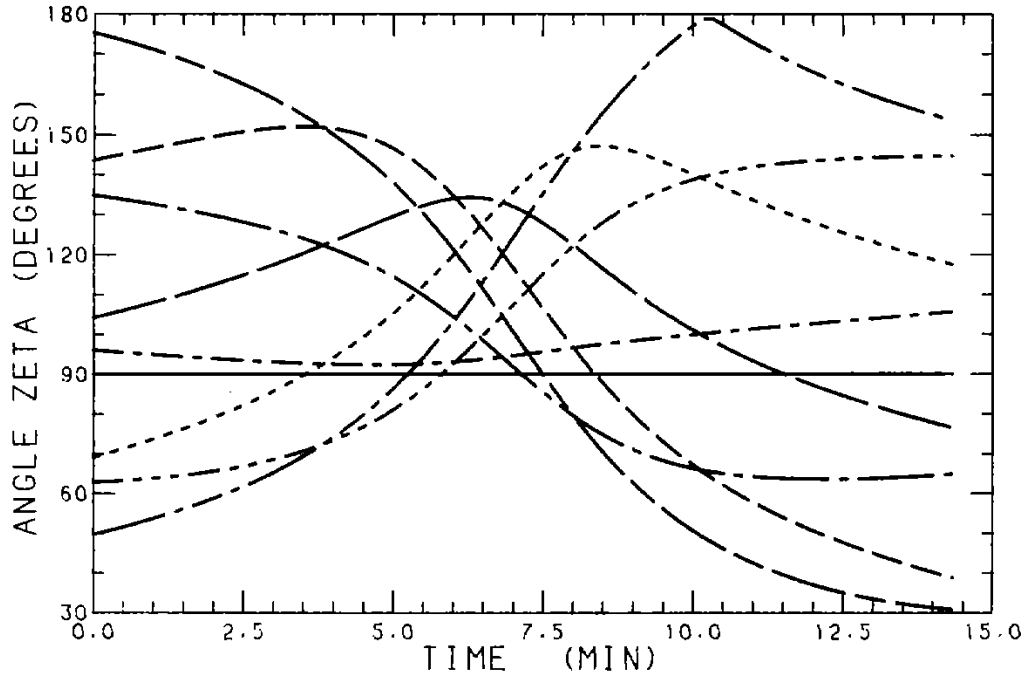

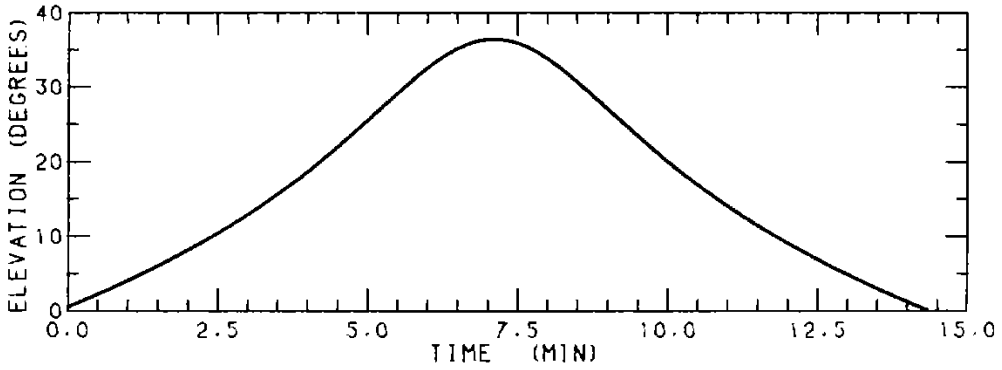

Fig. 5.8 - View of the satellite in the sixth orbit.

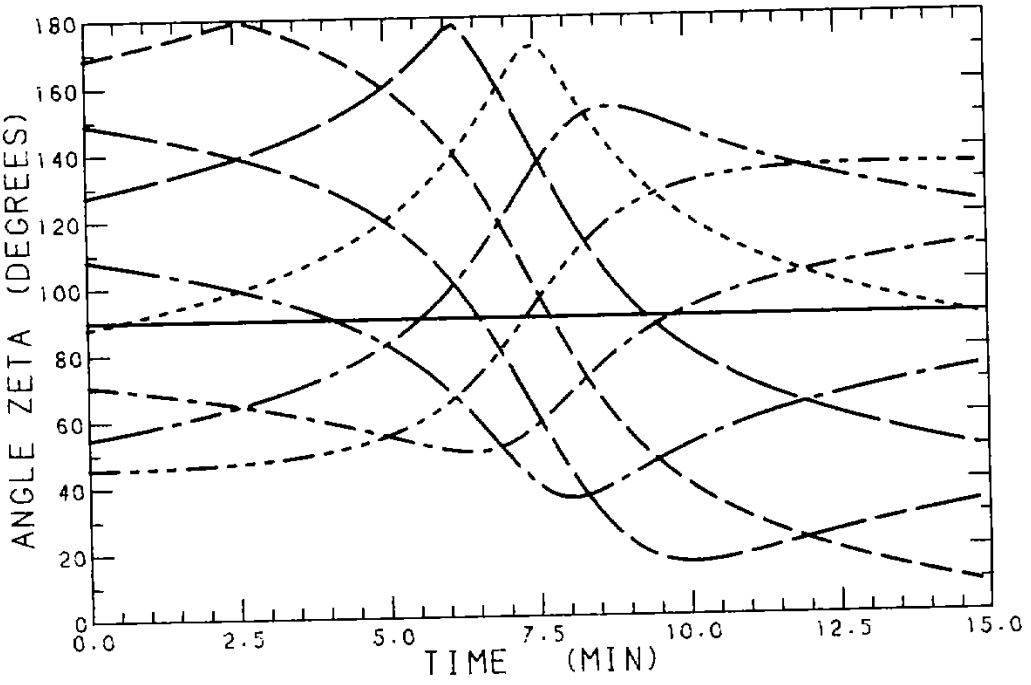

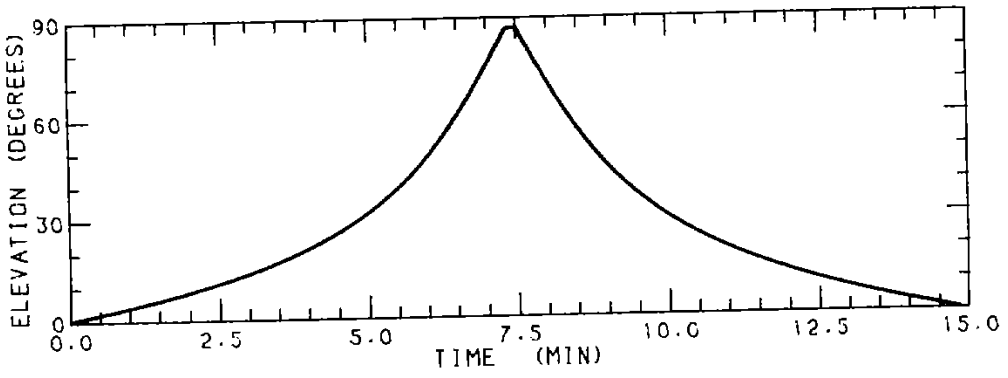

Fig. 5.9 - View of the satellite in the seventh orbit.

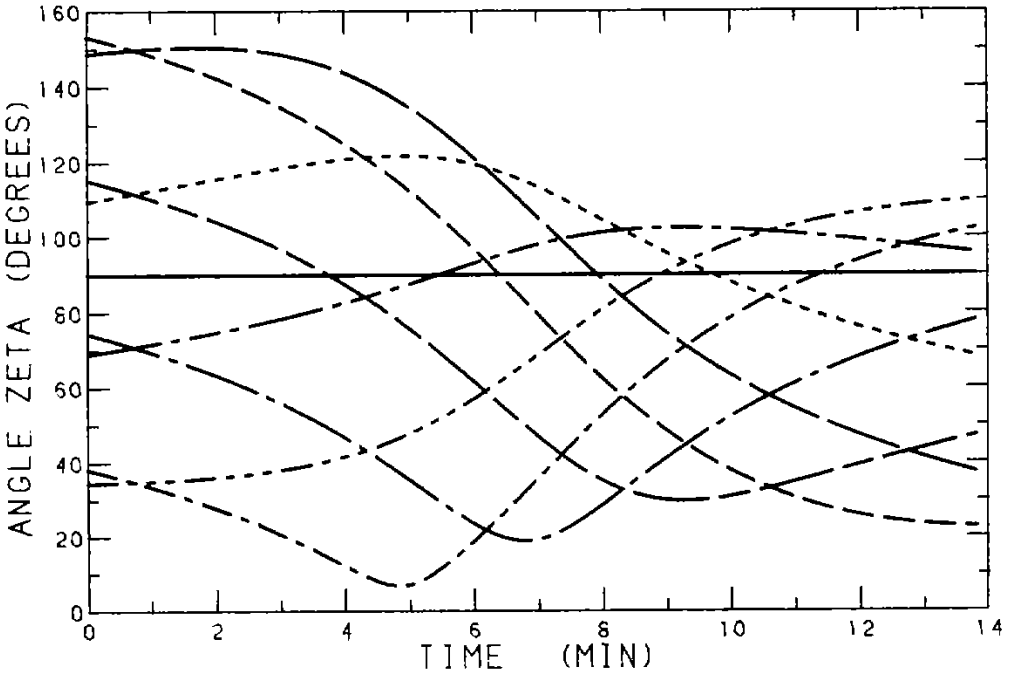

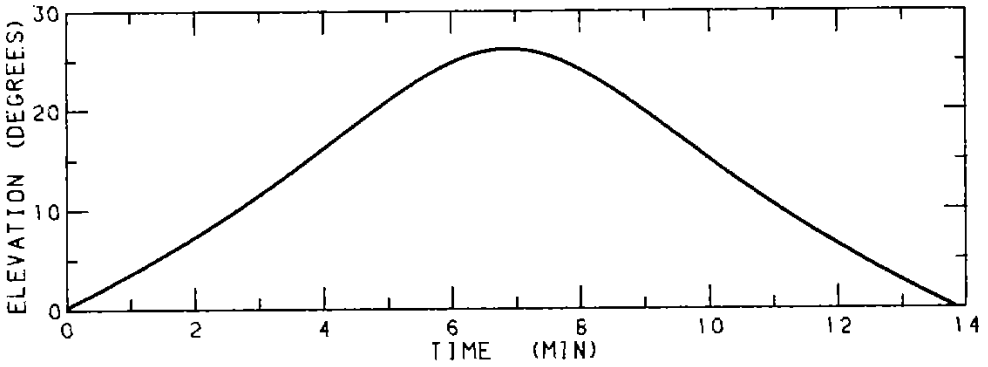

Fig. 5.10 - View of the satellite in the eighth orbit.

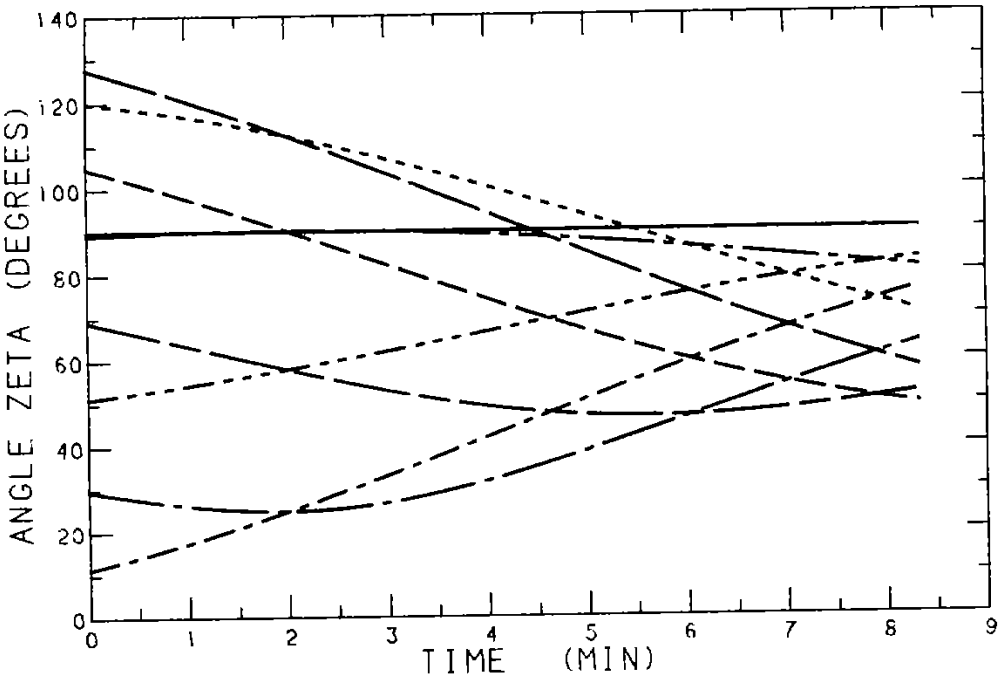

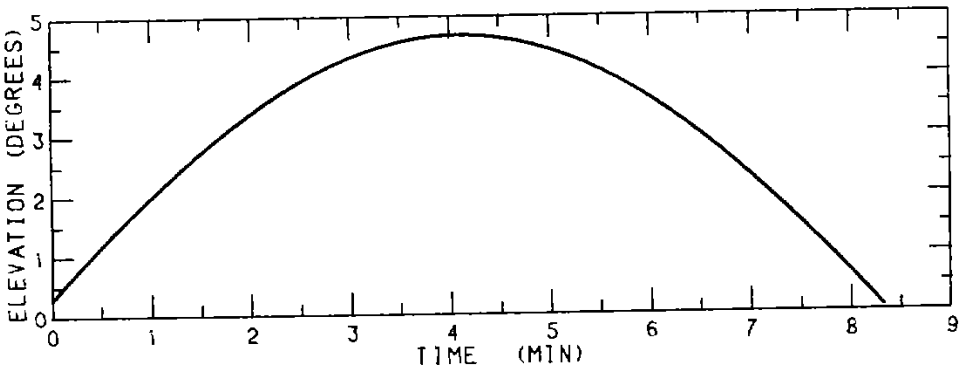

Fig. 5.11 - View of the satellite in the ninth orbit.

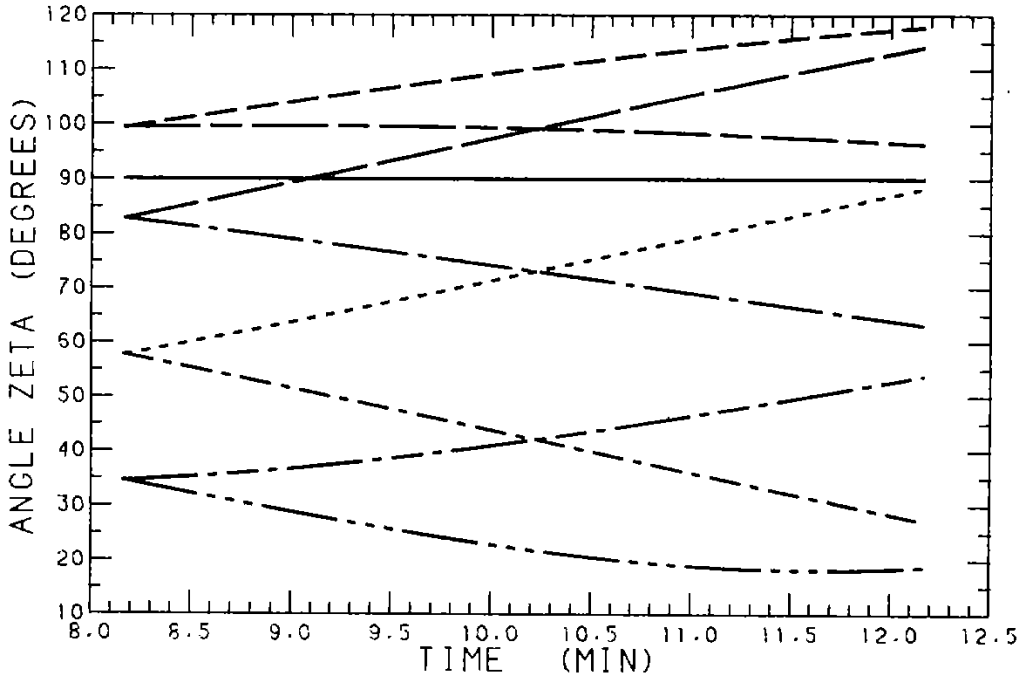

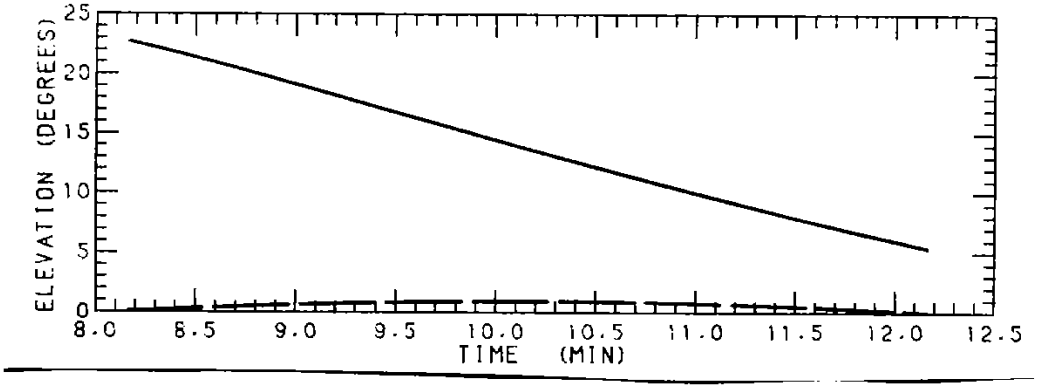

Fig. 5.12 - View of satellite from Cuiabá/Chui in the second orbit.

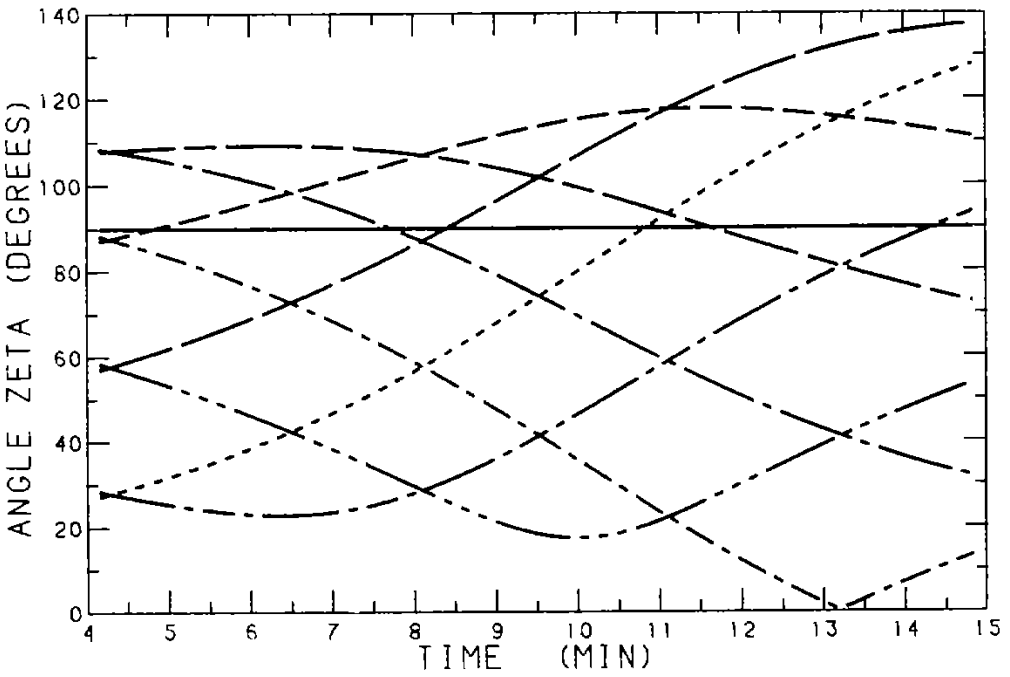

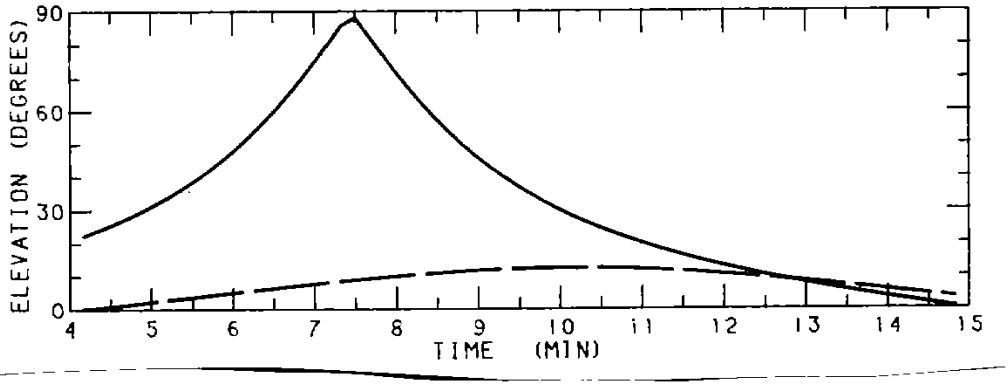

Fig. 5.13 - View of the satellite from Cuiabá/Chui in the third orbit.

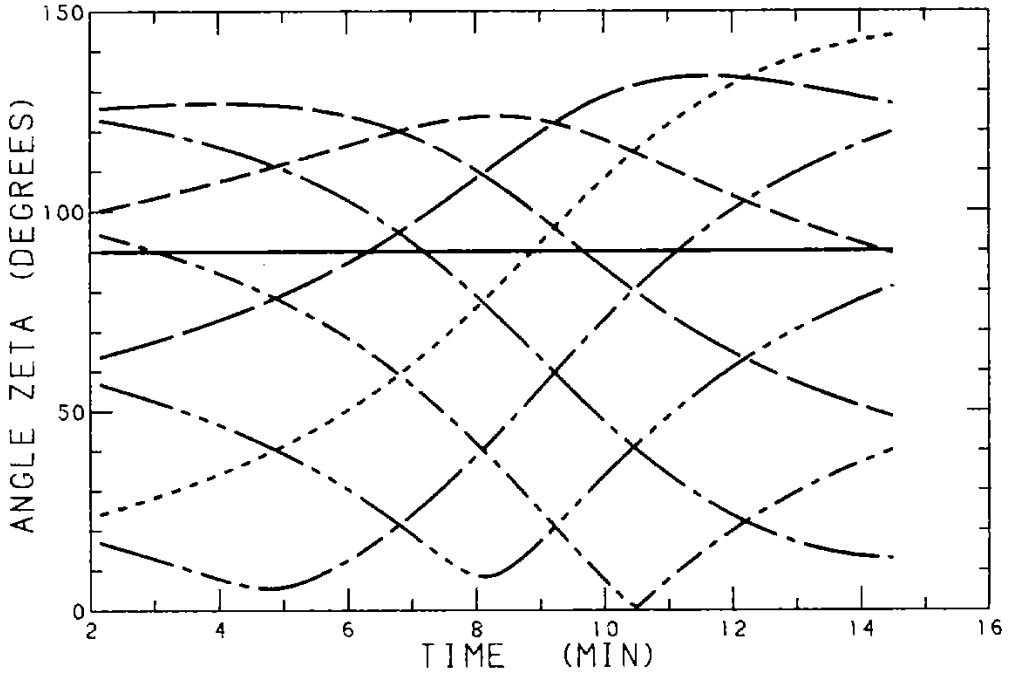

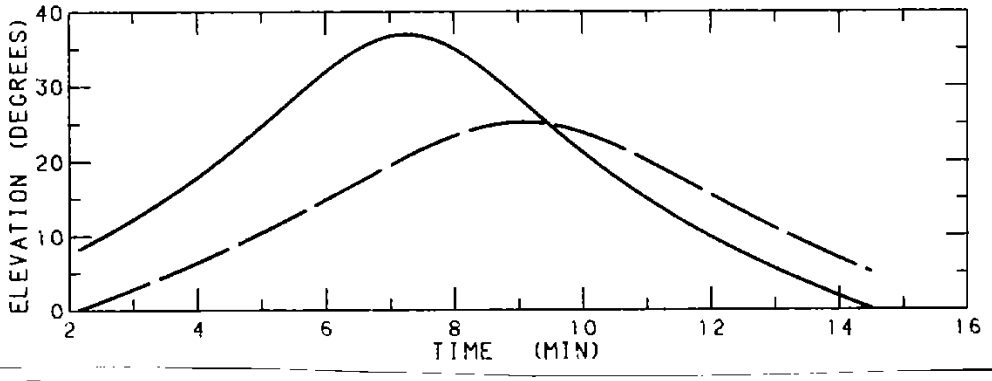

Fig. 5.14 - View of the satellite from Cuiabá/Chuí in the fourth orbit

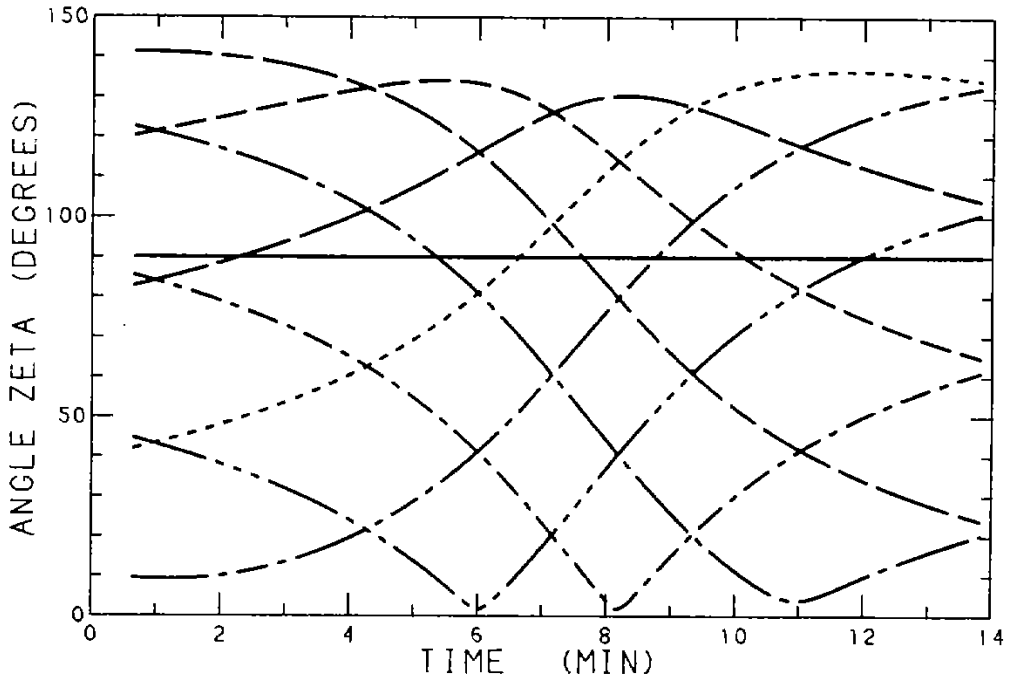

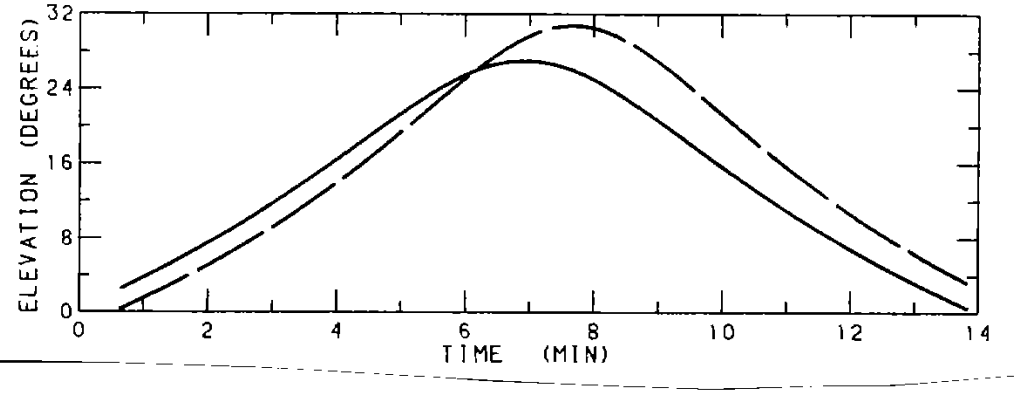

Fig. 5.15 - View of the satellite from Cuiabá/Chui in the fifth orbit.

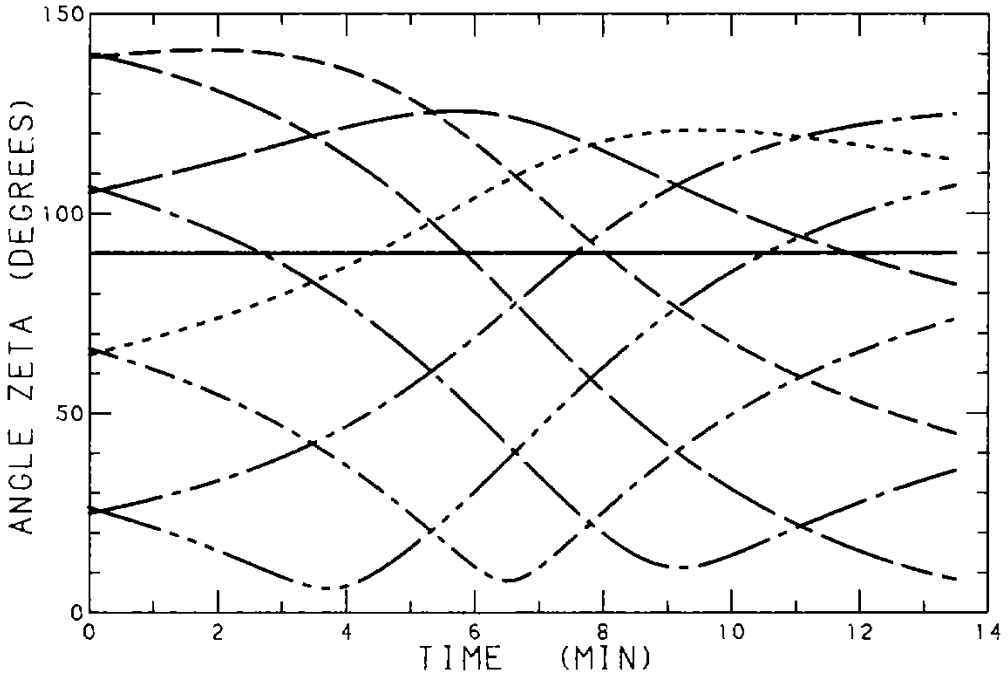

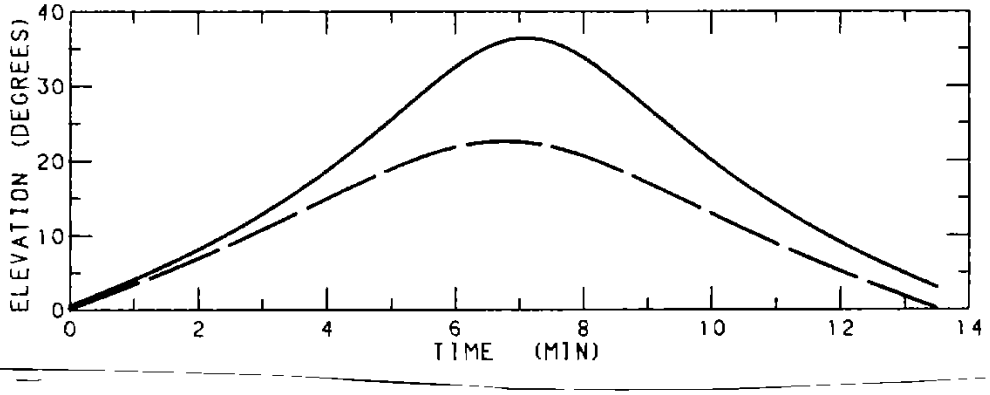

Fig. 5.16 - View of the satellite from Cuiabá/Chui in the sixth orbit.

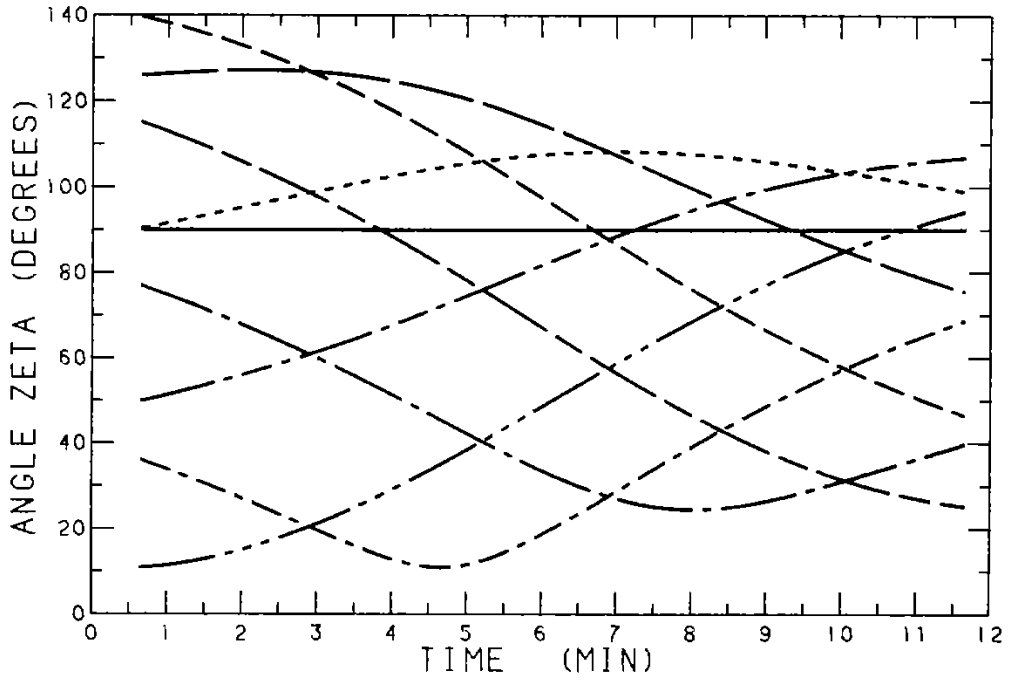

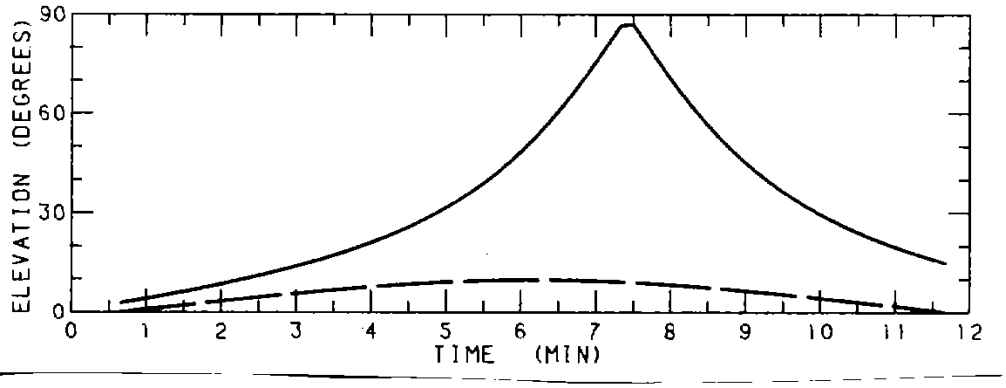

Fig. 5.17 - View of the satellite from Cuiab/Chui in the seventh orbit

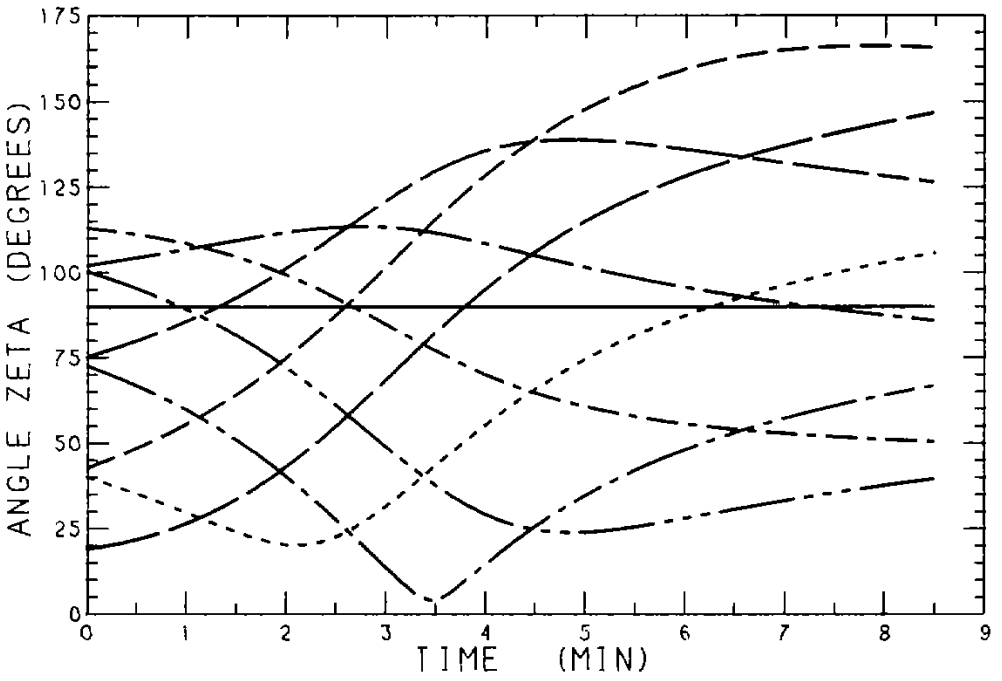

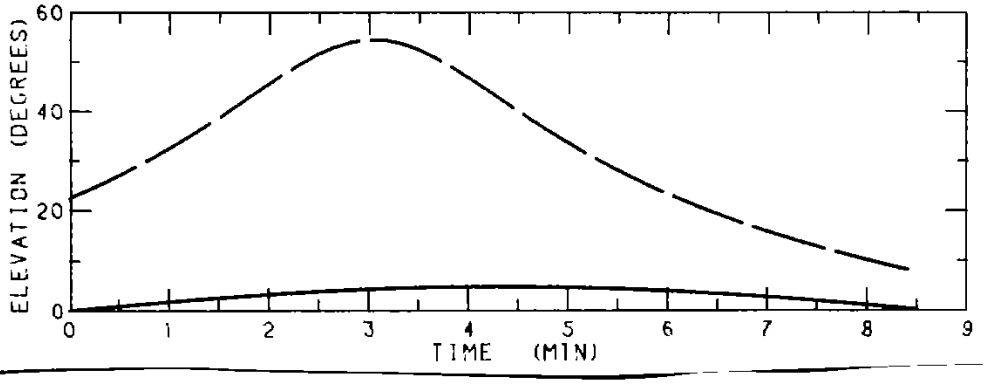

Fig. 5.18 - View of the satellite from Cuiabá/Oiapoque in the first orbit.

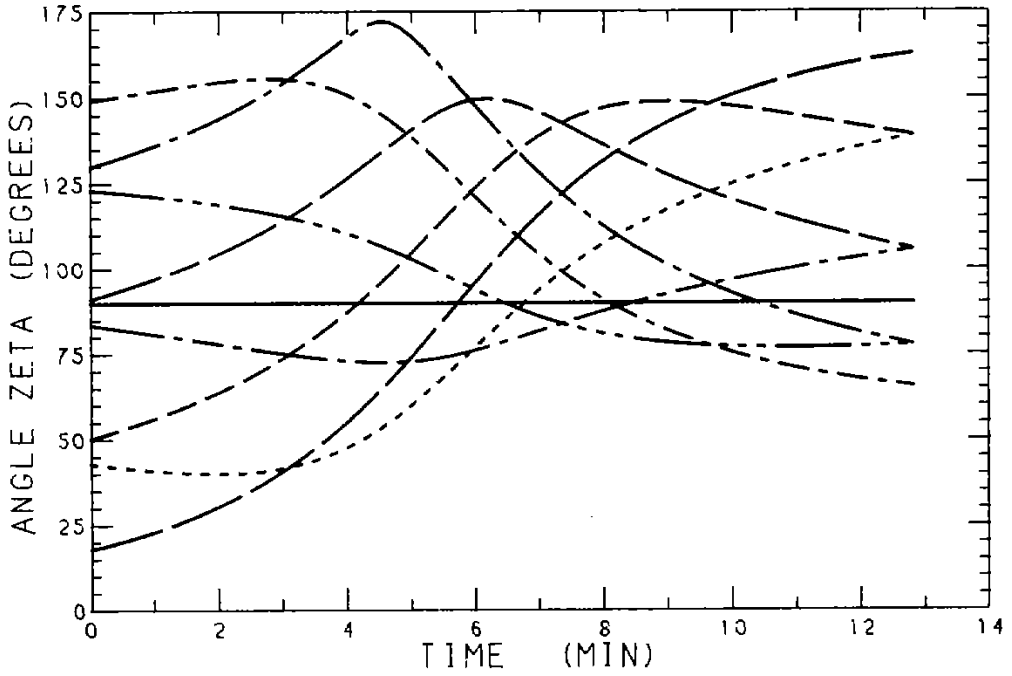

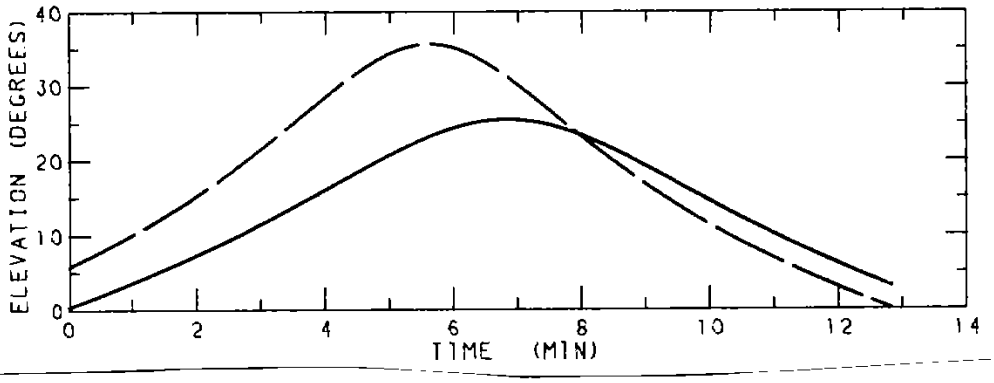

Fig. 5.19 - View of the satellite from Cuiabá/Oiapoque in the second orbit

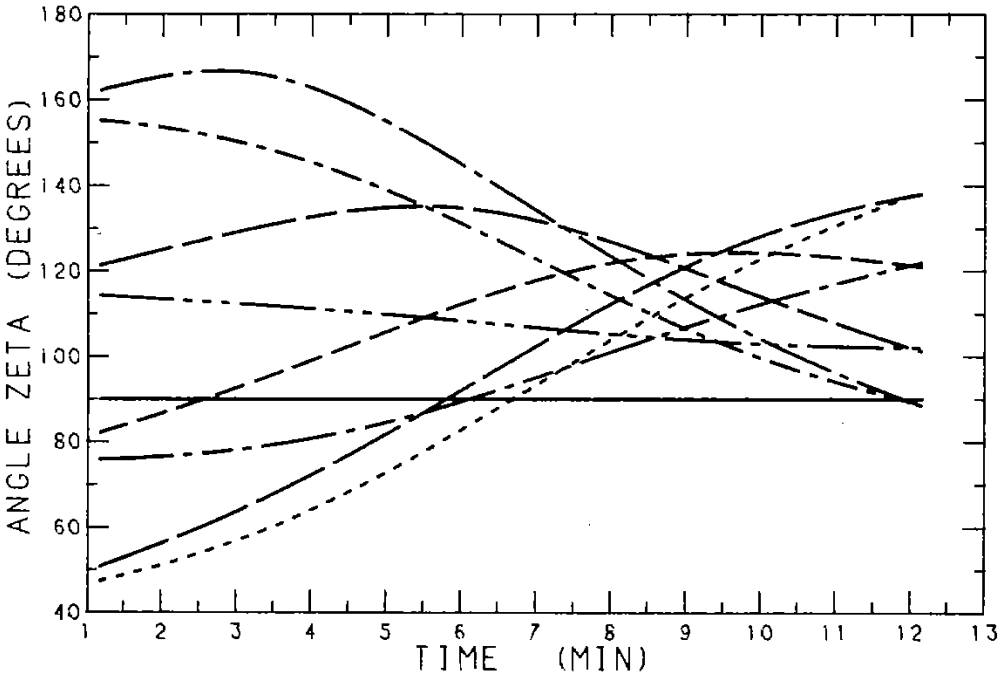

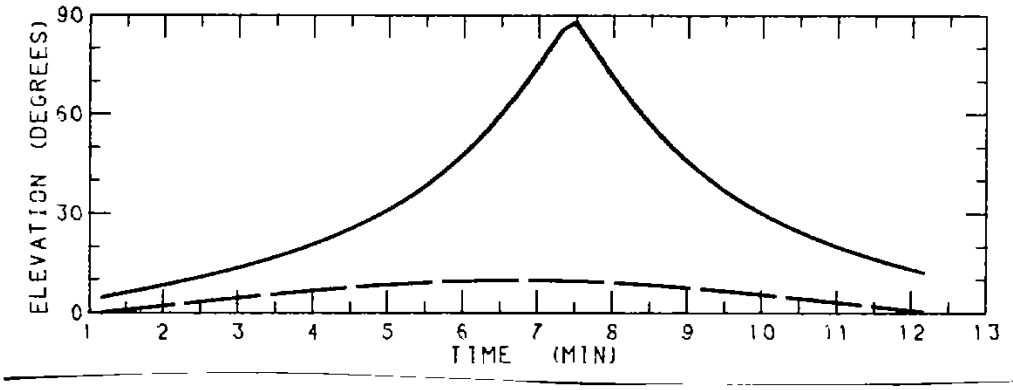

Fig. 5.20 - View of the satellite from Cuiabá/Oiapoque in the third orbit

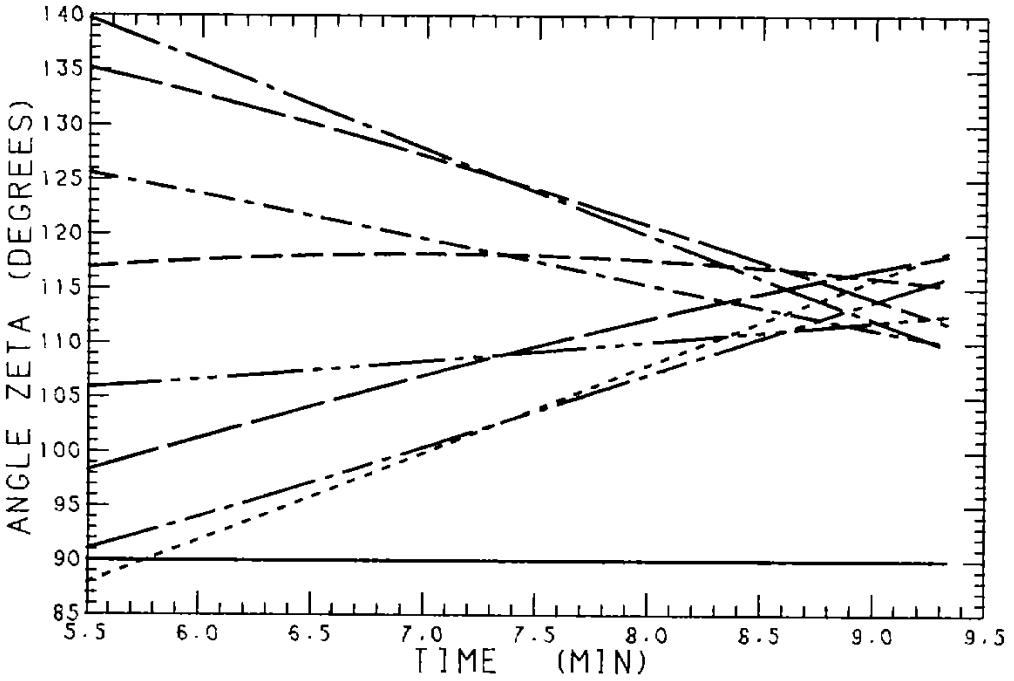

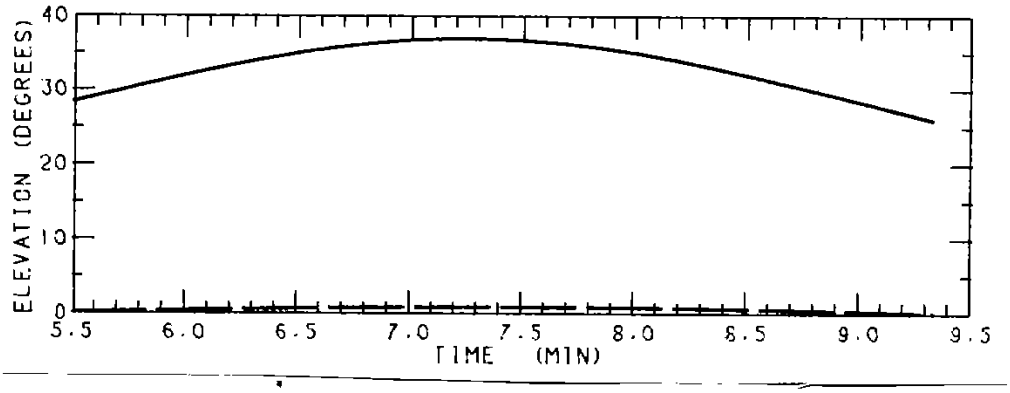

Fig. 5.21 - View of the satellite from Cuiabá/Oiapoque in the fourth orbit.

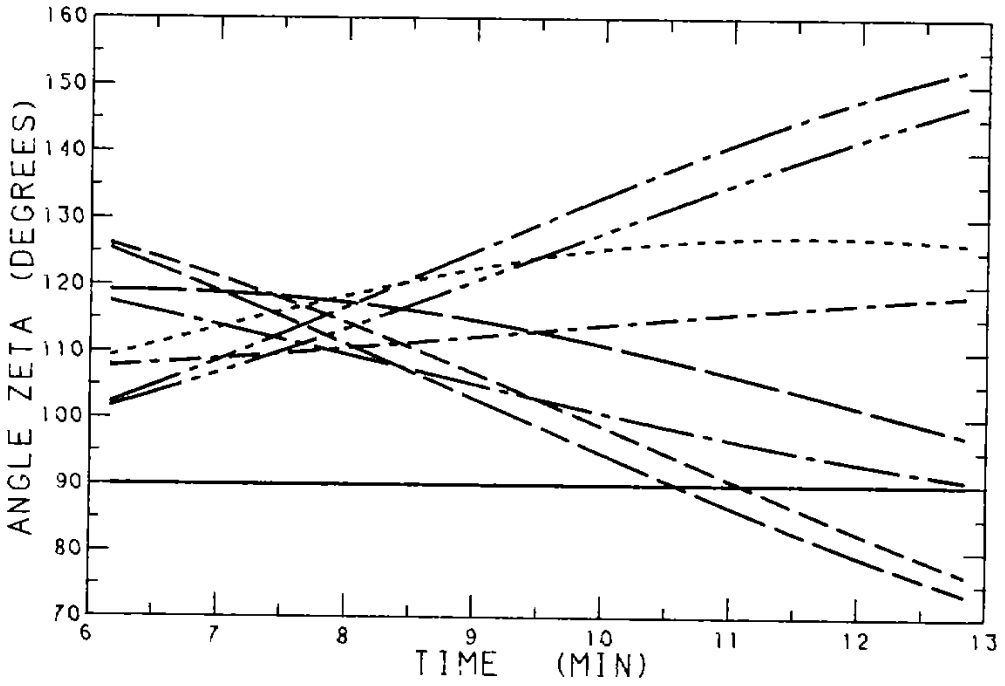

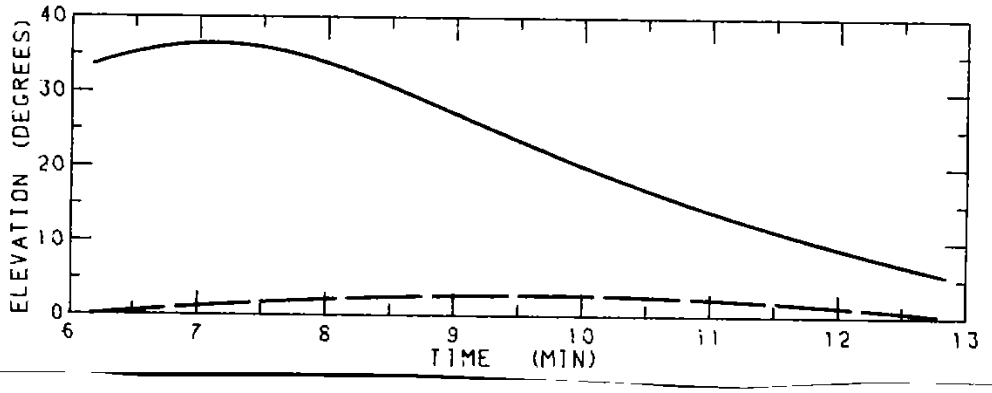

Fig. 5.22 - View of the satellite from Cuiabá/Oiapoque in the sixth orbit

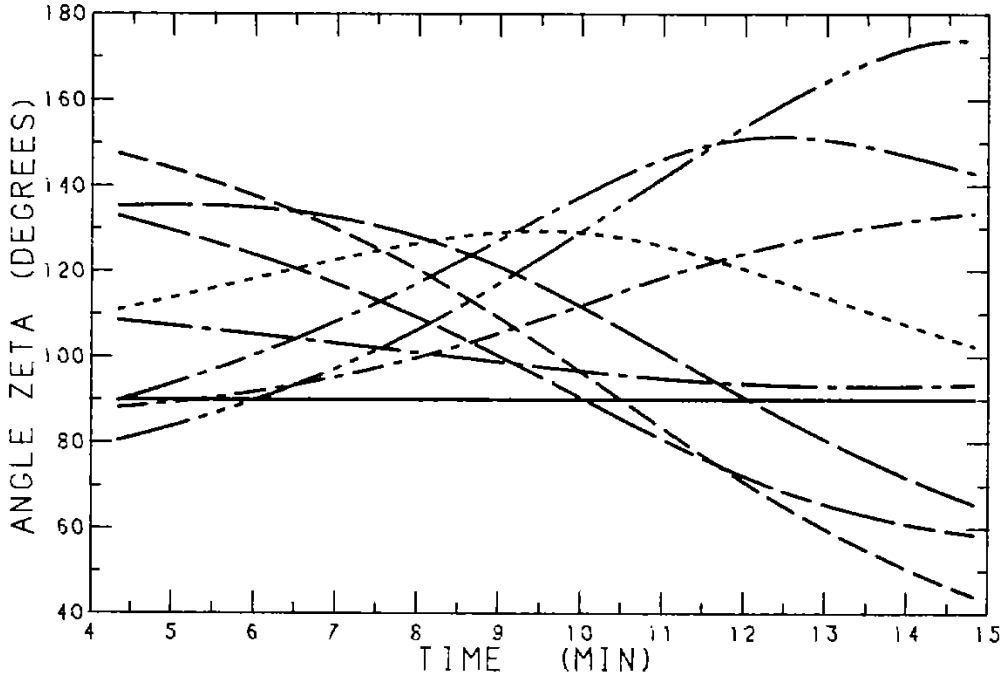

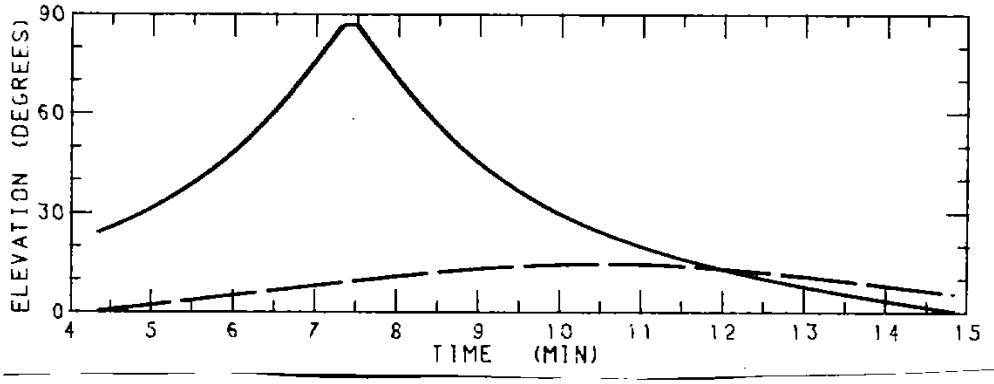

Fig. 5.23 - View of the satellite from Cuiabá/Oiapoque in the seventh orbit.

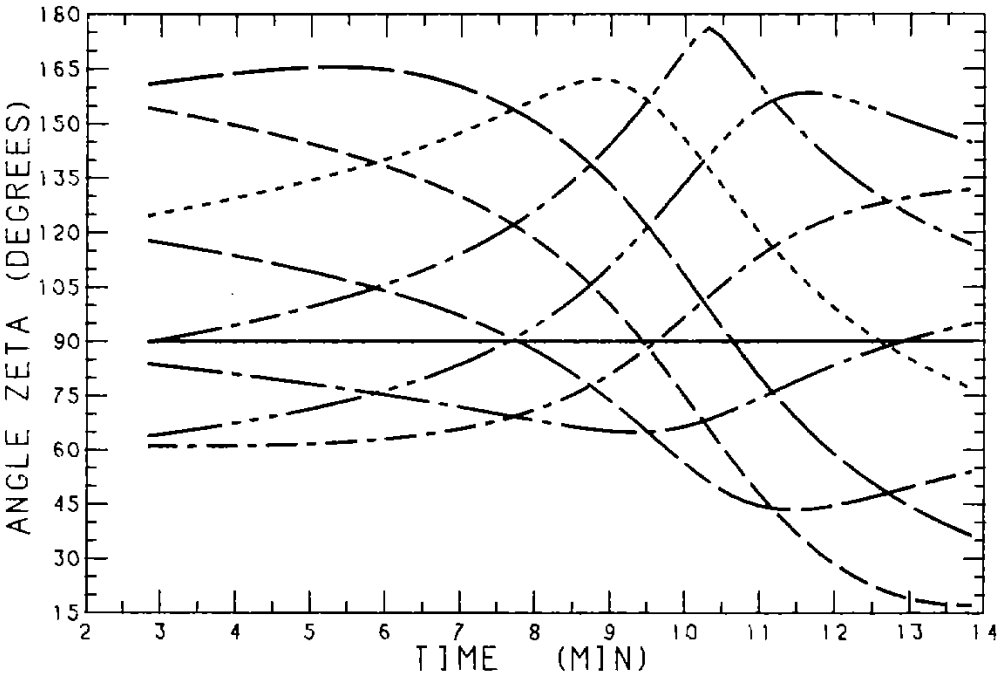

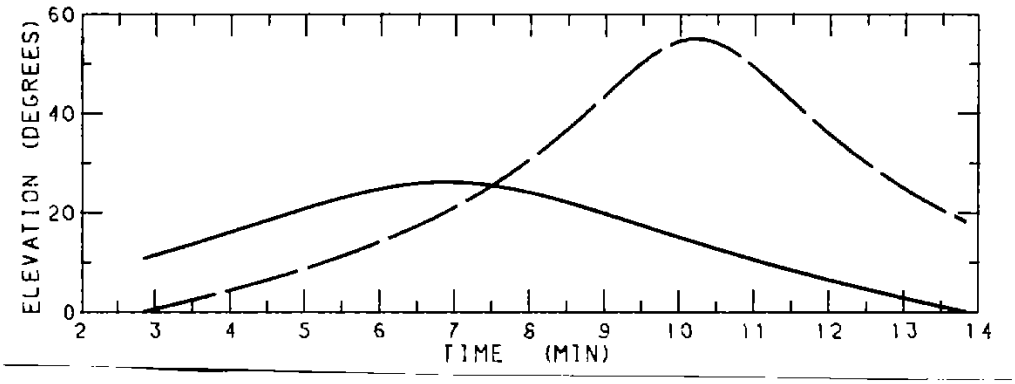

Fig. 5.24 - View of the satellite from Cuiabá/Oiapoque in the eighth orbit

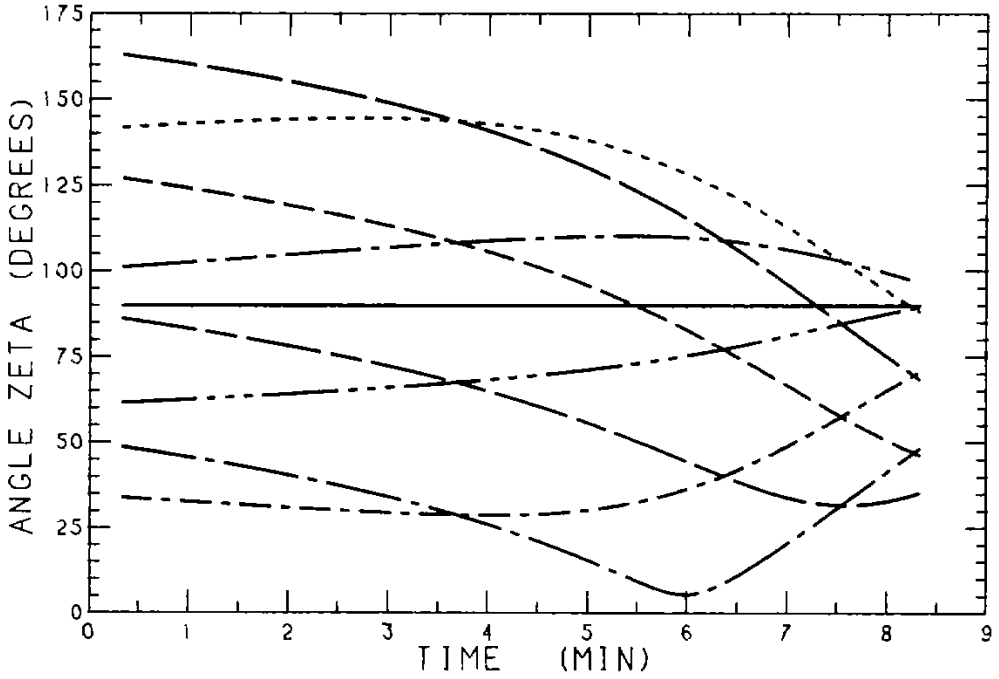

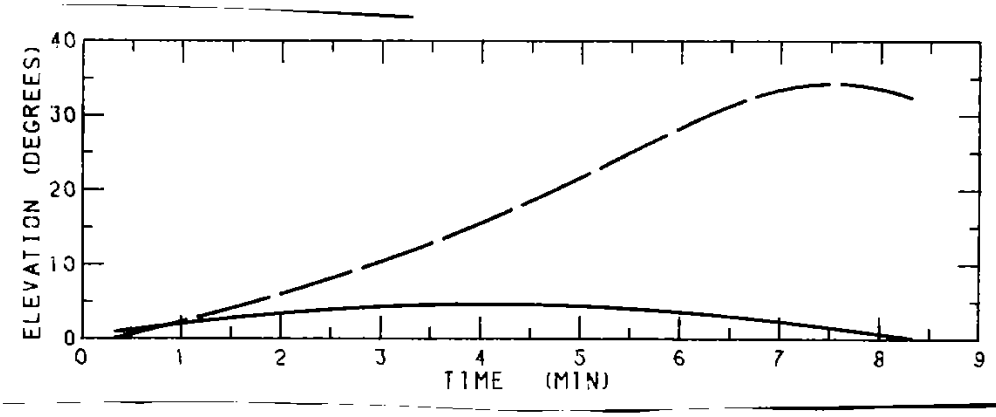

Fig. 5.25 - View of the satellite from Cuiabá/Oiapoque in the ninth orbit

6 - OBSERVATION AND COVERAGE

One of the problems in mission analysis is when and how to observe the satellite. After choosing the orbit and given the dispersions, a study is necessary for this purpose, mainly in the initial orbits, regarding orbit determination and control. In this section are shown a set of charts and diagrams which give a general information about the geometry of observation and contact between available stations and satellite.

The first topic is to define the geometry for available stations for tracking and orbit determination after burn-out. The stations considered are given in the Table 6.1.

TABLE 6.1

DATA OF THE OBSERVING STATIONS

STATION	λ^{o}(E)	ϕ^{o}
Cuiabá	- 56.100	- 15.53
Kourou	- 52.816	+ 5.25
Mas Palomas	- 15.340	+ 27.46

The Figure 6.1, split later as on p. 60, shows the Cuiabá station contacting the satellite at the end of the first orbit. The figure 6.2 shows that a five minute observation above 5^{o} of elevation is possible, and from figure 6.1 one can conclude that 10^{o} is the maximum elevation in this first passage. In the Figure 6.1, a nominal circular orbit is used because of the fixed altitude (700 km) of the visibility circle. In the case of the Figures 6.2 and 6.3, the lined part shows the actual intersection case of contact between the extremal eccentric orbits of an average altitude of 700 km and the circular orbits.

In general, more than one tracking station is desirable for preliminary orbit determination and in the Table 6.1, the available stations are given. In the figures 6.4, 6.5 and 6.6, one can see individual sub-satellite numbered trajectories for these stations for 0^{o}, 5^{o}, 10^{o} and 30^{o} visibility circles. These trajectories agree with the orbits of the first day (Figure 6.1).

Because of the spin stabilization and communication devices, the geometry of observation of the satellite from these stations is also important. The figures 6.7 through 6.13 depict the first three orbits for these stations, as described in the Section 5, each curve representing only one passage.

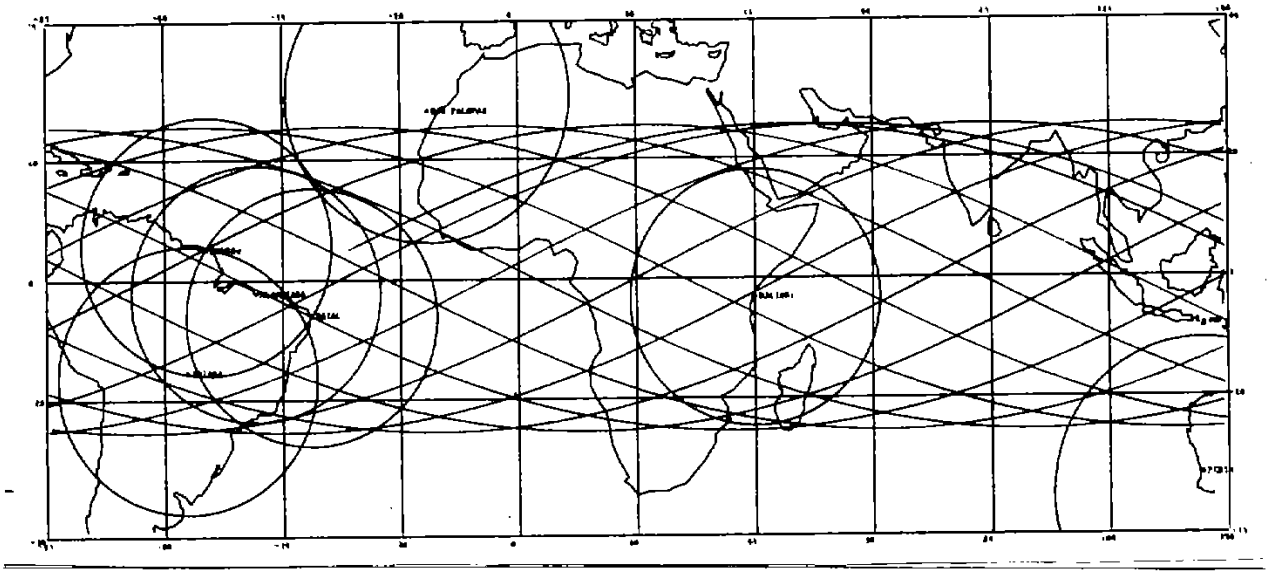

Fig. 6.1 - The first fifteen orbits of the first day.

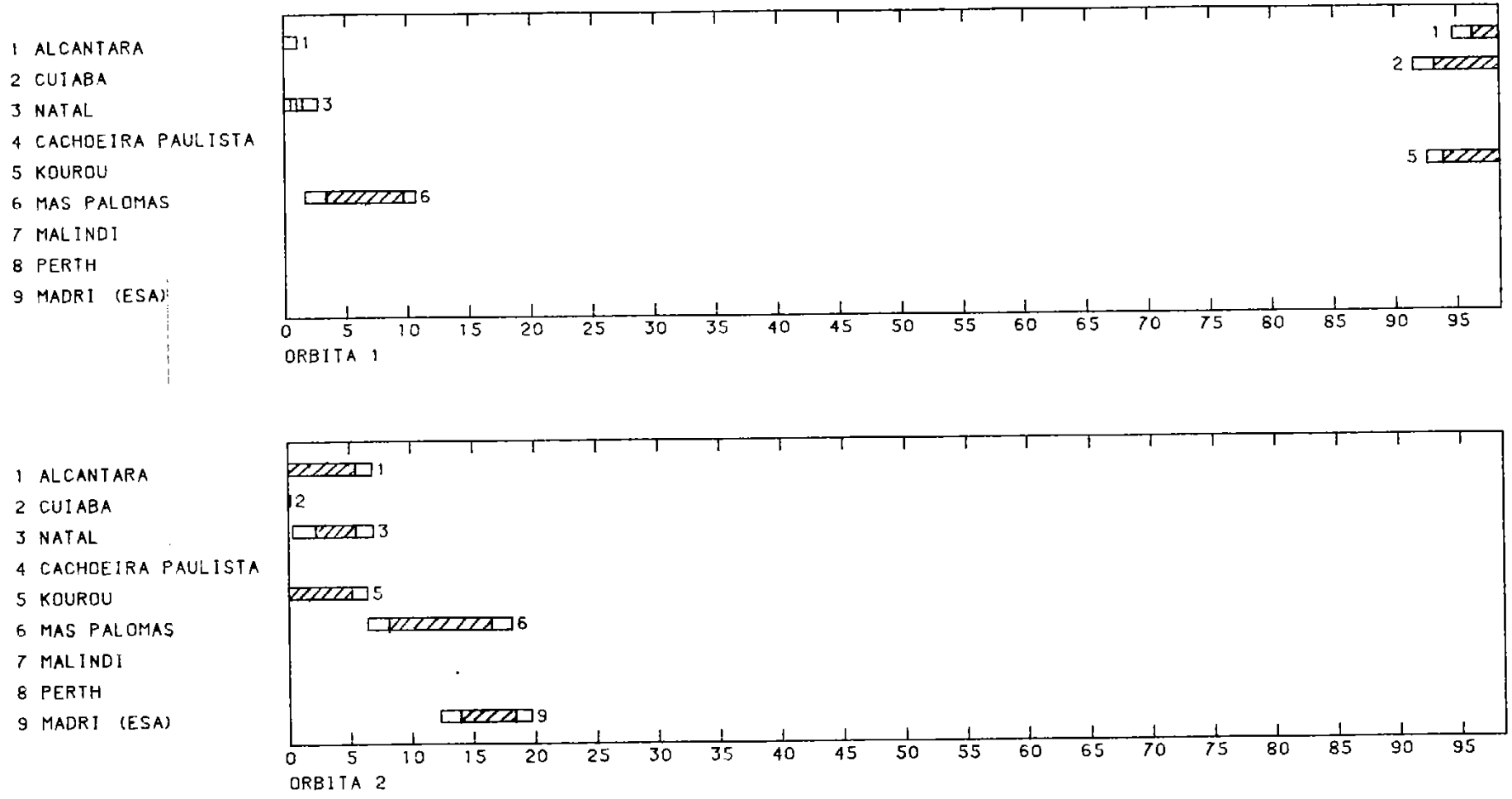

Fig. 6.2 - Contact time between the satellite and the ground stations for the orbits 1 and 2.

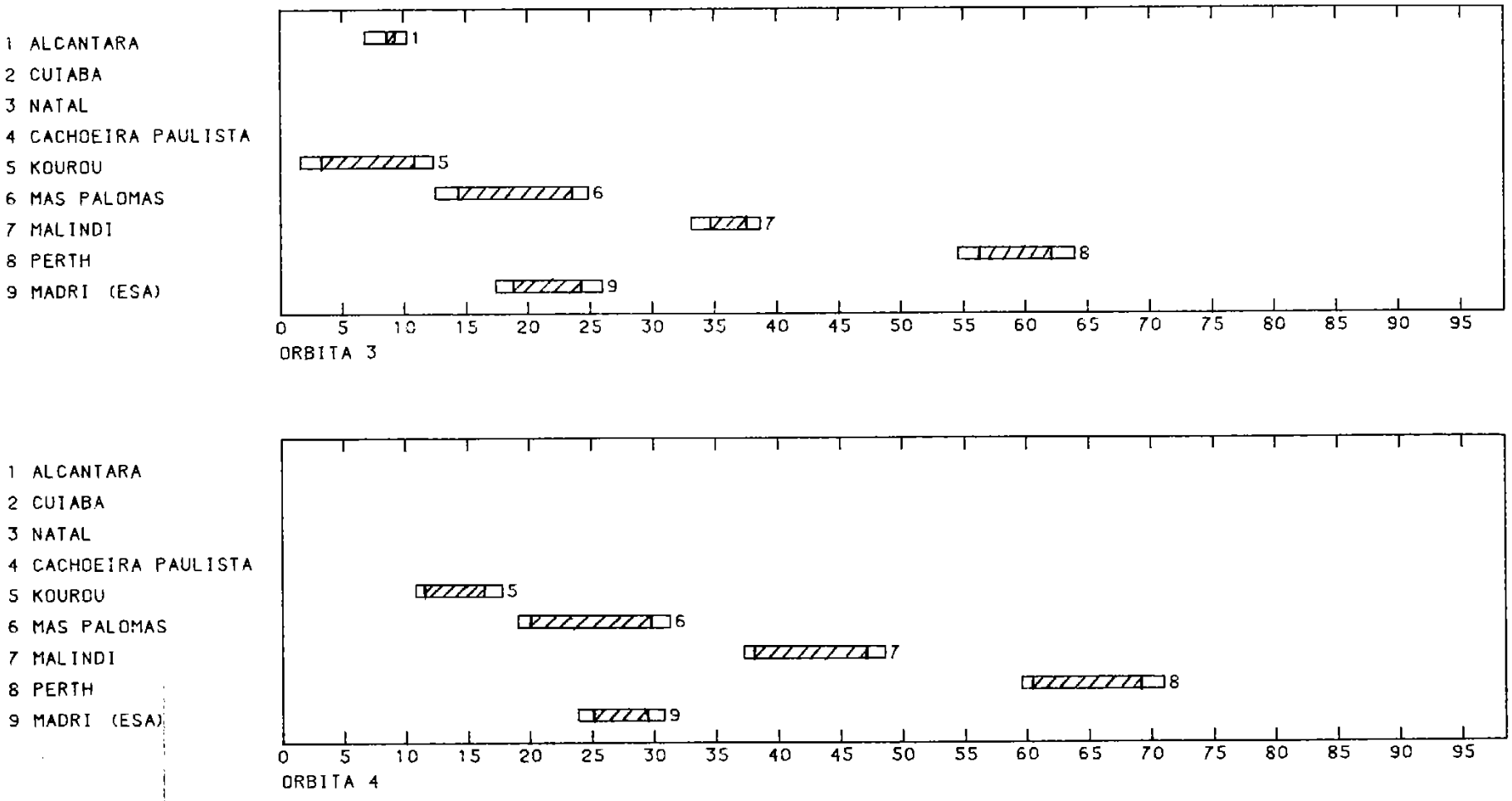

Fig. 6.3 - Contact time between the satellite and the ground stations for the orbits 3 and 4.

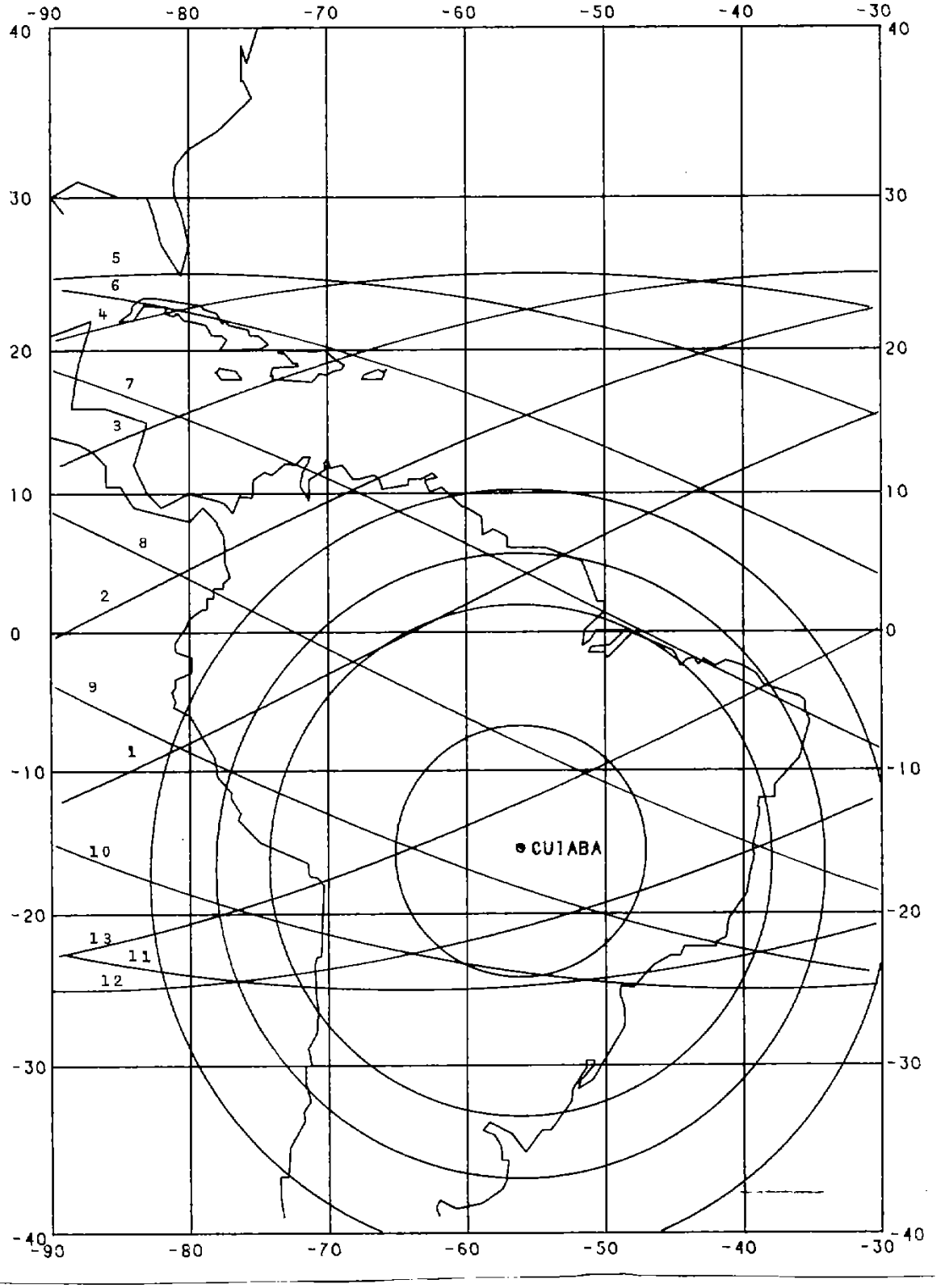

Fig. 6.4 - Visibility circles of the station Cuiabá for the elevation angles 0^{o}, 5^{o}, 10^{o}, 30^{o} along with the first day orbits.

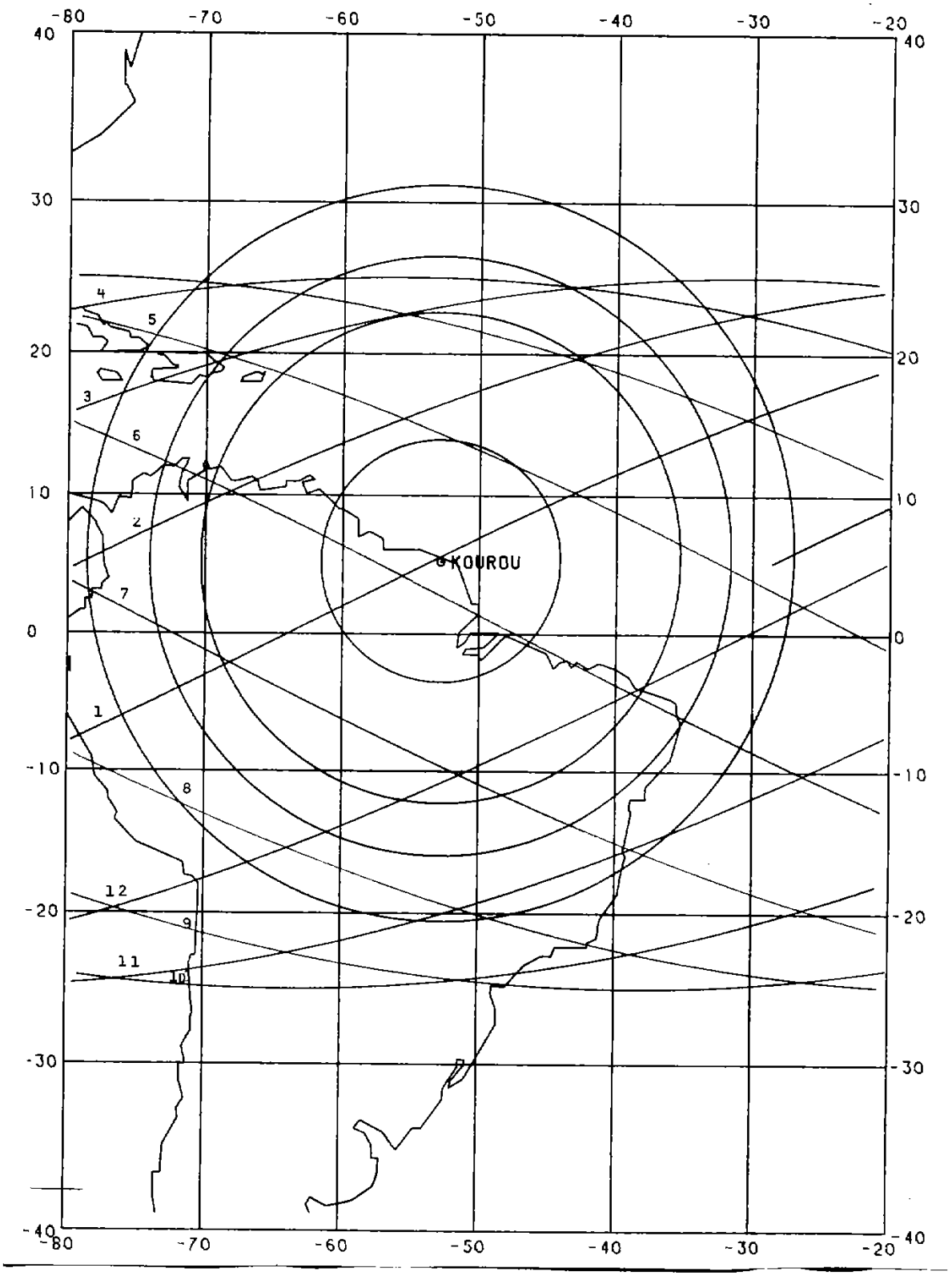

Fig. 6.5 - Visibility circles of the station Kourou for the elevation angles 0^{o}, 5^{o}, 10^{o}, 30^{o} along with the first day orbits.

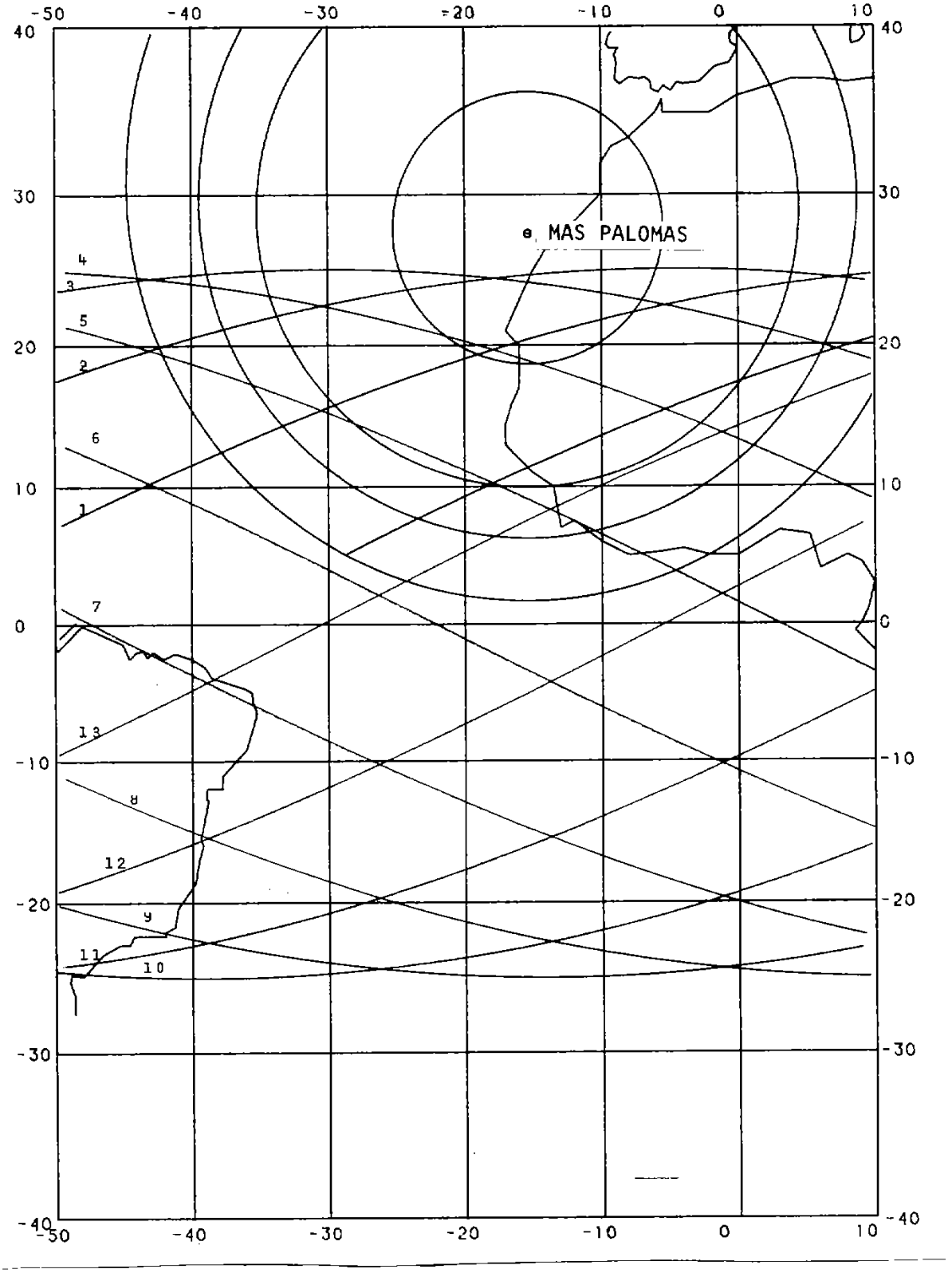

Fig. 6.6 - Visibility circles of the station Mas Palomas for the elevation angles 0^{o}, 5^{o}, 10^{o}, 30^{o} along with the first day orbits.

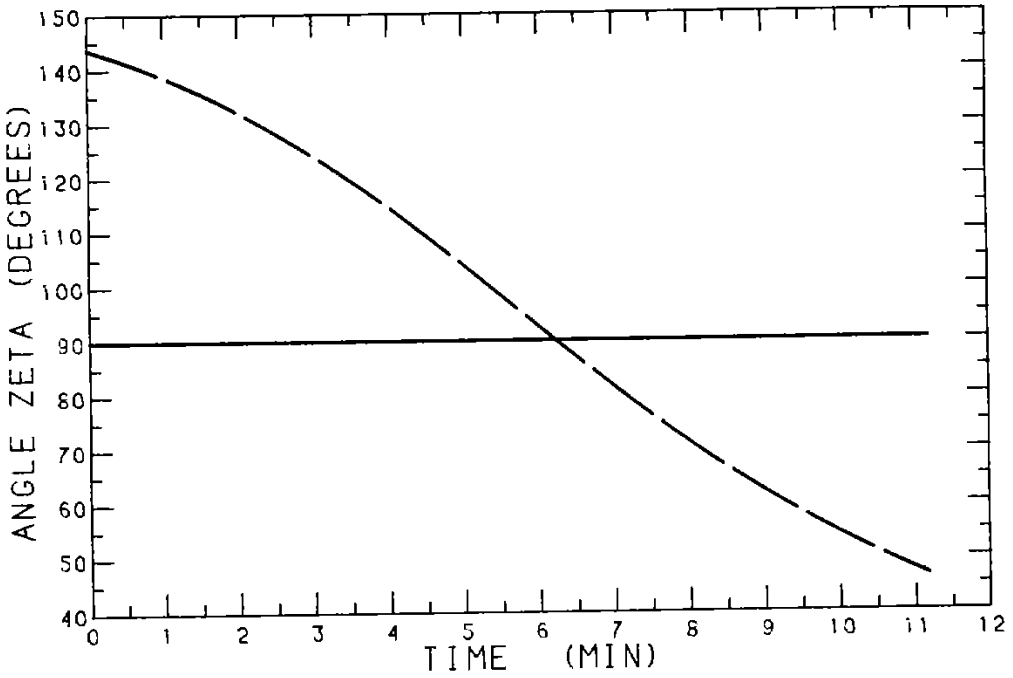

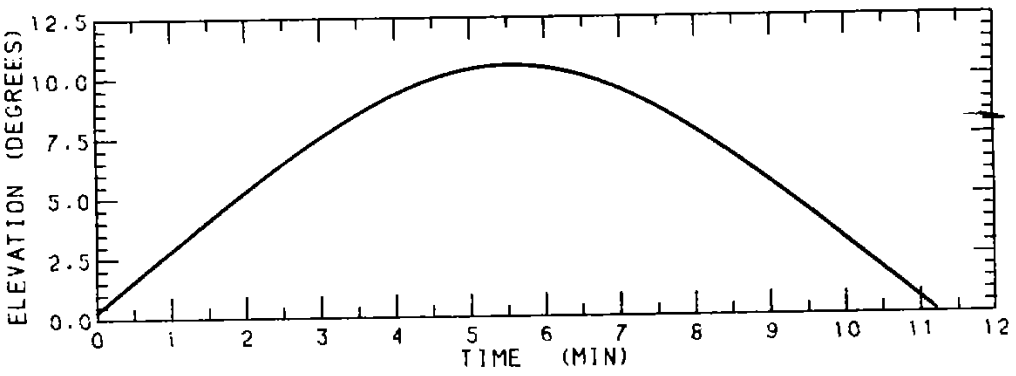

Fig. 6.7 - View of the satellite in the first orbit from Cuiabá.

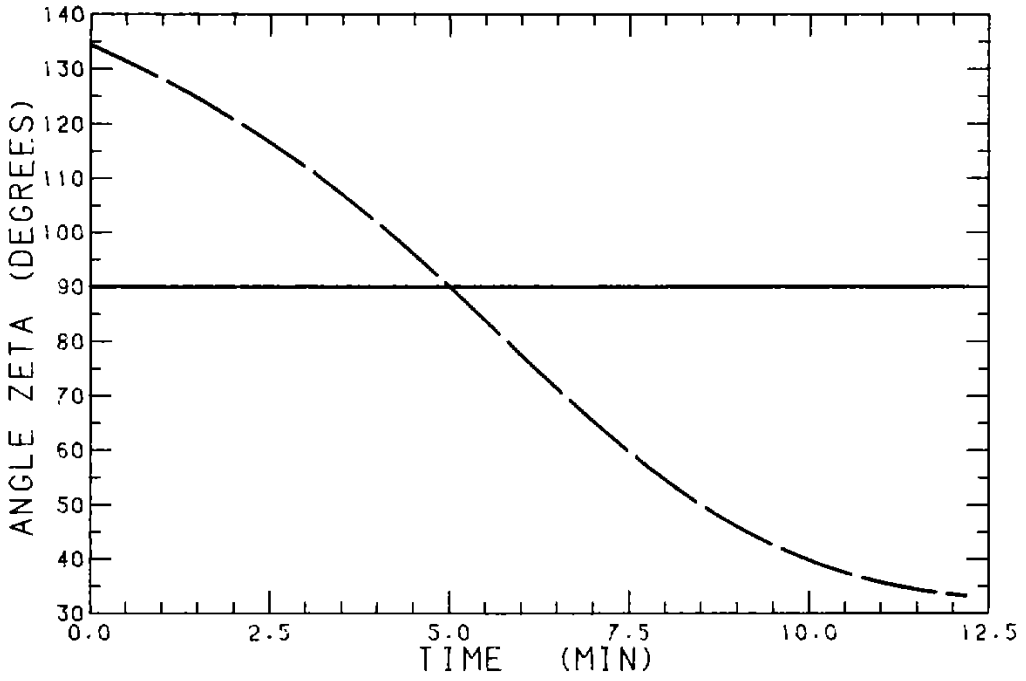

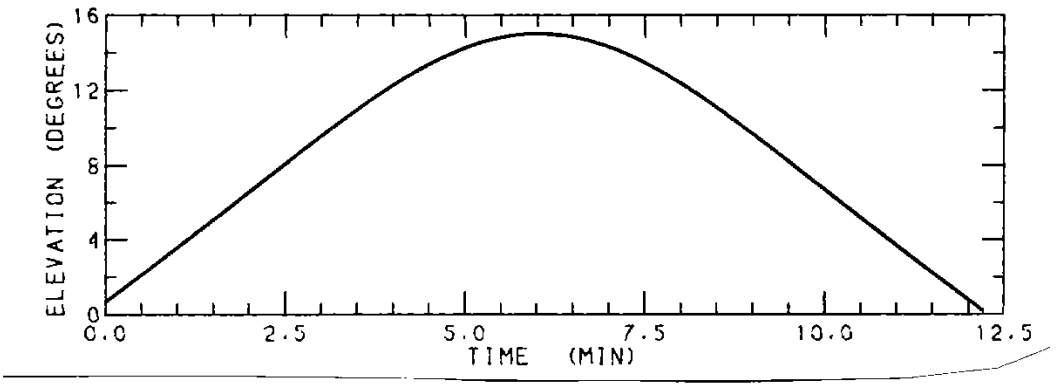

Fig. 6.8 - View of the satellite in the first orbit from Mas Palomas.

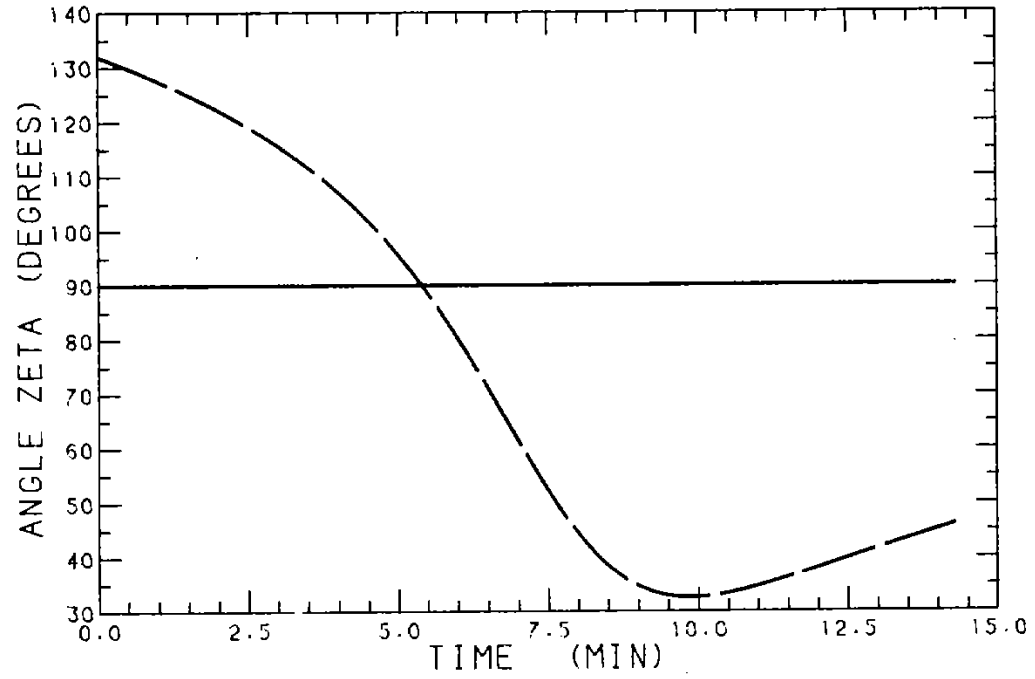

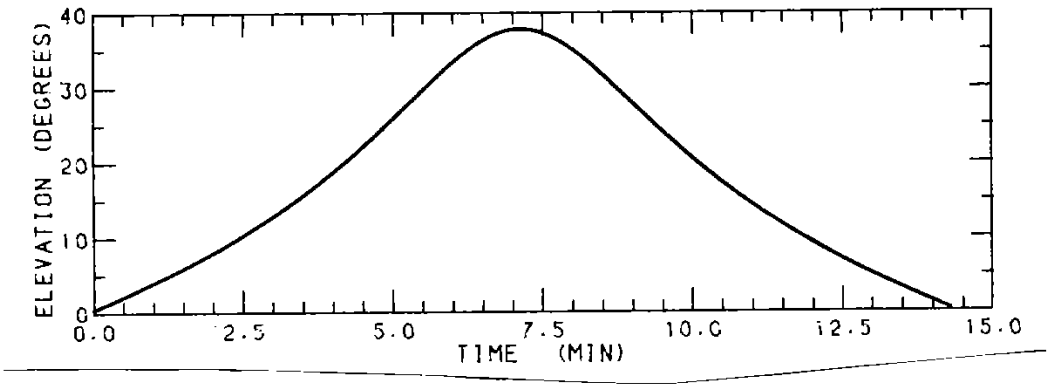

Fig. 6.9 - View of the satellite in the second orbit from Mas Palomas.

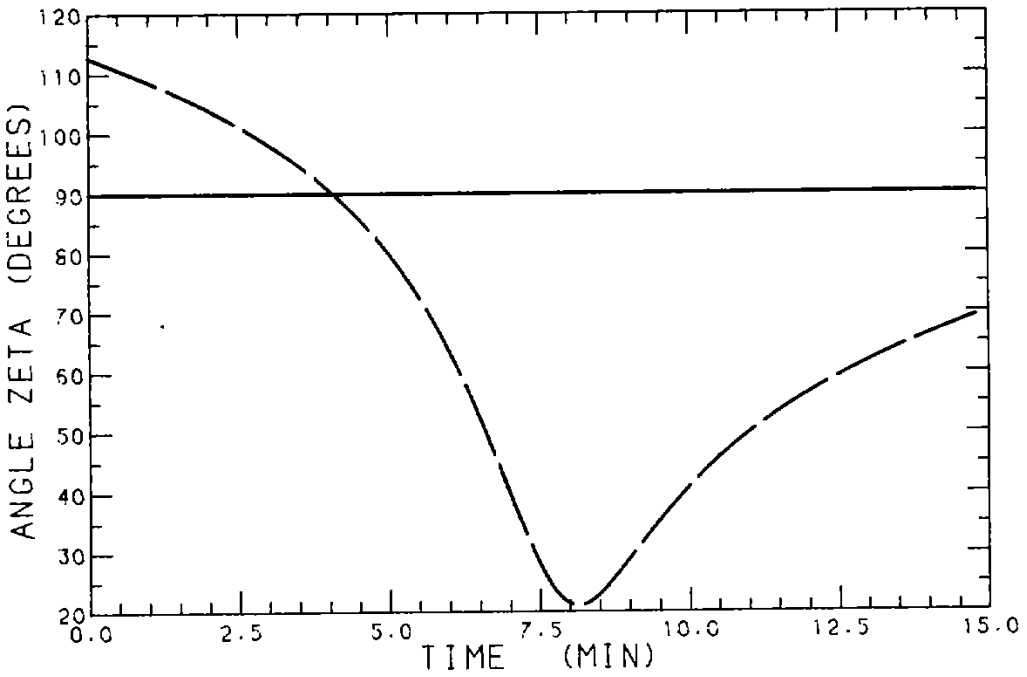

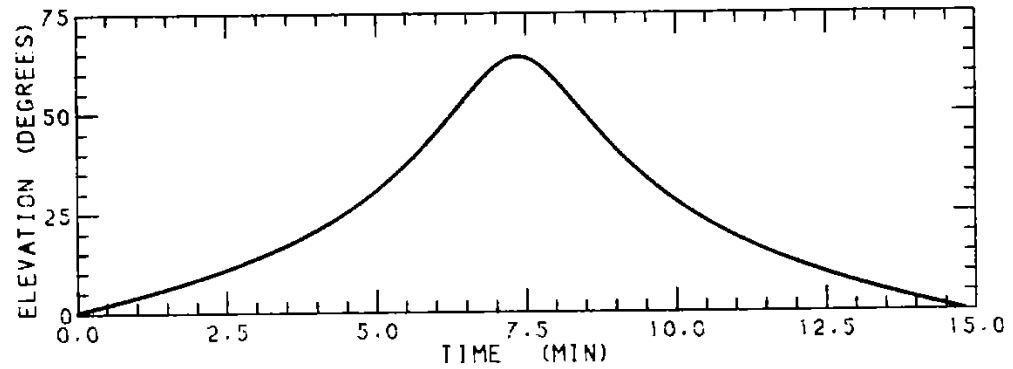

Fig.6.10 - View of the satellite in the third orbit from Mas Palomas.

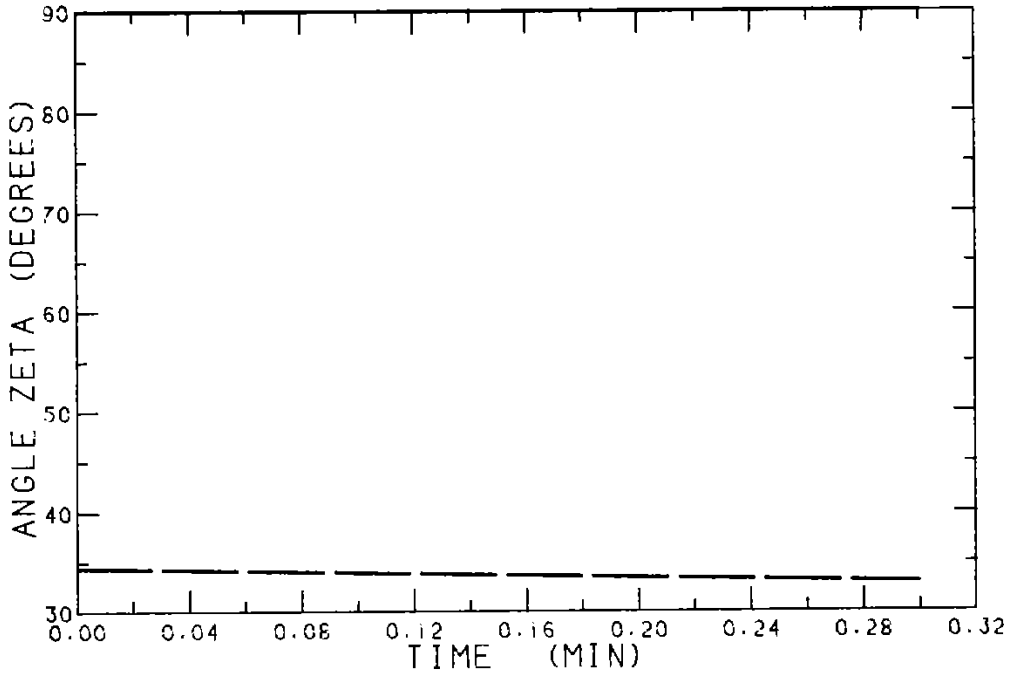

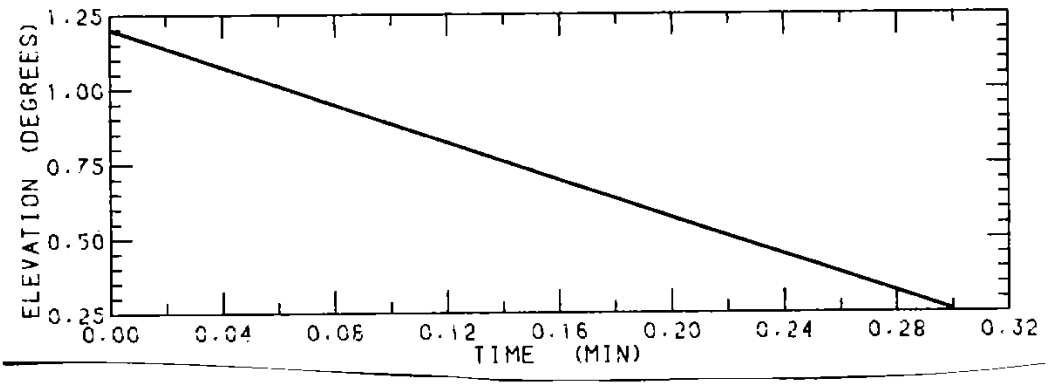

Fig. 6.11 - View of the satellite in the first orbit from Kourou.

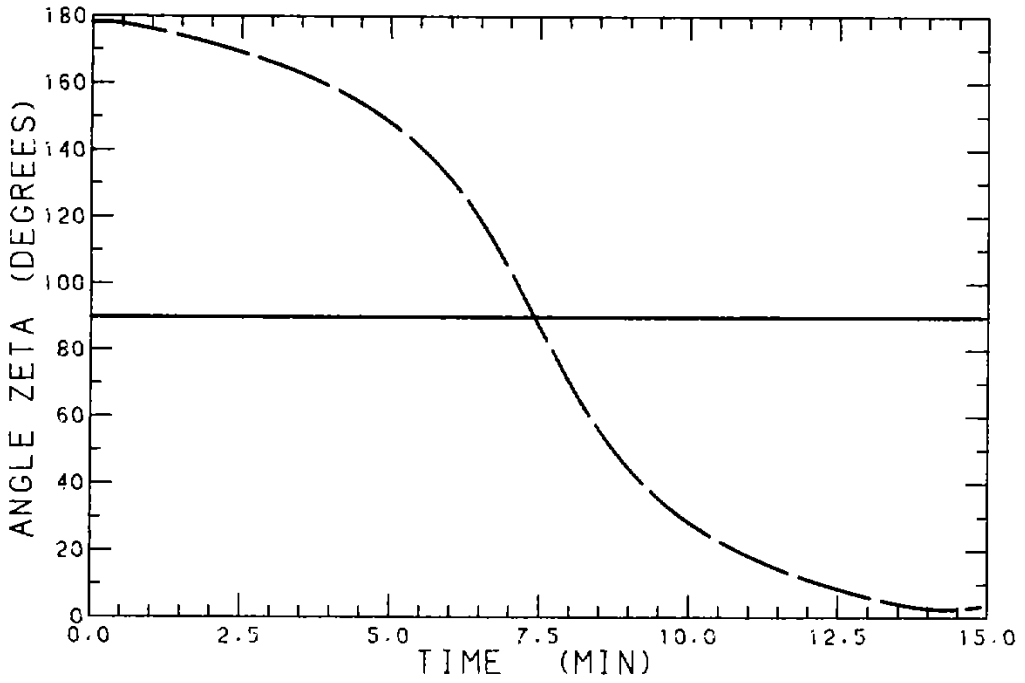

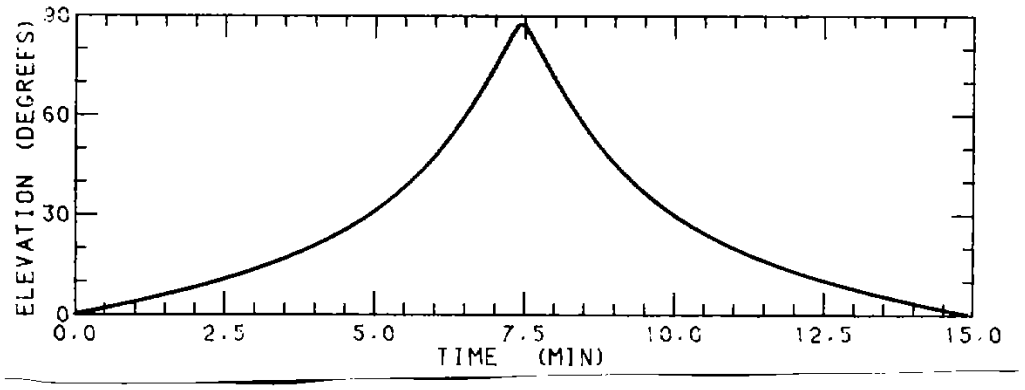

Fig. 6.12 - View of the satellite in the second orbit from Kourou.

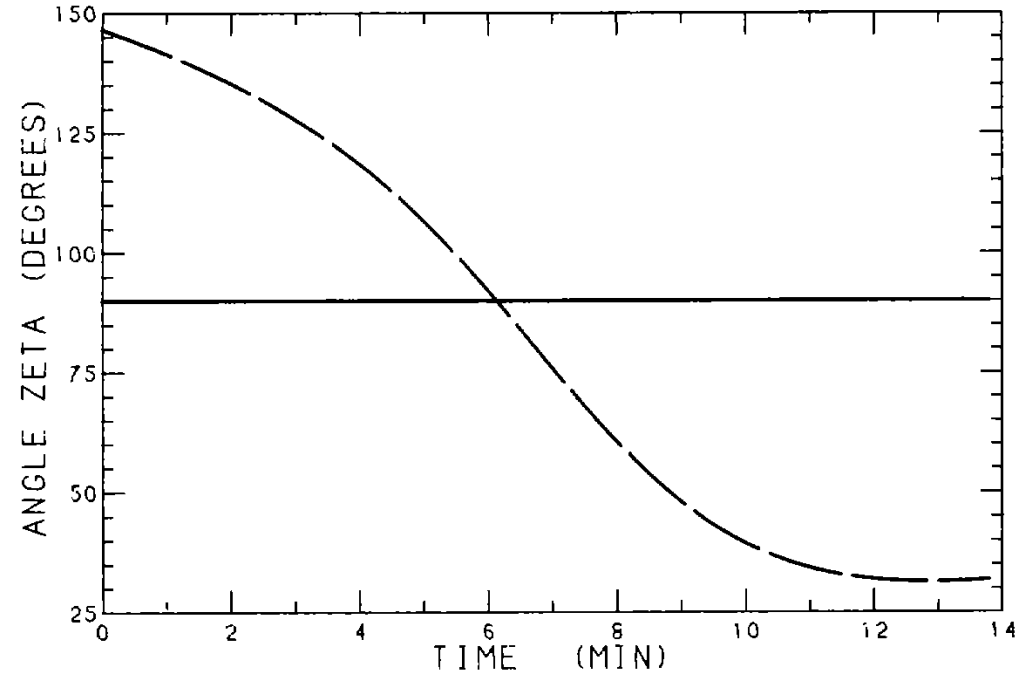

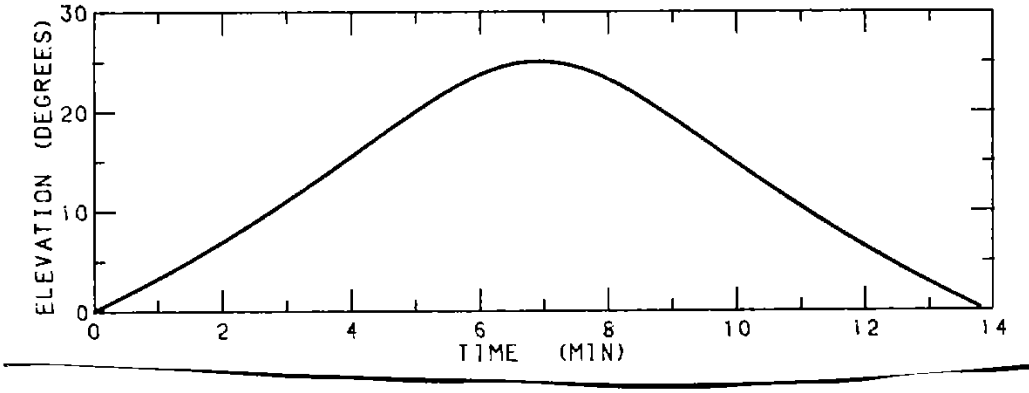

Fig. 6.13 - View of the satellite in the third orbit from Kourou.

In order to improve the view of the first day orbit, the Figure 6.1 is split into 15 figures (Figures 6.14 through 6.28). Each figure is now shown with only one numbered orbit.

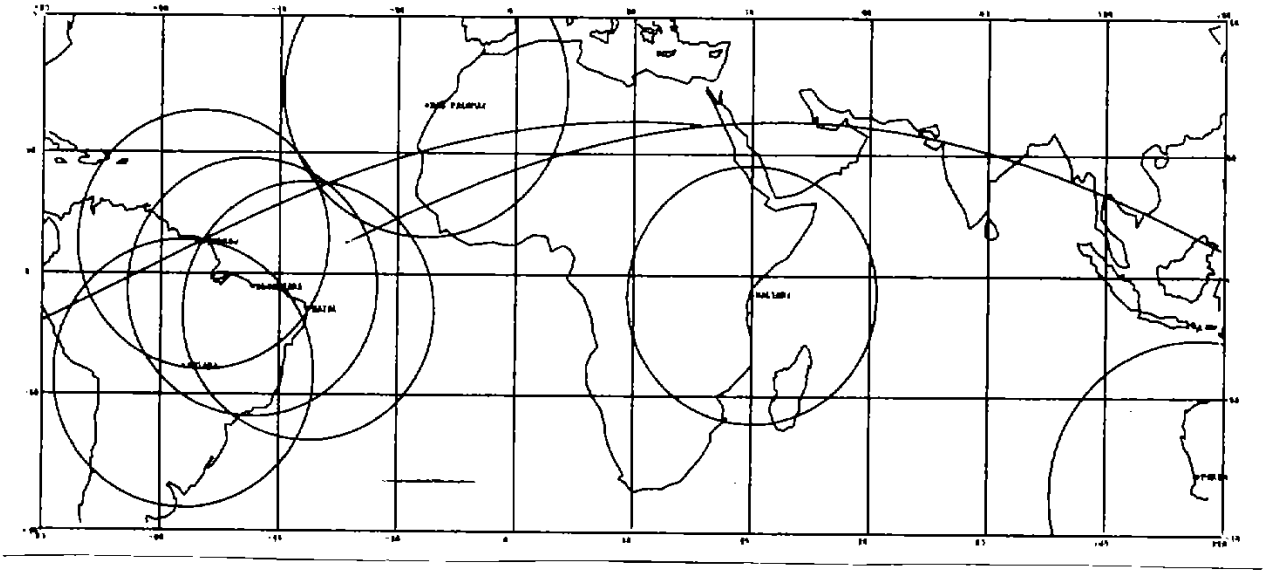

Fig. 6.14 - The orbit number one.

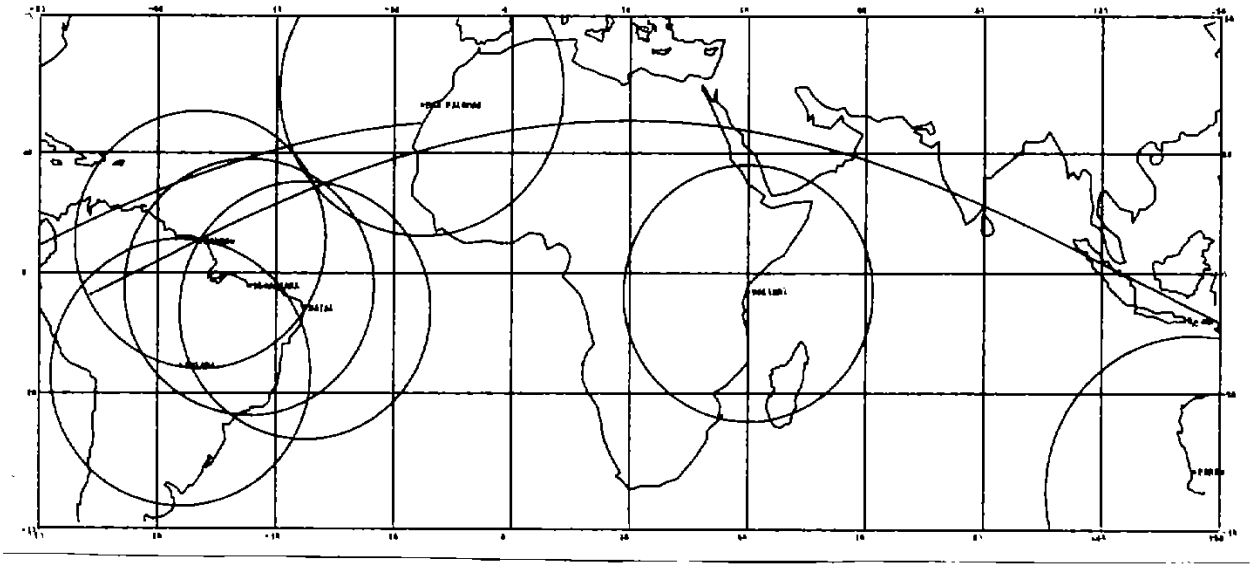

Fig. 6.15 - The orbit number two.

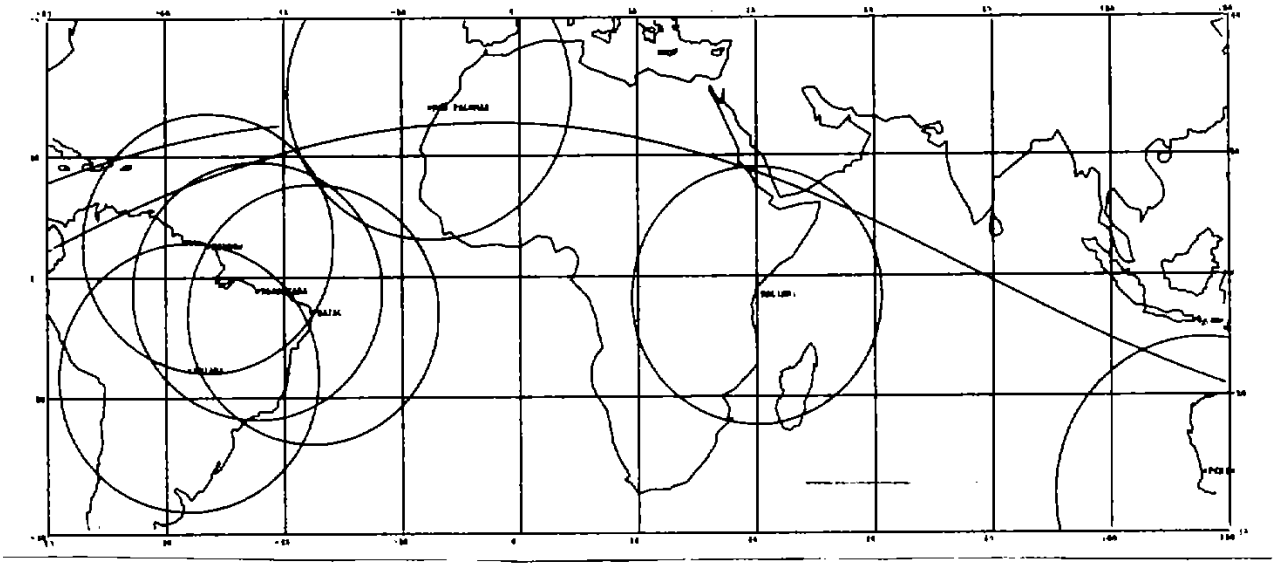

Fig. 6.16 - The orbit number three.

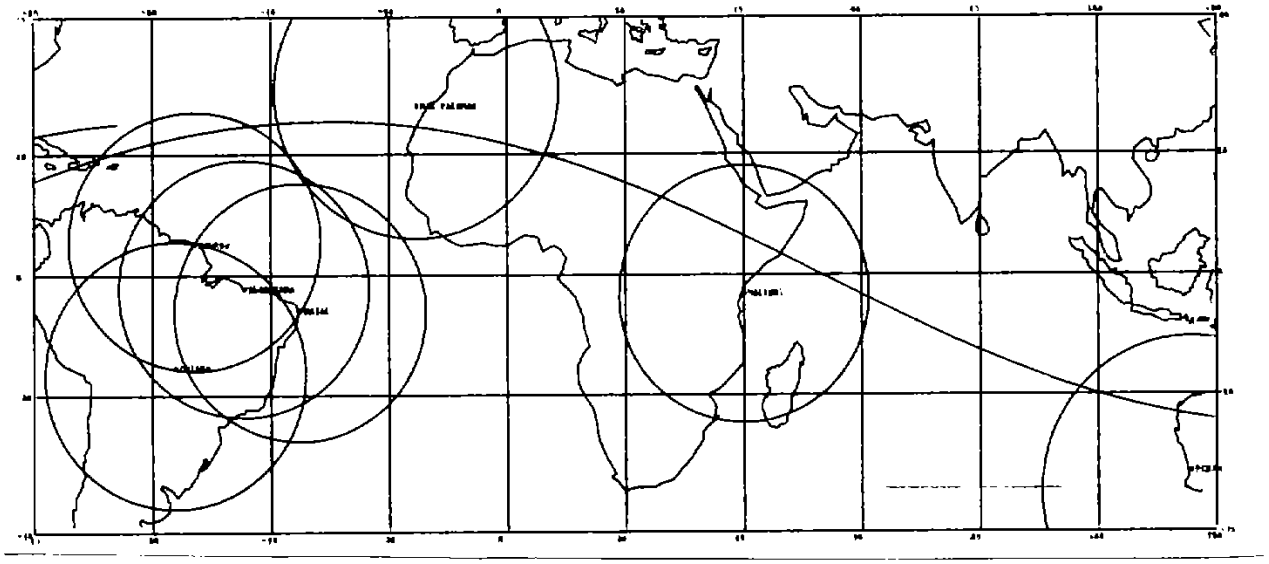

Fig. 6.17 - The orbit number four.

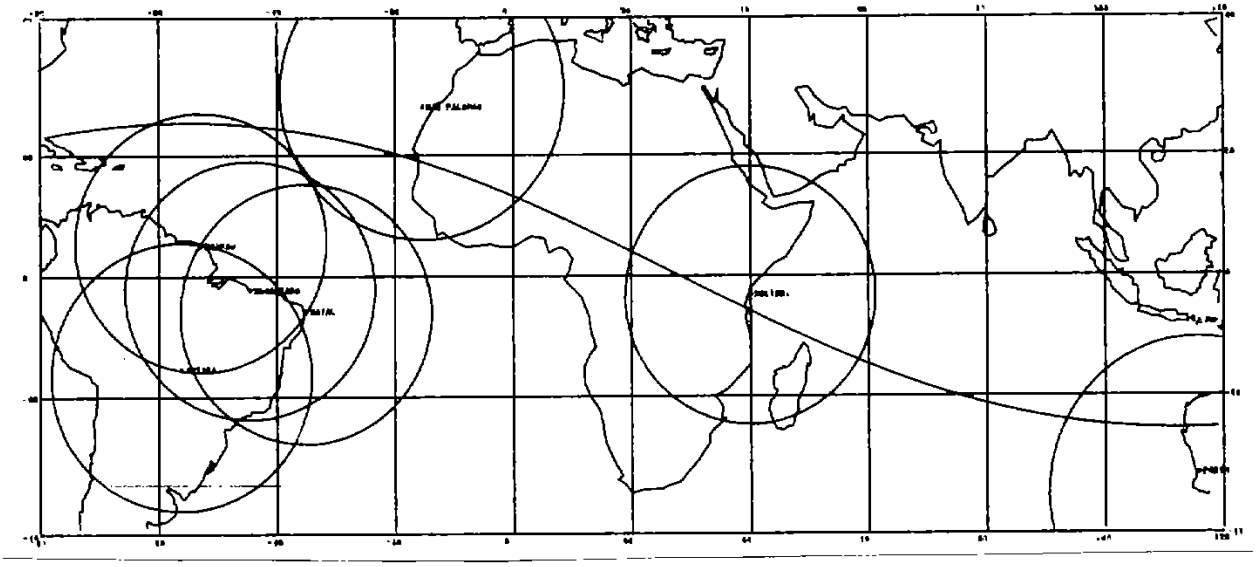

Fig. 6.18 - The orbit number five.

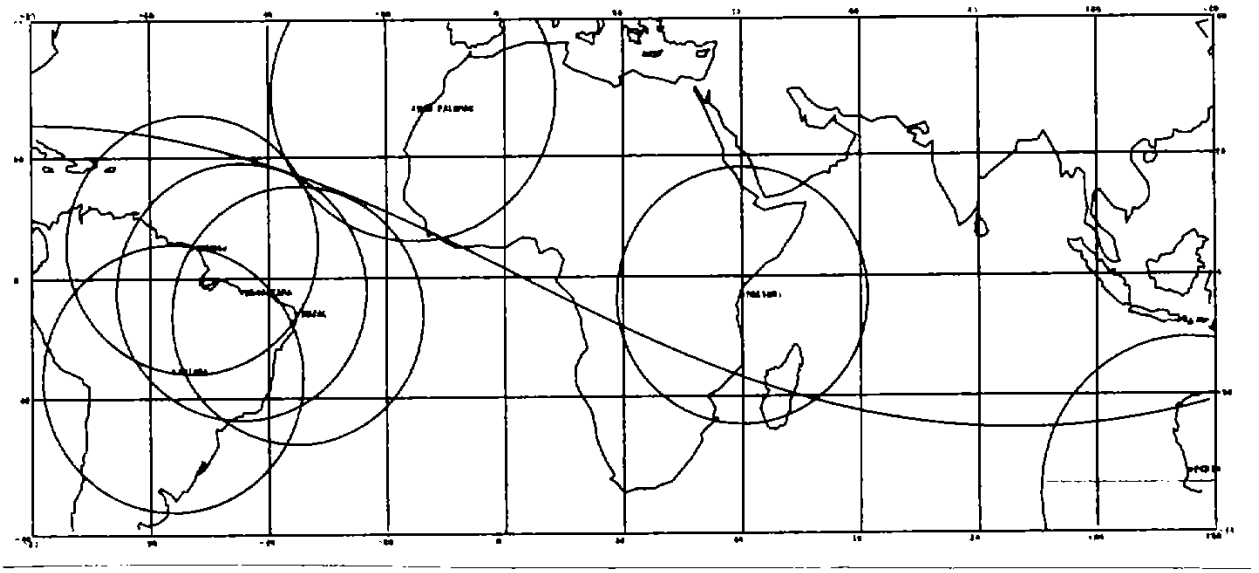

Fig. 6.19 - The orbit number six.

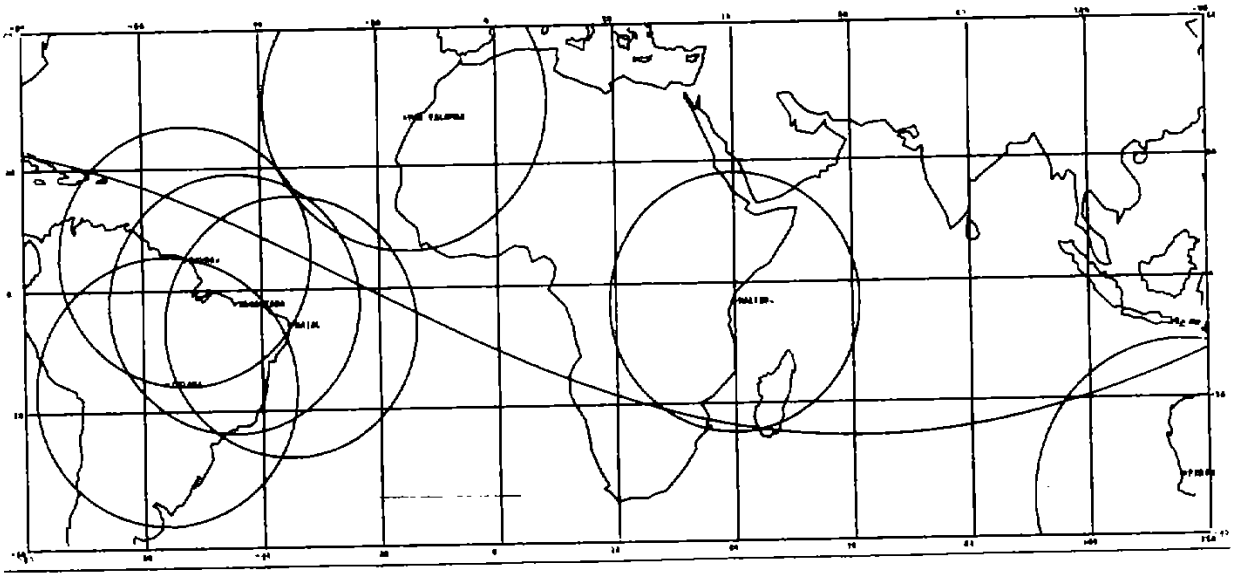

Fig. 6.20 - The orbit number seven.

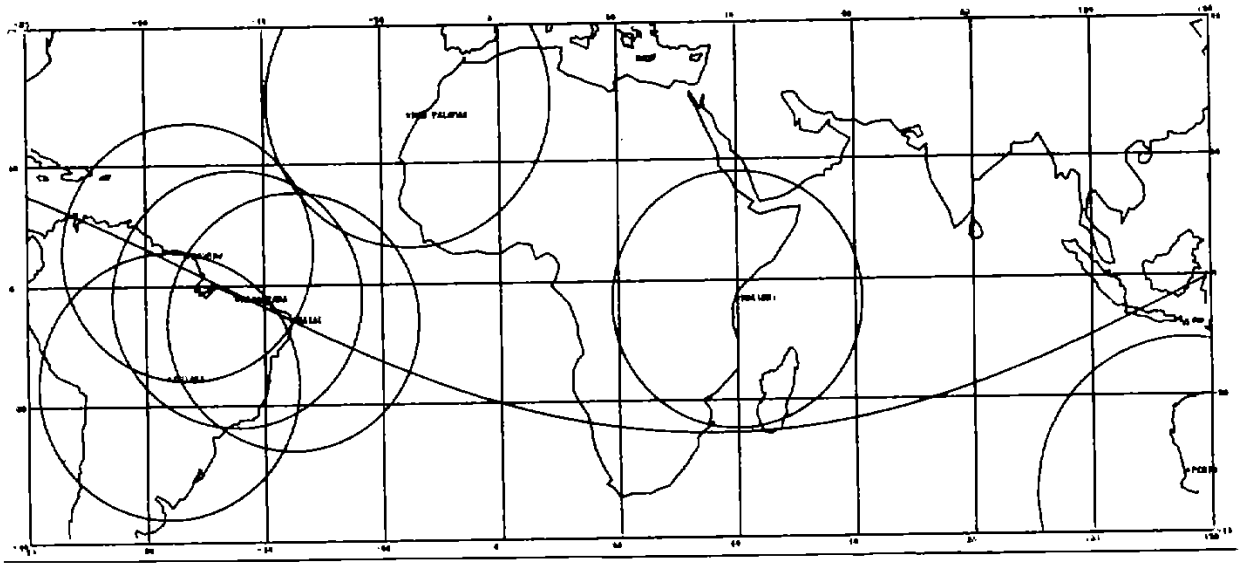

Fig. 6.21 - The orbit number eigth.

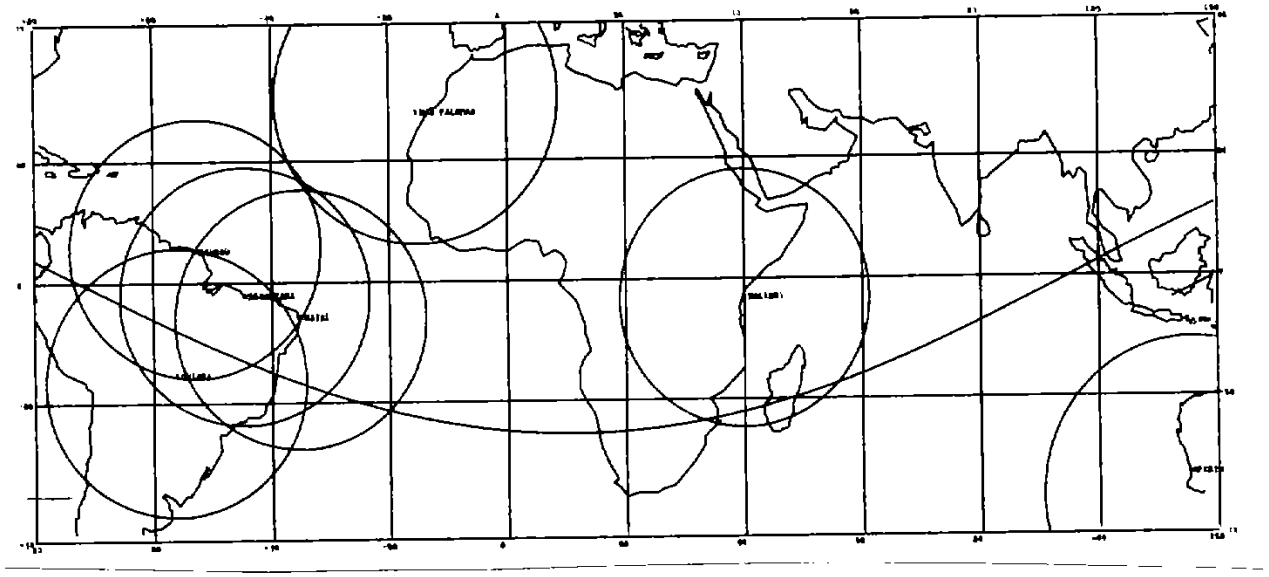

Fig. 6.22 - The orbit number nine.

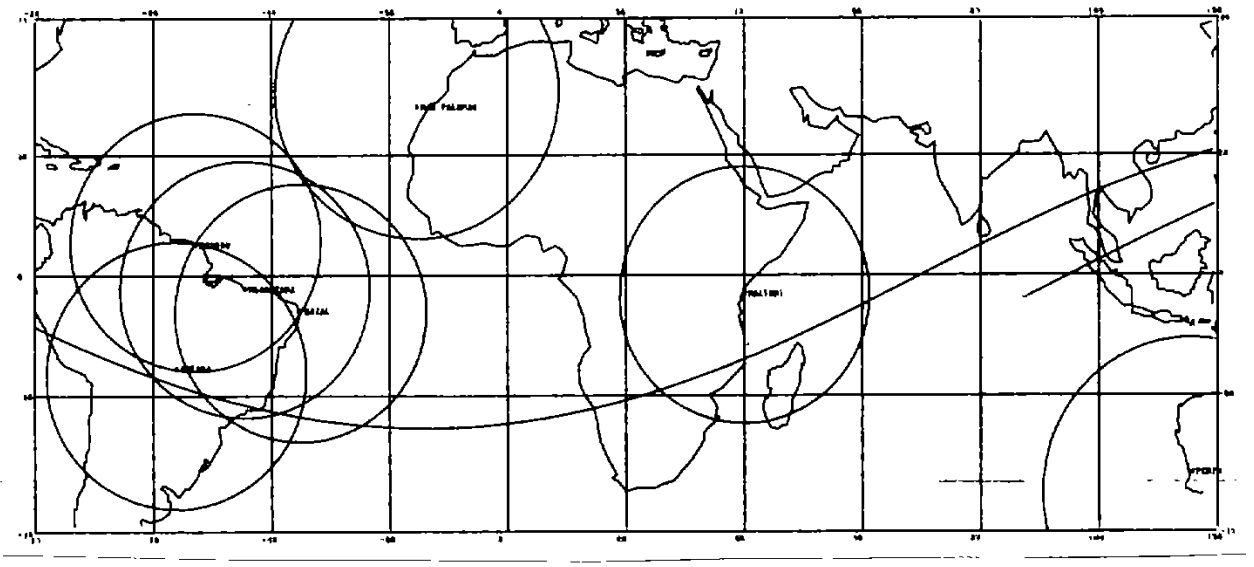

Fig. 6.23 - The orbit number ten.

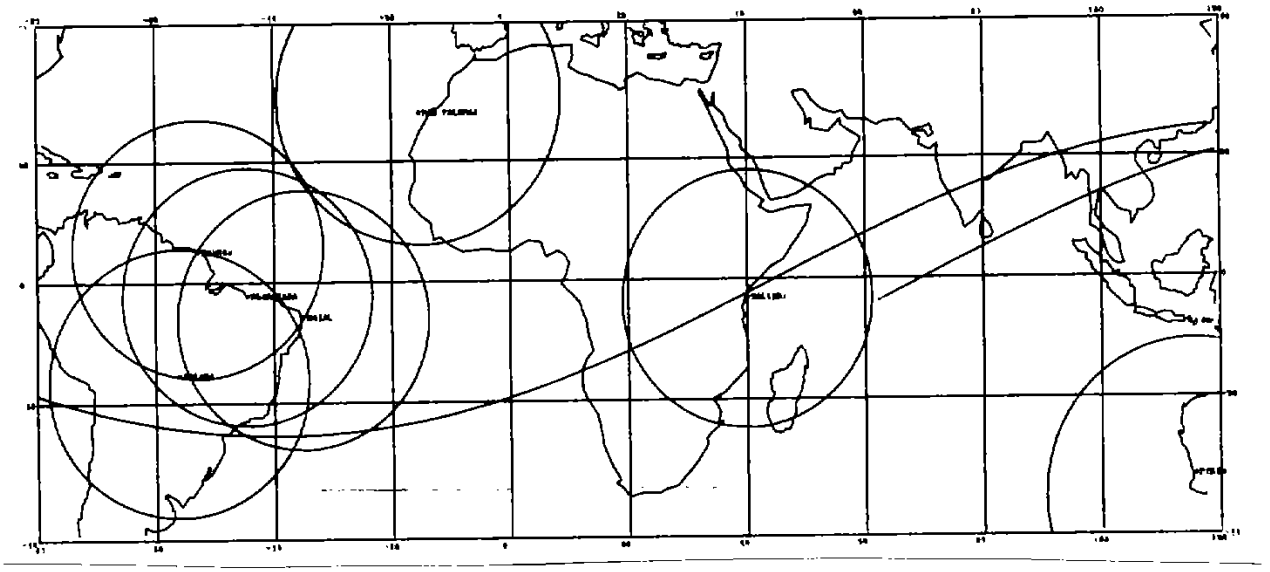

Fig. 6.24 - The orbit number eleven.

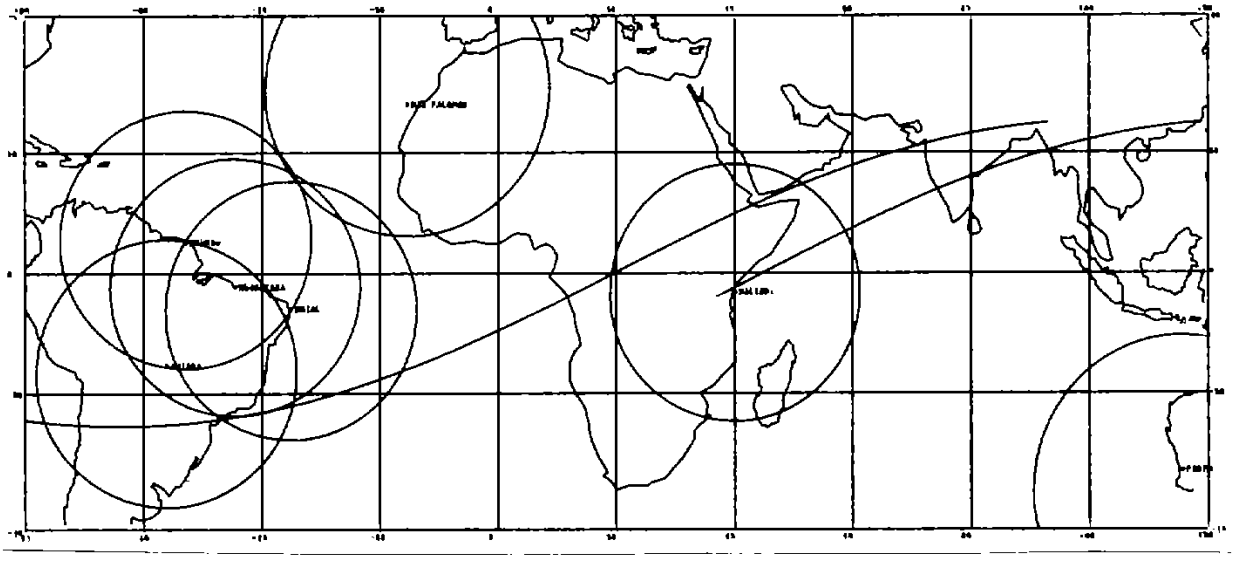

Fig.6.25 - The orbit number twelve.

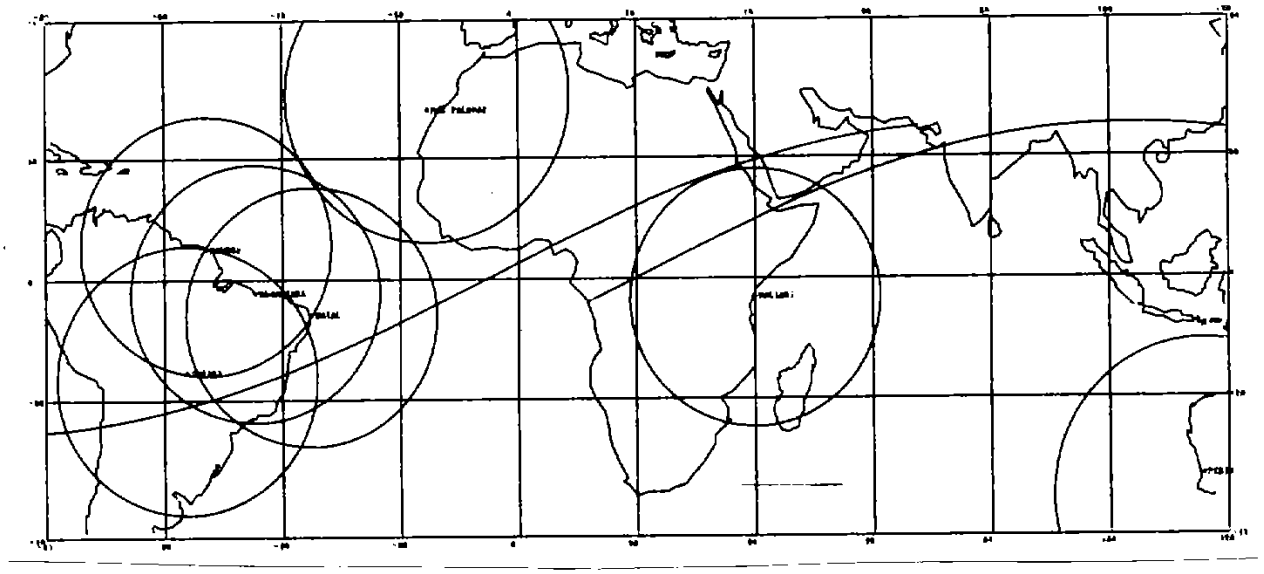

Fig. 6.26 - The orbit number thirteen.

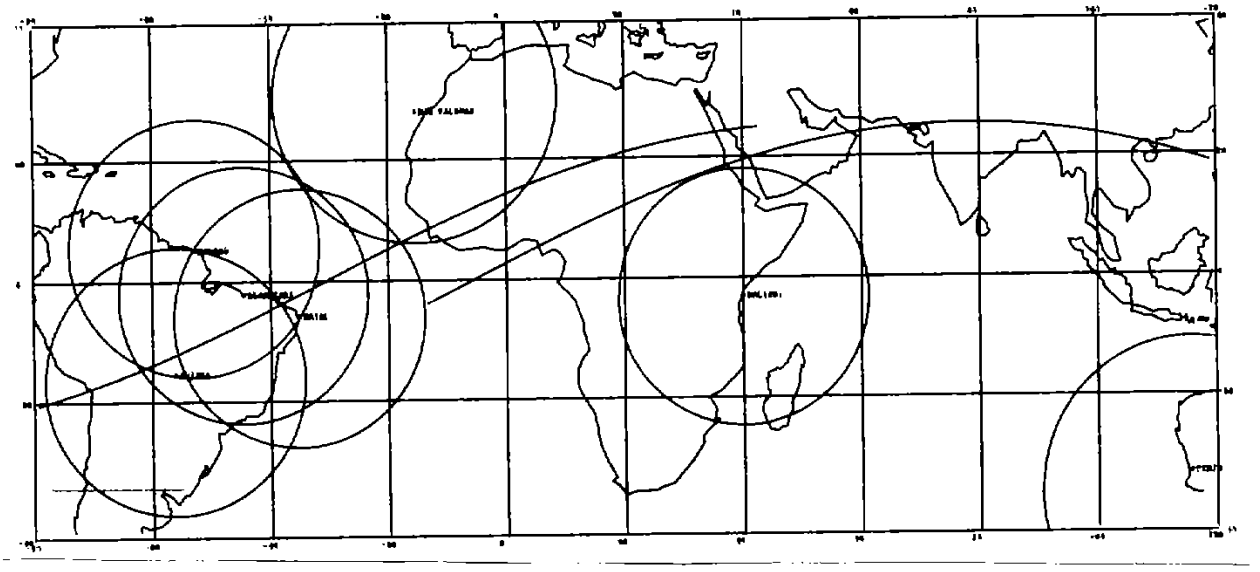

Fig. 6.27 - The orbit number fourteen.

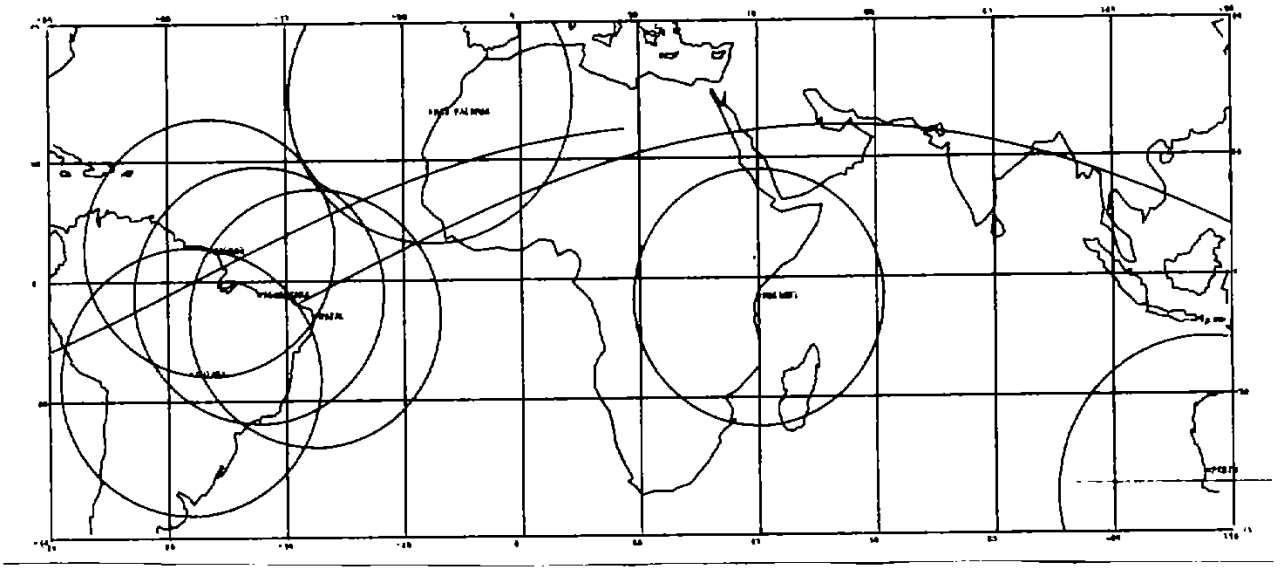

Fig. 6.28 - The orbit number fifteen.

REFERENCES

KONDAPALLI, R.R. Manual descritivo de uso do PRETEV - um programa para estimativa rápida do tempo de vida orbital de satelites artificiais. São José dos Campos, SP, INPE, junho de 1984. (INPE-3144-RPI/100).

KONDAPALLI, R.R.; MEDEIROS, V.M. Orbital geometry through launch data (in press).

MEDEIROS, V.M. Análise de missões: Definição da geometria orbital de satélites artificiais, São José dos Campos, SP, INPE, agosto de 1983. (INPE-2843-TDL/141).

APENDIX-A

In order to study the influence of inclination errors on the visibility of the satellite, 20^{o}, 25^{o} and 30^{o} inclination charts for 700 km are plotted in figures A.1, A.2, and A.3 respectively. The visibility circles of 400 km, 700 km and 1000 km with 5^{o} elevation above horizon line are also plotted for altitude dispersion analysis.

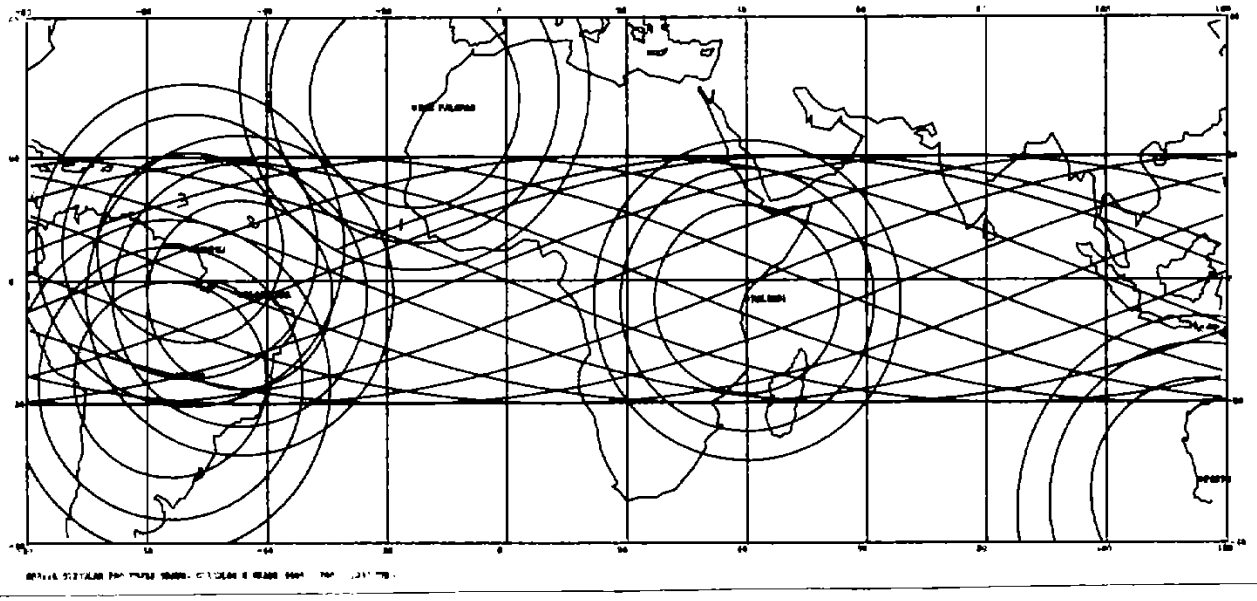

Fig. A.1 - 20^{o} inclination/700 km orbits chart.

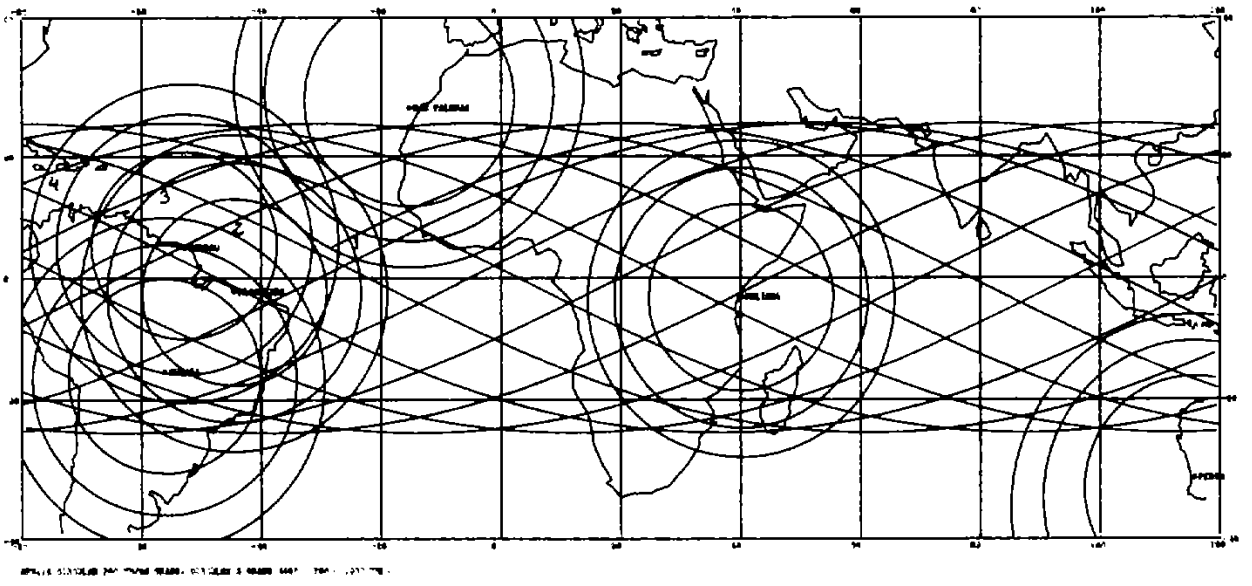

Fig. A.2 - 25^{o} inclination/700 km orbits chart.

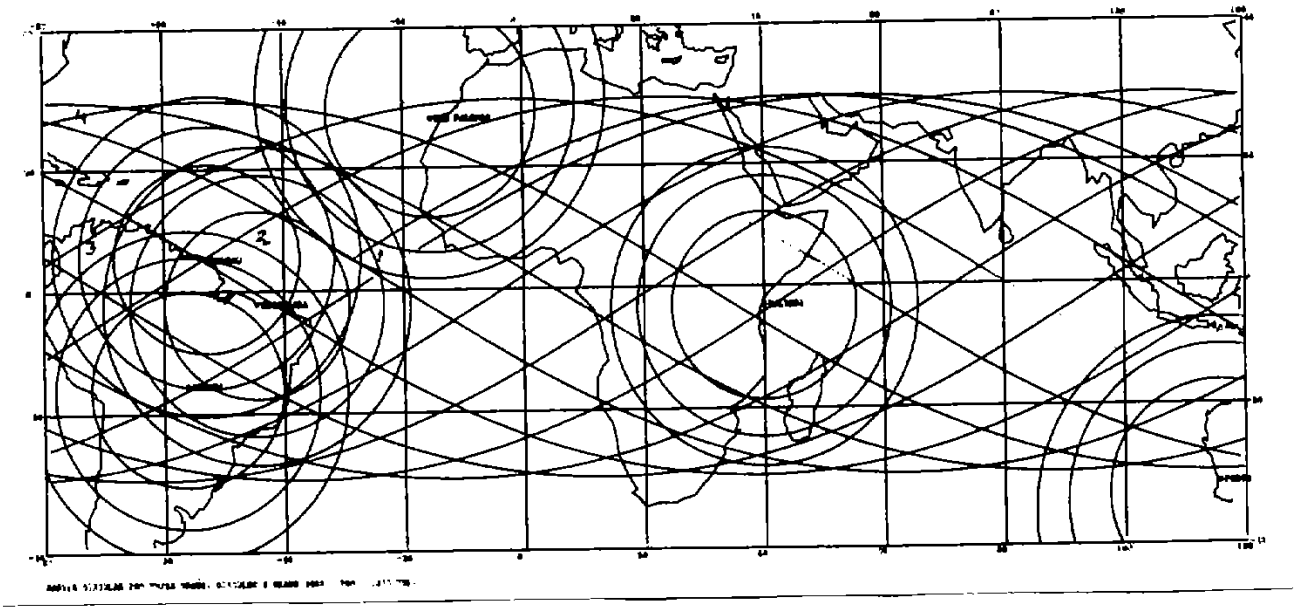

Fig. A.3 - 30^{o} inclination/700 km orbits chart.